THERMODYNAMICS OF ACID-BASE EQUILIBRIA SUBSTITUTED ANILINIUM IONS, PYRIDINIUM IONS, AND THIOPHENOL

A THESIS

Presented to

The Faculty of the Graduate Division

by

Edward Michael Perdue

In Partial Fulfillment

of the Requirements for the Degree

Doctor of Philosophy

in the School of Chemistry

Georgia Institute of Technology

August, 1973

THERMODYNAMICS OF ACID-BASE EQUILIBRIA

SUBSTITUTED ANILINIUM IONS,

PYRIDINIUM IONS, AND THIOPHENOL

Approved:

Charles L. Liotta, Chairman

Harry P. Hopkins, Jr.

Erling Grovenstein, Jr.

Date approved by Chairman: 8/15/73

ACKNOWLEDGMENTS

The author wishes to express his appreciation to his advisors, Dr. Charles L. Liotta, and Dr. Harry P. Hopkins, Jr., of Georgia State University, for their guidance and assistance throughout the course of this research. Dr. Liotta suggested this research problem and provided the author with financial support throughout the duration of this project. Dr. Hopkins, in whose laboratories this research was conducted, was instrumental in the development of experimental techniques. Both Dr. Liotta and Dr. Hopkins worked closely with the author in the analysis of experimental data.

An expression of appreciation and gratitude is also extended to Dr. Erling Grovenstein for his useful suggestions during the reading and critical evaluation of this manuscript.

The author would especially like to express his gratitude and appreciation to his wife, Kathy, for her patience and encouragement during the course of this research and for her diligence in the typing of this manuscript.

TABLE OF CONTENTS

Page

ACKNOWLEDGMENTS ii

LIST OF TABLES iv

LIST OF FIGURES vi

SUMMARY vii

Chapter

I. INTRODUCTION 1

Historical Background
Proposed Research

II. EXPERIMENTAL 14

Instrumentation and Equipment
Materials
Procedure

III. RESULTS 42

Anilinium Ions and Pyridinium Ions
Thiophenol

IV. DISCUSSION 58

Anilinium Ions
Pyridinium Ions
Thiophenol

V. CONCLUSIONS 93

VI. RECOMMENDATIONS 95

APPENDIX 97

BIBLIOGRAPHY 151

VITA 157

LIST OF TABLES

Table		Page
1.	Commercial Source and Method of Purification of the Organic Compounds Used in this Research	28
2.	Switch Positions for Electrical Measurements and Sample Introduction in the Solution Calorimetry System	41
3.	Enthalpies of Ionization of Substituted Anilinium Ions	43
4.	Enthalpies of Ionization of Substituted Pyridinium Ions	44
5.	Enthalpies of Solution of 4-Chloropyridine-HCl and 4-Bromopyridine-HCl in Aqueous Perchloric Acid and Sodium Hydroxide Solutions	45
6.	Thermodynamics of Ionization of Substituted Anilinium Ions in Aqueous Solution at 25°C	50
7.	Thermodynamics of Ionization of Substituted Pyridinium Ions in Aqueous Solution at 25°C	51
8.	The pK_a of Thiophenol in Aqueous Solution at 25°C	56
9.	Enthalpy of Neutralization of Thiophenol	57
10.	Kirkwood-Westheimer Treatment of Substituted Anilinium Ions	66
11.	Comparison of the Thermodynamics of Ionization of Thiophenol and Phenol in Aqueous Solution and in the Gas Phase at 25°C	76

LIST OF TABLES (Continued)

Table		Page
12.	Calculated Gas Phase Entropies of Thiophenoxide and Phenoxide Anions	89
13.	Equipment List for the Solution Calorimetry System	113
14.	Absorbance Data for Thiophenol and Thiophenoxide Anion in Aqueous Solution at 37,950 cm^{-1}	127
15.	Summary of the Experimental Data for the Determination of the pK_a of Thiophenol in a Standard KH_2PO_4-Na_2HPO_4 Buffer Solution	128
16.	Structural Parameters Used in the Kirkwood-Westheimer Treatment of Substituted Anilinium Ions and Pyridinium Ions	133
17.	Van der Waals Volumes and Overlapping Volume Increments for A-B Groups	137
18.	Entropy Contributions of the Fundamental Vibrational Frequencies in Thiophenoxide and Phenoxide Anions	148

LIST OF FIGURES

Figure		Page
1.	Vacuum-jacketed Reaction Vessel	15
2.	Container Lid with Associated Equipment	17
3.	Sample Introduction System	19
4.	Sample Bag Assembly	20
5.	Heater and Thermistor Probes	22
6.	Electrical Circuit Diagram for the Thermistor Drift Rate Determinations	24
7.	Electrical Circuit Diagram for Sample Introduction and for Heat Capacity Determinations	25
8.	A Plot of $\Delta\overline{G}°$ versus $\Delta\overline{S}°$ for the Ionization of the Substituted Anilinium Ions and Pyridinium Ions Included in this Study	52
9.	A Plot of $\Delta\overline{G}°$ versus $\Delta\overline{H}°$ for the Ionization of the Substituted Anilinium Ions and Pyridinium Ions Included in this Study	54
10.	A Thermodynamic Cycle for the Entropy of Proton Transfer in the Thiophenol-Phenol System	87
11.	The Spherical Molecular Cavity Model of Kirkwood-Westheimer Electrostatic Theory	130

SUMMARY

The research described herein is a detailed investigation of the relative contributions of the enthalpy and entropy of ionization to the Gibbs free energies of ionization of substituted anilinium ions, pyridinium ions, and thiophenol. Enthalpies of ionization ($\Delta\overline{H}°$) were determined calorimetrically in aqueous solution at 25°C. Entropies of ionization ($\Delta\overline{S}°$) were calculated from the experimental enthalpies and literature Gibbs free energies of ionization ($\Delta\overline{G}°$). In the case of thiophenol, $\Delta\overline{G}°$ was calculated from the pK_a, which was determined spectrophotometrically in a standard buffer solution.

In an analysis of the experimental data for substituted anilinium ions and pyridinium ions, it was found that plots of $\Delta\overline{G}°$ versus $\Delta\overline{H}°$ and $\Delta\overline{G}°$ versus $\Delta\overline{S}°$ were linear for both acid systems. The magnitude of the slopes of the $\Delta\overline{G}°/\Delta\overline{H}°$ plots for both anilinium ions and pyridinium ions indicate that substituent effects are manifested primarily in the enthalpy rather than the entropy of ionization. (In contrast, substituent effects in the ionization of neutral organic acids such as phenols and benzoic acids are primarily due to entropy changes). Furthermore, the slopes of the $\Delta\overline{G}°/\Delta\overline{S}°$ plots for both anilinium ions and pyridinium ions

agree well with the predictions of Kirkwood-Westheimer electrostatic theory.

The experimental data for substituted anilinium ions and pyridinium ions were also analyzed in terms of Hepler's theory of substituent effects. These analyses reveal that β values for these acid systems are far greater than the value of 280° suggested by Hepler, and that, rather than being constant, β values vary substantially from one acid system to another.

A comparison of the thermodynamics of ionization of thiophenol and phenol reveals that the greater acidity of thiophenol is primarily due to a more positive entropy of ionization. Furthermore, a comparison of the aqueous and gas phase thermodynamic functions for the following proton transfer reaction

$$C_6H_5SH + C_6H_5O^- \rightleftharpoons C_6H_5S^- + C_6H_5OH$$

shows that the more positive entropy of ionization of thiophenol is almost entirely due to "looser" solvation of the thiophenoxide anion in aqueous solution.

While the volume change for the above proton transfer reaction can be satisfactorily accounted for in terms of a van der Waals contribution and a small contribution due to electrostriction of solvent, none of the theoretical formu-

lations which were employed in this analysis were able to quantitatively account for the large positive entropy change observed for this reaction.

CHAPTER I

INTRODUCTION

Historical Background

One of the foremost problems in the field of acid-base equilibria is the lack of a quantitative theoretical formulation which adequately describes the acid ionization process. Various factors which can influence acidity must be encompassed in such a theory. These factors include (1) the nature of the functional group from which the acidic proton is removed, (2) the relative inherent stabilities of the acid and its conjugate base, and (3) the influence of solvent on the stabilities of the acid and its conjugate base. Furthermore, since most known acids are organic compounds, a successful theory must also account for substituent-induced changes in the acidities of these acids.

The thermodynamic quantity most commonly used as a measure of acidity is the standard Gibbs free energy of ionization ($\Delta\overline{G}°$), which can easily be obtained from pK_a determinations. Consequently, most current theories tend to treat the acid ionization process only in terms of $\Delta\overline{G}°$ values. Unfortunately, $\Delta\overline{G}°$ represents the net effect of all the factors mentioned above and, therefore, provides little information concerning the relative importance of each factor

in determining the acidity of a given compound. An analysis of the thermodynamic components of $\Delta\bar{G}°$, the standard enthalpy ($\Delta\bar{H}°$) and entropy ($\Delta\bar{S}°$) of ionization, might be expected to contribute significantly to the development of a more suitable theory of the acid ionization process. However, before such an analysis can be undertaken, these parameters must be determined for a wide variety of acids.

Despite the limitations of a formulation based solely on $\Delta\bar{G}°$ values, several such theories have been proposed to account for substituent-induced changes in the acidities of organic acids. Substituent effects are most clearly illustrated in a symmetrical proton transfer reaction such as

$$HA_1 + A_2 \rightleftharpoons A_1 + HA_2 \qquad (1)$$

where HA_1 and HA_2 are two structurally similar organic acids differing only by a charged or dipolar substituent, and A_1 and A_2 are the respective conjugate bases. In an analysis of the influence of charged substituents on the pK_a's of carboxylic acids, Bjerrum[1] suggested that, for symmetrical proton transfer reactions such as eq 1, pK_a differences can be accounted for in terms of purely electrostatic field effects. If the proton and charged substituent are treated as point charges separated by a distance r in a solvent continuum whose dielectric constant D is that of the bulk

solvent, the work required to transfer the proton from r to infinity in the electrostatic field of the charged substituent can be calculated from classical electrostatic theory. The pK_a difference between the unsubstituted and substituted acids (ΔpK) is then given by

$$\Delta pK = \frac{Nze^2}{2.303RTDr} \qquad (2)$$

where R is the gas constant, T is the absolute temperature, N is Avogadro's number, ze is the charge of the substituent, and e is the proton charge.

Bjerrum's equation can be extended to include dipolar substituents if the dipole moment (μ) of the substituent is treated as a point dipole located at a distance r from the acidic proton. The pK_a difference between the unsubstituted and substituted acids is then given by

$$\Delta pK = \frac{Ne\mu\cos\phi}{2.303RTDr^2} \qquad (3)$$

where ϕ is the angle between the dipole moment vector and a line connecting the point dipole with the acidic proton, and all other symbols are the same as those previously defined. This equation, which was proposed by Eucken[2], underestimates the magnitude of dipolar substituent effects. A similar

equation was proposed by Smallwood[3], who suggested that all solute-solvent interactions should cancel in a symmetrical proton transfer reaction such as eq 1. The substituent effects observed in aqueous solution should therefore equal the calculated substituent effects for the gas phase proton transfer reaction. Accordingly, Smallwood's equation for ΔpK assumes that $\mathcal{D}=1$ (the dielectric constant of a vacuum) and does not depend on the dielectric constant of the solvent. However, this equation overestimates the magnitude of dipolar substituent effects, so the best model of dipolar field effects apparently lies somewhere between the two extreme models proposed by Eucken and Smallwood.

In 1938, Kirkwood and Westheimer[4-7] proposed an electrostatic theory which proved to be much more successful than prior theories of the acid ionization process. Assuming the organic acid to be imbedded in a cavity of low dielectric constant immersed in a solvent continuum whose dielectric constant is that of the solvent, Kirkwood and Westheimer have shown that the size and shape of the cavity are instrumental in determining the magnitude of substituent effects on the ionization of organic acids. In order to incorporate the transmission of substituent effects through the molecular cavity, these workers introduced the concept of an "effective" dielectric constant ($\mathcal{D}_{eff}$), which can be calculated from a knowledge of the size and shape of the molecular cavity, the dielectric constant of the cavity (usually set equal to 2.0),

and the dielectric constant of the solvent. Because of insurmountable mathematical difficulties, the initial studies were limited to spherical and prolate ellipsoidal cavities. Later, however, Sarmousakis[8] extended the theory to include oblate ellipsoidal cavities.

Since the original model of Kirkwood and Westheimer was proposed, other researchers have suggested modifications which, in some cases, give better agreement between theoretical and experimental results. For example, when dealing with acid-base equilibria in aqueous media, Tanford[9] suggested that improved agreement with experimental results could be obtained if the radius of the cavity was increased by 1.0 Å for charged substituents and 1.5 Å for dipolar substituents, an adjustment which has the net effect of burying the charge or dipole further inside the molecular cavity. The Tanford modification and the original electrostatic field model of Kirkwood and Westheimer are both widely used today in the analysis of substituent effects on the ionization of organic acids[10].

Another model of substituent effects which has been widely used is the inductive model, in which substituent effects are attributed to successive polarization of the bonds between the substituent and the reaction center[11-13]. The magnitude of substituent effects will thus depend on both the nature of the substituent and on the number and

nature of the bonds and transmission paths through which polarization effects are propagated.

Qualitatively, the inductive and field models differ in that, while the inductive model emphasizes the importance of the number of bonds between the substituent and the reaction site, the hybridization of these bonds, and the number of possible transmission paths, the electrostatic field model primarily emphasizes the distance between the substituent and the reaction center and, in the case of dipolar substituents, the angle between the dipole moment vector and a line which connects the point dipole with the acidic proton. Numerous researchers have synthesized and studied acid systems which were designed to test each theory by taking advantage of these qualitative differences in the two models[14-28]. Stock[29] has recently summarized the results of these investigations and, in general, better agreement between theoretical and experimental results was obtained using the field model of Kirkwood and Westheimer.

While quantitative approaches such as the field and inductive models have been only partially successful in the area of acid-base equilibria, Hammett[30] has shown that substituent effects for meta- and para-substituted benzene derivatives can be predicted surprisingly well by the following empirical relationship:

$$\Delta pK = - \left[\frac{A}{2.303RTr^2}\right] \left[\frac{B_1}{D} + B_2\right] \quad (4)$$

where A, B_1, and B_2 are constants which are independent of temperature and solvent, and all other parameters have been previously defined. It is interesting to note that this equation is identical in form with the electrostatic equation of Kirkwood and Westheimer (see Calculation 5 in the Appendix). Since A depends only on the substituent and its position in the benzene ring relative to the acidic functional group, and B_1 and B_2 depend only upon the reaction, Hammett suggested that eq 4 could be represented by:

$$\Delta pK = \rho\sigma \quad (5)$$

where $\sigma = - A/2.303R$ and $\rho = \left[\frac{1}{r^2T}\right] \left[\frac{B_1}{D} + B_2\right]$.

According to eq 5, the effect of a substituent on a given reaction will depend on some intrinsic property of the substituent (σ) and on the sensitivity of that particular reaction to substituent effects (ρ). The σ-values of various substituents are based on the ionization of substituted benzoic acids in water at 25°C, for which a ρ-value of 1.0 is arbitrarily assigned. The resulting σ-values are appli-

cable in a large number of reactions, failing only when resonance interactions between a substituent and the reaction center become significant[31]. Furthermore, as predicted by eq 5, ρ-values have been found to be dependent upon the reaction, the solvent medium, and the temperature[32].

Before a complete theory of substituent-induced changes in acidity can be developed, not only $\Delta\bar{G}°$, but also $\Delta\bar{H}°$ and $\Delta\bar{S}°$ values must be known for a wide variety of organic acids. While reliable $\Delta\bar{G}°$ values have now been obtained in aqueous solution for a majority of the known organic acids, $\Delta\bar{H}°$ values and $\Delta\bar{S}°$ values are known for only a few acid systems. In a recent review article, Larson and Hepler[33] have summarized the available thermodynamic data for the acid ionization process. Thus far, most studies have been limited to neutral organic oxygen-containing acids such as phenols and benzoic acids. Positively charged organic acids such as protonated amines and sulfur-containing organic acids such as thiols have generally been neglected. Before a successful theory of the acid ionization process can be fully developed, these types of acid systems must be carefully studied to determine the effect of the nature of the acidic functional group on the thermodynamics of ionization of organic acids.

Proposed Research

Anilinium Ions and Pyridinium Ions

In ionogenic processes such as the ionization of phenols[33] and carboxylic acids[34,35], it has been established that entropy changes are primarily responsible for the substituent-induced changes in the acidities of these acids in aqueous solution. The study of systems involving organic cation acids would determine the relative importance of the enthalpy and entropy of ionization in an isoelectric reaction. Substituted anilinium ions and pyridinium ions provide suitable systems for such a study. In the case of anilinium ions, only the uncharged conjugate base can undergo resonance interactions with a substituent; however, in pyridinium ions, both the cation acid and its conjugate base are susceptible to resonance effects. Therefore, a comparison of the two systems should reflect the relative importance of resonance interactions in charged and uncharged species in aqueous solution. Furthermore, since the proton-dipole distance is shorter in substituted pyridinium ions than in anilinium ions, electrostatic theory predicts that substituent-induced $\Delta\bar{G}°/\Delta\bar{S}°$ ratios should be more negative for substituted pyridinium ions than for the corresponding anilinium ions. Thus, a study of the thermodynamics of ionization of these two acid systems should provide a substantial amount of data which is needed for the refinement

of current acid ionization theories.

The pK_a's of several substituted anilinium ions have been determined by both Bolton[36-38] and Biggs[39] with an agreement at 25°C of better than 0.01 pK_a units (± 14 cal/mol in $\Delta\bar{G}°$). However, an analysis of the temperature dependence of the pK_a data of both Biggs and Bolton provides $\Delta\bar{H}°$ values which differ by as much as 500-1000 cal/mol for many of the substituted anilinium ions. This leads to a variation in $\Delta\bar{S}°$ values between the two investigators of as much as three cal/deg-mol.

Van de Poel and Slootmaekers[40] have calorimetrically determined the thermodynamic parameters of ionization for a number of substituted anilinium ions. Unfortunately, the range of substituents studied did not include any highly electron-withdrawing substituents where direct resonance interaction between the substituent and the reaction center is possible in the uncharged species.

Other calorimetric studies include Christensen's[41] study on the thermodynamics of ionization of protonated amines, which included a few anilinium ions, and O'Hara's[42] determination of $\Delta\bar{H}°$ values for *o*-, *m*-, and *p*-toluidinium ions. The calorimetric values are somewhat different from the spectrophotometrically determined values of Bolton[36-38].

The pK_a's of a large number of 3- and 4-substituted pyridinium ions in aqueous solution have been determined by

Fischer and coworkers[43], who, on the basis of relative pK_a values, concluded that only electron-donating 4-substituents undergo resonance interactions with the reaction center.

Recently, the thermodynamics of ionization of several substituted pyridinium ions were reported by Christensen and coworkers[44]. However, since only three 4-substituted pyridines (including 4-hydroxypyridine, which is believed to exist as the pyridone tautomer in aqueous solution[45]) were included in this study, a thorough examination of resonance effects in the pyridine system was not possible. Furthermore, the positive slope obtained in a plot of $\Delta\overline{G}°$ versus $\Delta\overline{S}°$ from the results of these workers is in contradiction with the negative slope which is predicted by electrostatic theory and with the experimental slopes found in other organic acid systems[34,35].

In addition, a few substituted pyridinium ions have been studied by Bates and Hetzer[46] and by Sacconi and coworkers[47]. The results of these researchers are in good agreement with the values reported by Christensen and coworkers.

The first part of this thesis research was undertaken to provide the necessary calorimetric data to accurately establish the enthalpies of ionization for a large number of substituted anilinium ions and pyridinium ions in aqueous solution at 25°C. Standard entropies of ionization were then

calculated from the experimental enthalpies and literature Gibbs free energies of ionization. The thermodynamic parameters obtained in this study were then analyzed in terms of Hepler's theory of substituent effects[48,49] and compared with the predictions of electrostatic theory[4-8].

Thiophenol

During the past several years, numerous investigators have extensively studied the thermodynamics of ionization of phenol and substituted phenols. In a recent review article, Larson and Hepler[33] have summarized the available data for this series of compounds. As previously mentioned, it is now generally accepted that the variation of the pK_a's of substituted phenols is almost completely due to changes in the entropy of ionization. In contrast, very little reliable data is available on the sulfur analog of phenol, thiophenol. The pK_a of thiophenol has been determined by several researchers[50,51] and is reported to be approximately 6.5. These results show that thiophenol is three and a half orders of magnitude more acidic than phenol (pK_a = 9.97). The relative acidities are clearly demonstrated in the proton transfer reaction shown in eq 6

$$PhSH + PhO^- \rightleftharpoons PhS^- + PhOH \qquad (6)$$

for which the aqueous Gibbs free energy of proton transfer is

calculated to be $\Delta\bar{G}^{\circ}_{t}(aq) = -4.75$ kcal/mol. At the present time, however, it is not known whether this difference in acidity is due to bond energies, anion stabilities, solute-solvent interactions, or a combination of these factors.

In the second part of this thesis research, the thermodynamic parameters $\Delta\bar{G}^{\circ}$, $\Delta\bar{H}^{\circ}$, and $\Delta\bar{S}^{\circ}$ were determined for the ionization of thiophenol in aqueous solution. These values were combined with literature values for the ionization of phenol in aqueous solution at 25° in order to calculate the thermodynamic parameters for the proton transfer reaction given in eq 6. In addition, the gas phase thermodynamic parameters $\Delta\bar{G}^{\circ}_{t}(g)$, $\Delta\bar{H}^{\circ}_{t}(g)$, and $\Delta\bar{S}^{\circ}_{t}(g)$ were calculated by a combination of semi-empirical (CNDO/2) results and statistical thermodynamic methods. The thermodynamic functions for the proton transfer reaction were then analyzed in terms of current solution theories in order to provide a better understanding of the nature and magnitude of solute-solvent interactions.

CHAPTER II

EXPERIMENTAL

Instrumentation and Equipment

Solution Calorimetry System

All calorimetric determinations were obtained in the laboratories of Dr. Harry P. Hopkins, Jr., of Georgia State University using a high precision solution calorimetry system which is similar to the system described by Hepler[52]. A complete list of all equipment used in the construction of the calorimetry system is given in the Appendix.

Reactions were carried out in a silvered vacuum-jacketed reaction vessel which was fabricated by the glass-blower at Georgia Tech. The design of the reaction vessel is shown in Figure 1 and the procedure used to silver the reaction vessel is given in the Appendix. Two externally accessible glass tubes which extend into the interior of the reaction vessel have been incorporated into the vessel in such a manner that the integrity of the vacuum jacket is maintained. The heater and thermistor probes which are placed in these tubes are thus able to maintain excellent thermal contact with the solution without the risk of any possible harm which might come to the probes as a result of chemical contact with the solution.

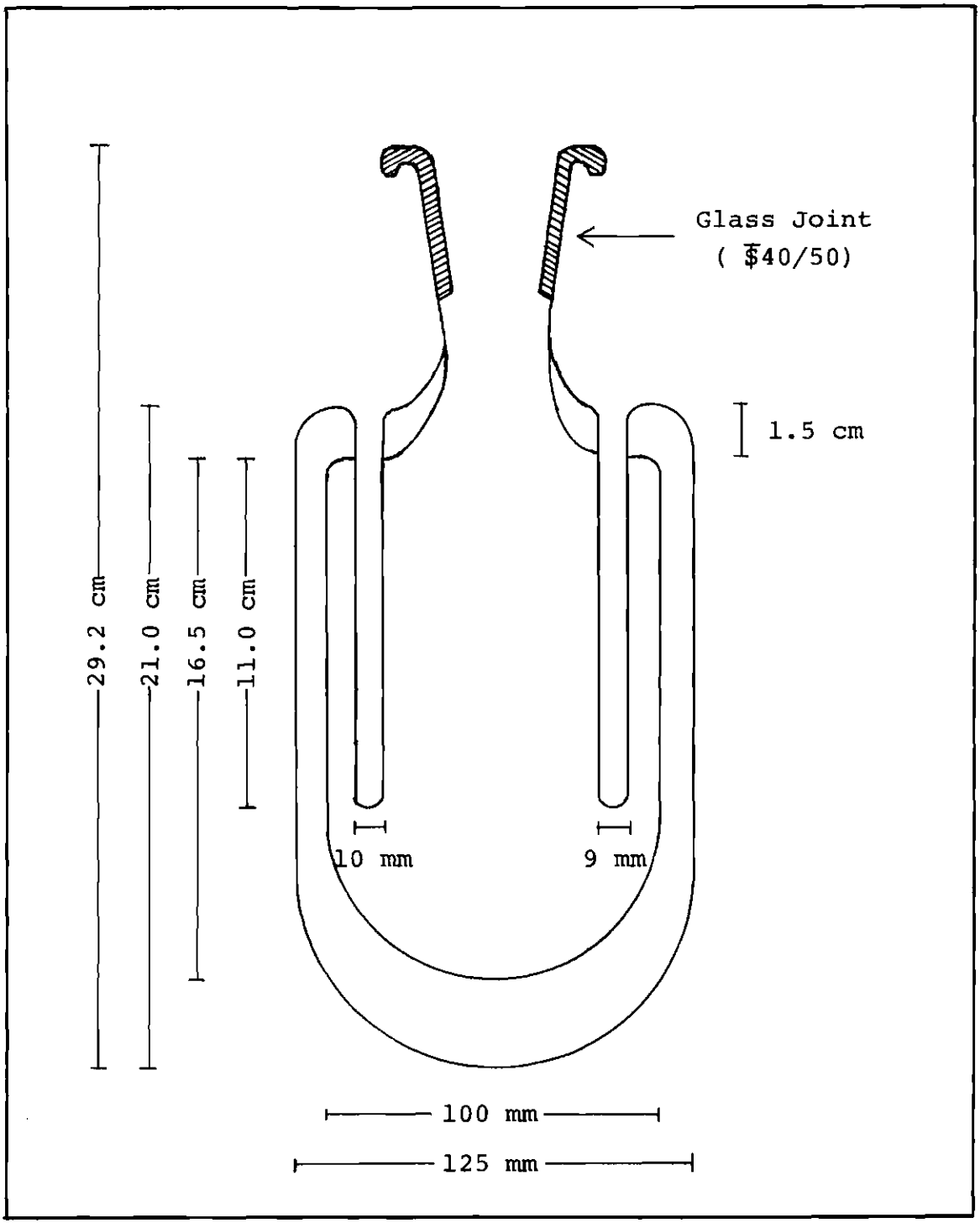

Figure 1. Vacuum-jacketed Reaction Vessel.

The reaction vessel, which has a capacity of approximately one liter, is suspended inside a water-tight stainless steel container and placed in a thermally regulated water bath during a calorimetric determination. The lid of the container, to which the reaction vessel is attached via a ₮40/50 stainless steel male joint, serves as a mounting plate for the stirring motor, the sample introduction motor, and the internal receptacle, a small electrical connector by which the heater and thermistor probes of the reaction vessel are connected with the external electrical instrumentation. The construction of the container lid and all associated equipment is given in Figure 2.

A unique feature of this calorimetry system is a sample introduction system which eliminates the problem of random heat effects due to sample introduction. With this mechanism, samples may be introduced smoothly and simply with only a small and highly reproducible heat effect of about 0.01 calories or less. Basically, the sample introduction system involves cutting a polyethylene sample bag with a sharp cutting blade at an appropriate time during a calorimetric determination. The sample container, which also serves as a completely adequate stirrer, is attached to the end of the stirrer shaft.

The cutting blade is constructed from a single-edged stainless steel razor blade and attached with silver solder

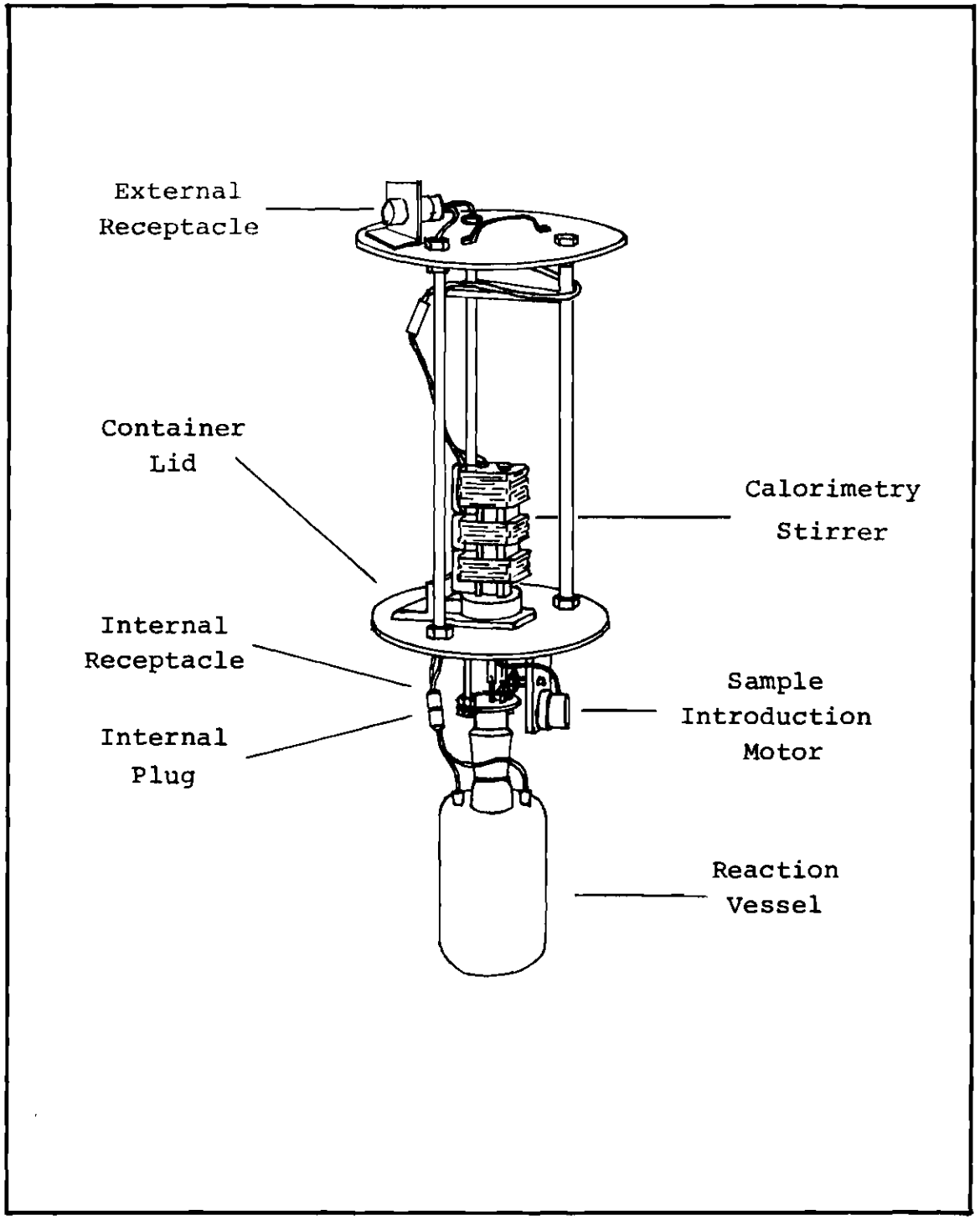

Figure 2. Container Lid with Associated Equipment

at a right angle to one end of a piece of 1/32 inch O.D. stainless steel rod. This connecting rod is attached to the sample introduction motor by a set of gears in such a manner that the position of the cutting blade can be manually adjusted. When power is supplied to the motor for a given length of time, the blade is turned by a fixed amount of arc, thus striking and cutting the spinning sample bag. The entire sample introduction system is shown on Figure 3.

A pattern of the sample bags used in this research was machined into a thin aluminum plate (13.7 cm x 4.1 cm x 1 cm). A sealing edge of 0.32 cm was used to assure that the edges of the bag would be completely sealed. The aluminum pattern was then attached to the heating unit of a commercially available polyethylene bag sealing iron. To make a sample bag, a double thickness of 3/4 mil polyethylene is placed between two thin sheets of Teflon and the heated pattern is pressed down firmly on the Teflon sheets for a few seconds. The sealed sample bag may be cut out with scissors.

The Teflon sample form shown in Figure 4 is used to shape the sample bag, to seal a sample in the bag, and to attach the sample bag to the stirrer shaft. When the sample form is attached to the stirrer shaft by means of a 1/4 inch polypropylene tubing connector, the resulting sample container is a tight cylindrical bag which is closed by the tightened tubing connector.

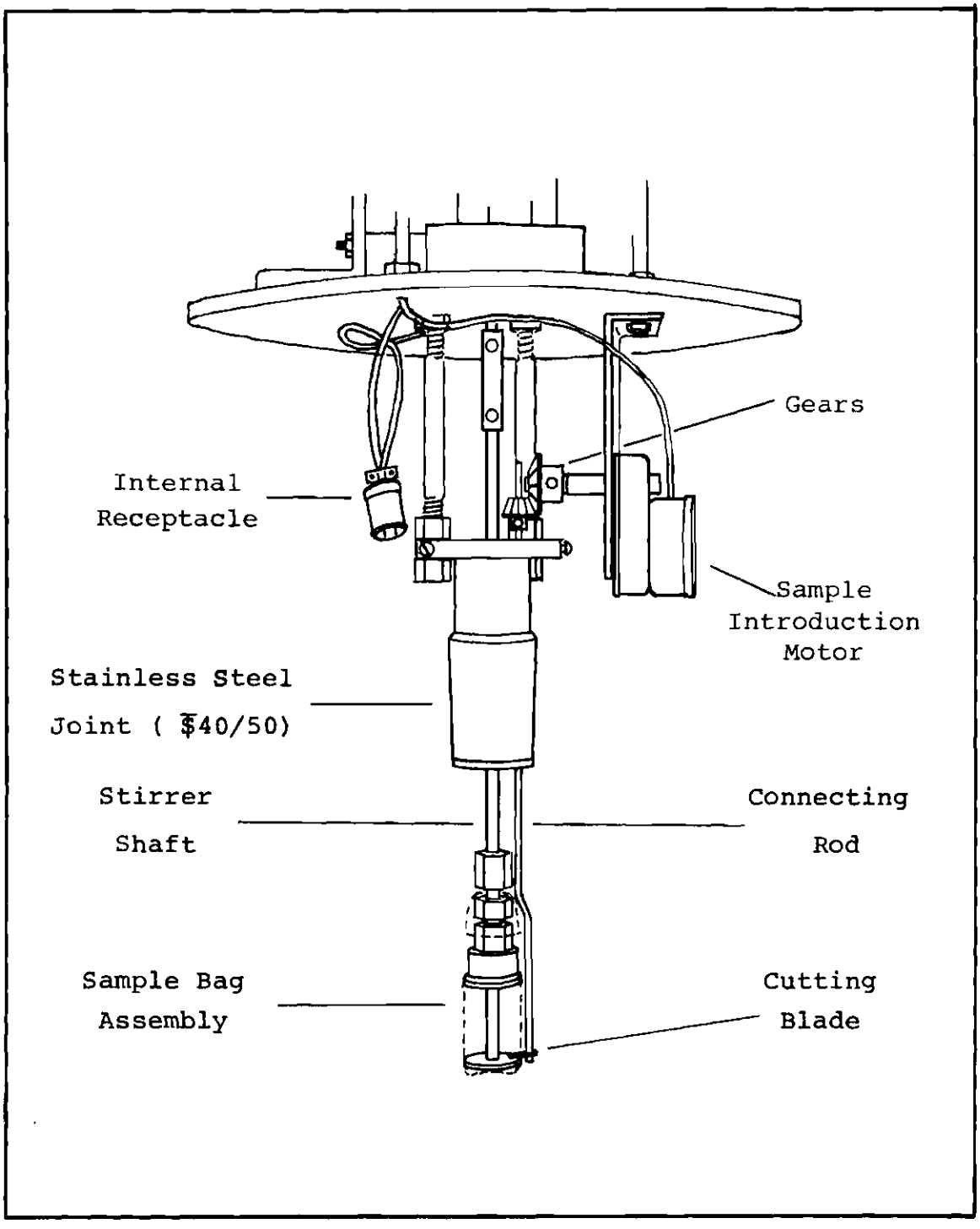

Figure 3. Sample Introduction System

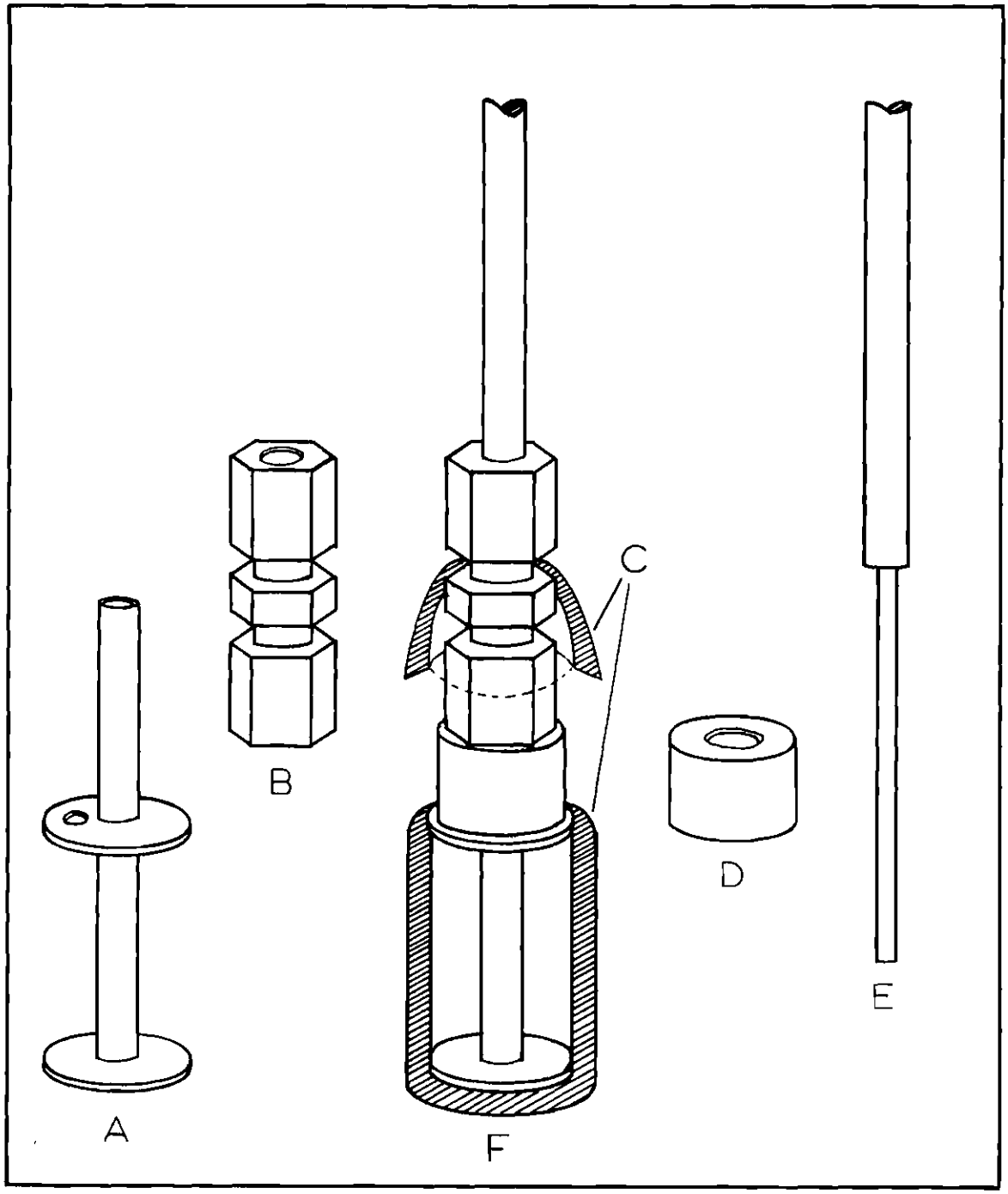

Figure 4. Sample Bag Assembly : (A) Teflon sample form; (B) Polypropylene tubing connector; (C) Polyethylene sample bag; (D) Teflon washer; (E) Stirrer shaft; (F) Assembled sample container attached to stirrer shaft.

The heater probe, which is placed in one of the glass tubes of the reaction vessel, is constructed from a 12 foot length of Manganin wire (11.92 ohms/ft.). The wire is wrapped tightly around a heater form which is constructed from an 11 cm length of 1/4 inch nylon rod. After the heater wires are connected to insulated copper leads, the entire probe is covered with a thin coat of epoxy cement and allowed to dry.

The thermistor probe, which is placed in the other glass tube of the reaction vessel, is constructed from two 100 ohm thermistors. After the thermistors are connected in parallel to insulated copper leads, the thermistor probe is covered with a thin coat of epoxy cement and allowed to dry.

The leads from the two probes are passed through #00 rubber stoppers and the probes are placed in the glass tubes of the reaction vessel. After the tubes have been filled with mineral oil, the external openings are closed with the rubber stoppers and sealed with epoxy cement. The leads from both probes are connected to the internal plug, which is connected to the internal receptacle during a calorimetric determination. The construction of both probes is shown in Figure 5.

In order to connect the internal receptacle, which is inside the stainless steel container, with the electrical

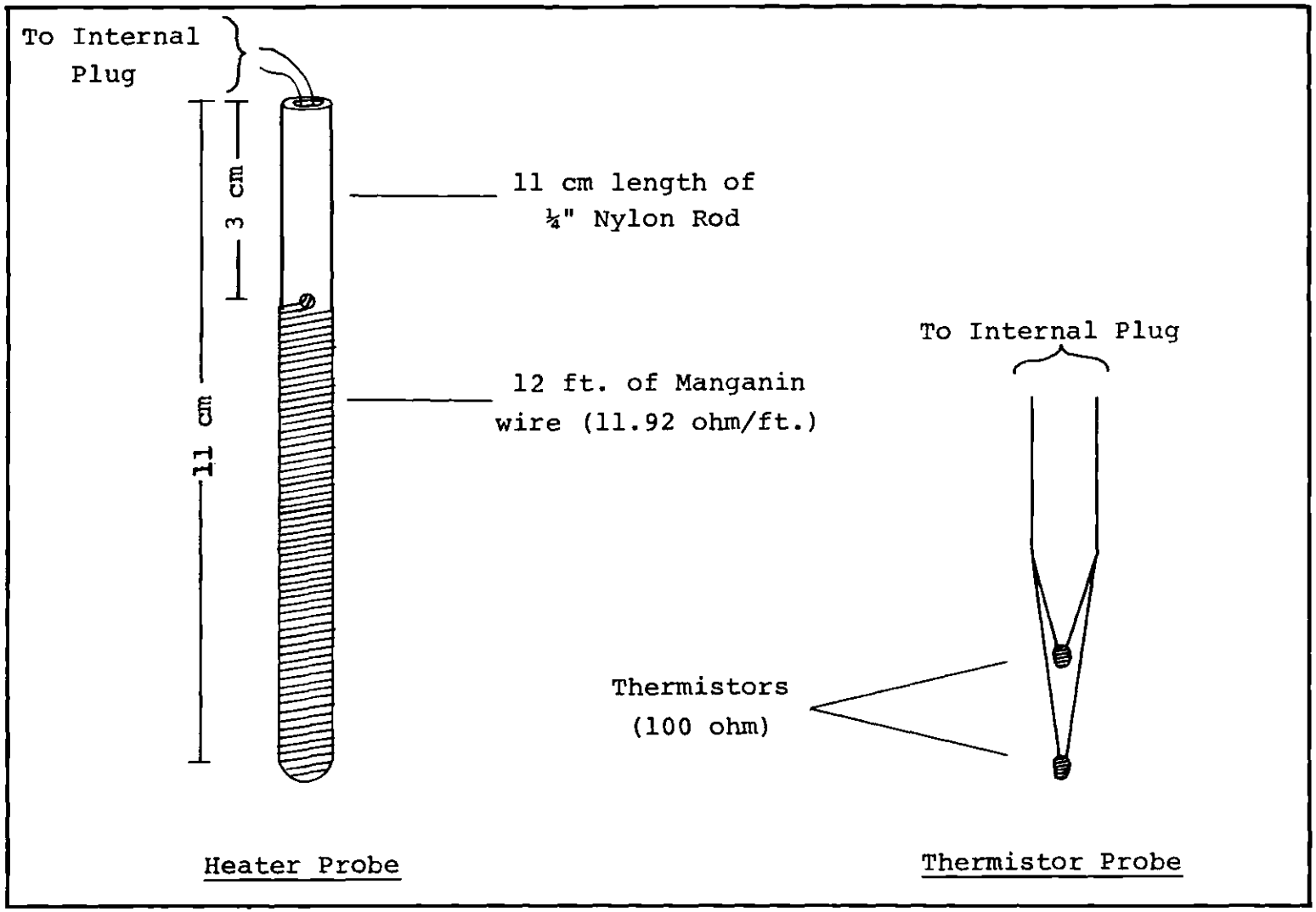

Figure 5. Heater and Thermistor Probes

instrumentation, insulated copper leads were run through hollow support rods to an external receptacle which is mounted at the very top of the container lid (see Figure 2). The leads from all the electrical instrumentation are connected to an external plug, which plugs into the external receptacle during a calorimetric determination.

The external electrical circuits are shown in Figure 6 and Figure 7. The circuit in Figure 6 is used to measure the resistance of the thermistor probe and to measure the rate of resistance change of the thermistor probe (in sec/ mΩ). The resistance of the thermistor probe is determined with a Mueller bridge whose output is connected to a galvanometer. The difference between the resistance of the thermistor probe and the resistance of the variable resistor on the Mueller bridge appears as a scale deflection on the galvanometer. The use of Switch F, shown in Figure 6, permits the output of the Mueller bridge to be sent either directly to the galvanometer (high sensitivity position) or through a 1000 ohm resistor in series with the galvanometer (low sensitivity position). The rate of resistance change of the thermistor probe is obtained using a digital timer (with automatic reset) by measuring successively the time interval required for the resistance of the thermistor probe to change by one milliohm.

In order to relate the resistance change in the

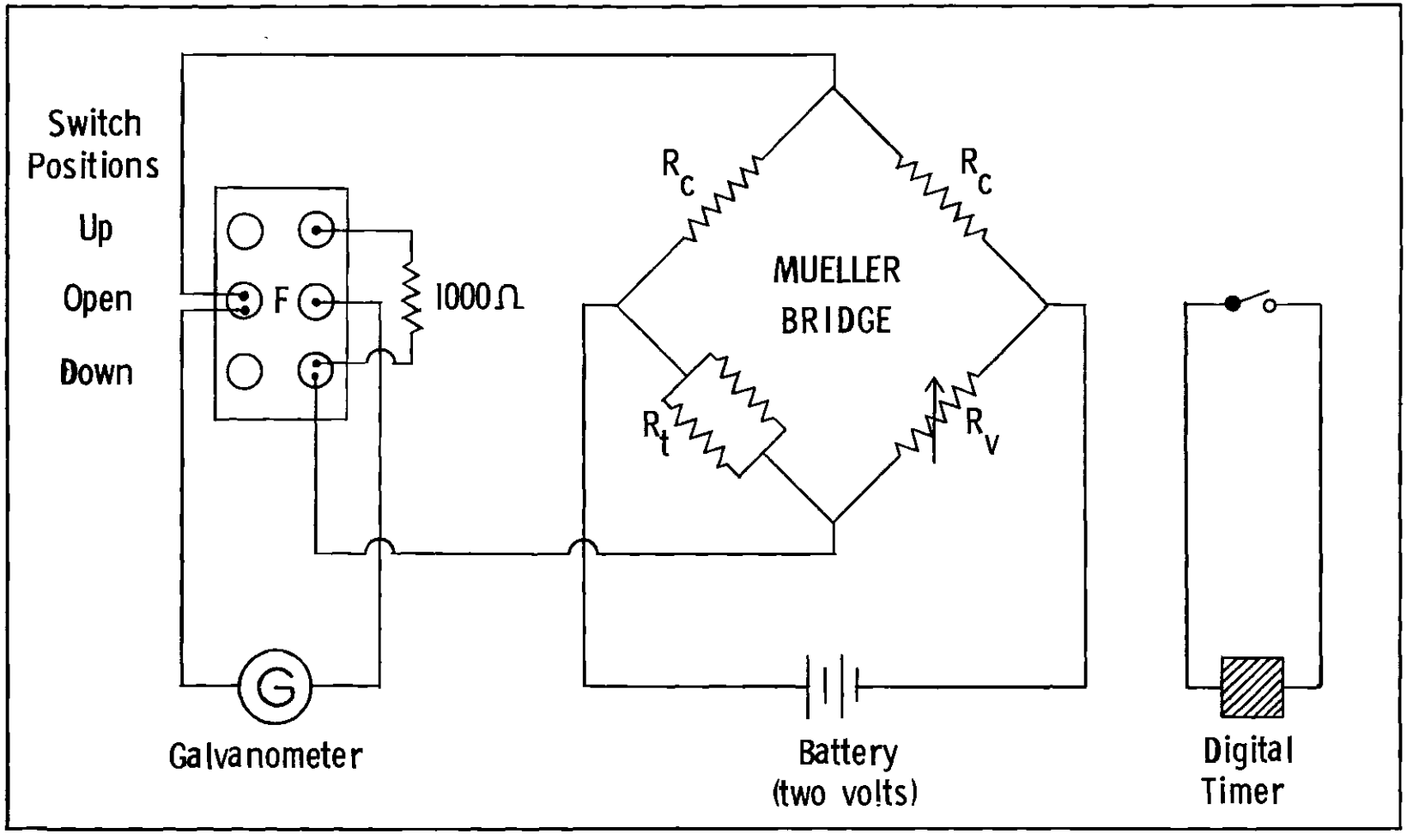

Figure 6. Electrical Circuit Diagram for the Thermistor Drift Rate Determinations.

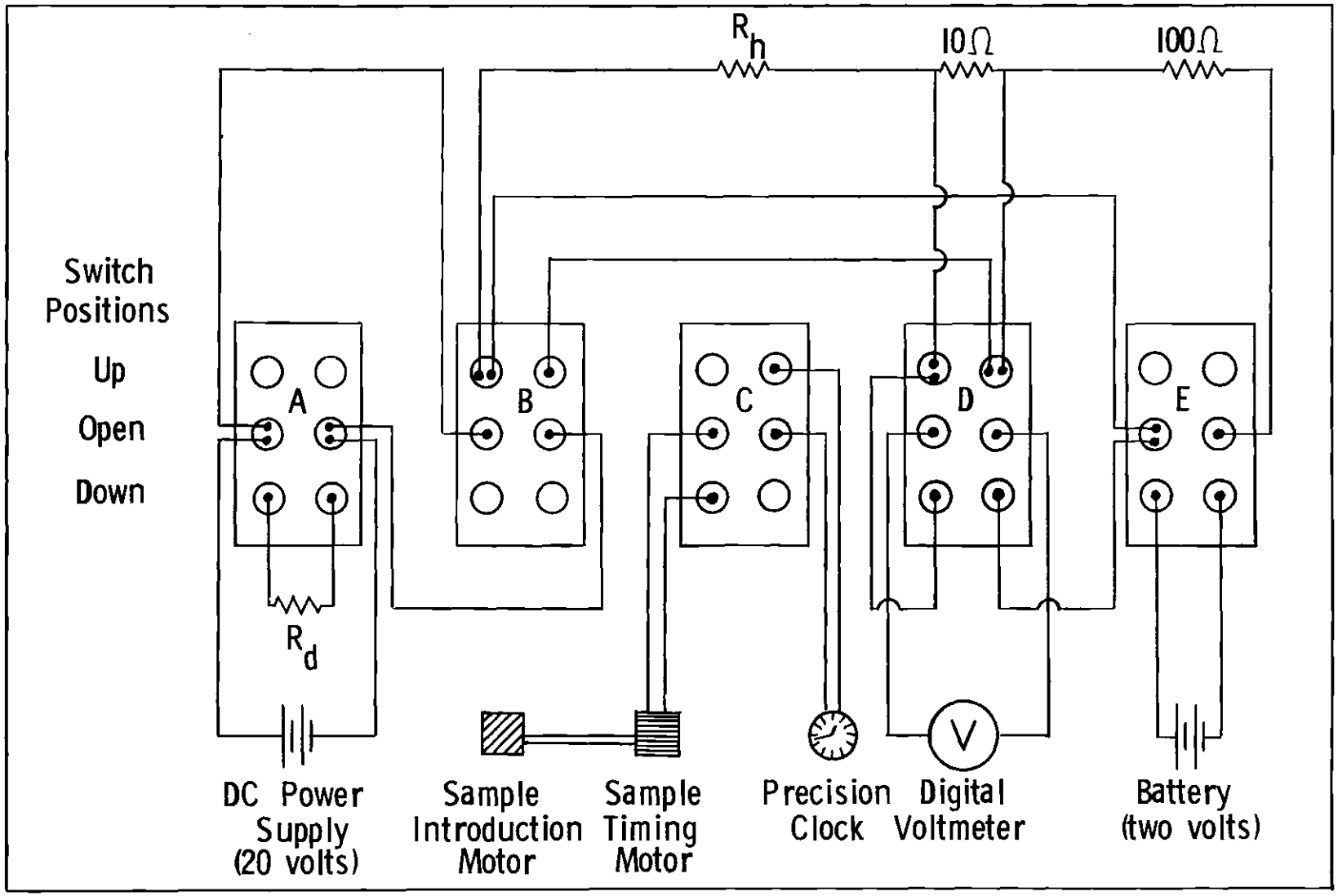

Figure 7. Electrical Circuit Diagram for Sample Introduction and for Heat Capacity Determinations.

thermistor probe to the heat evolved in a chemical reaction, the heat capacity of the calorimetry system must be determined. By passing a known current through the heater probe for a given length of time, the heat capacity of the system can be calculated from the known amount of heat evolved and the resulting resistance change in the thermistor probe. The circuit used for electrical calibration is shown in Figure 7. The current, which is supplied by a DC power supply, is determined by measuring the potential drop across a standard 10 ohm resistor in series with the heater probe. Voltage measurements are obtained with a digital voltmeter and time measurements are obtained with a precision clock. Switches B and C are attached together so that the heater and clock will be turned on and off at exactly the same time. The two volt battery shown in Figure 7 is used to determine the resistance of the heater probe, which can be calculated from the ratio of the potential drop across the heater to the potential drop across the standard 10 ohm resistor. The procedures used to make the various measurements mentioned above will be described in detail later in this chapter.

Ultraviolet Spectrophotometer

All UV absorbance measurements used in the determination of the pK_a of thiophenol were obtained on a Beckman Acta V UV-Visible Spectrophotometer equipped with a thermally regulated cell holder (25.0 ± 0.1°C).

Melting Point Apparatus

A Mel-temp melting point apparatus was used to obtain melting points. All reported values are uncorrected.

Nuclear Magnetic Resonance Spectrometer

All n.m.r. spectra were obtained on a Varian A-60A nuclear magnetic resonance spectrometer.

Differential Scanning Calorimeter

All melting curves used for purity determinations were obtained on a Perkin-Elmer DSC-1 differential scanning calorimeter.

Weighing Balances

All sample weights were determined either with a Mettler Type H6 balance or with a Cahn Model G Ratio Electrobalance.

Computer Facilities

All computer calculations were carried out using the computer facilities at Georgia State University. A list of all programs is given in the Appendix.

Materials

All of the compounds studied in this research are listed in Table 1. The commercial source and method of purification of each compound are also given. 4-Chloropyridine and 4-bromopyridine, which are commercially available only as the hydrochloride salts, were used without further purification. All other solid compounds were purified

Table 1. Commercial Source and Method of Purification of the Organic Compounds Used in this Research

Compound Studied	Commercial Source	Method of Purification
Aniline	Aldrich	Distillation
4-Bromoaniline	Eastman	Sublimation
4-Chloroaniline	Eastman	Sublimation
4-Cyanoaniline	Aldrich	Sublimation
4-Ethoxyaniline	Aldrich	Distillation
4-Ethylaniline	Aldrich	Distillation
4-Fluoroaniline	Eastman	Distillation
4-Iodoaniline	Aldrich	Sublimation
4-Methoxyaniline	Aldrich	Sublimation
4-Methylaniline	Aldrich	Sublimation
4-Nitroaniline	Eastman	Sublimation
3-Bromoaniline	Eastman	Distillation
3-Chloroaniline	Eastman	Distillation
3-Cyanoaniline	See Text	Sublimation
3-Ethoxyaniline	Pfaltz and Bauer	Distillation
3-Ethylaniline	Aldrich	Distillation
3-Fluoroaniline	Aldrich	Distillation
3-Iodoaniline	Pfaltz and Bauer	Distillation
3-Methoxyaniline	Aldrich	Distillation
3-Methylaniline	Eastman	Distillation
3-Nitroaniline	Eastman	Sublimation
Pyridine	Aldrich	Distillation
4-Aminopyridine	Aldrich	Sublimation
4-Bromopyridine-HCl	Aldrich	None
4-Chloropyridine-HCl	Aldrich	None
4-Cyanopyridine	Aldrich	Sublimation
4-Methoxypyridine	See Text	Distillation
4-Methylpyridine	Aldrich	Distillation
3-Aminopyridine	Aldrich	Sublimation
3-Bromopyridine	Aldrich	Distillation
3-Chloropyridine	Aldrich	Distillation
3-Cyanopyridine	Aldrich	Sublimation
3-Methylpyridine	Aldrich	Distillation
Thiophenol	Eastman	Distillation

by vacuum sublimation at pressures below one mm. Purity determinations by differential scanning calorimetry[53] showed all solid samples to be at least 99.5 percent pure. The purified solid samples were stored in sealed glass ampules until they were used. Because of the tendency of some of the liquid compounds (especially the liquid anilines) to photolyze, liquid samples were vacuum distilled daily in a distillation apparatus completely wrapped with aluminum foil. Without these precautions, reproducible results could not be obtained.

3-Cyanoaniline was obtained by the reduction of 3-nitrobenzonitrile, using the method of Dyson and coworkers[54]. To five grams (0.034 moles) of 3-nitrobenzonitrile and 16 grams (0.135 g-atom) of tin, 36 ml of ice cold concentrated HCl was slowly added with stirring. The heat of reaction was sufficient to reflux the mixture, so the solution was cooled occasionally to slow down the reaction. When the reaction ceased, the solution was warmed on a steam bath for fifteen minutes. During the total reaction time of about twenty minutes, the acid-insoluble starting material went into solution and the product amine hydrochloride then precipitated out of solution. After cooling the solution to 0°C, 100 ml of ice cold 5 N NaOH was slowly added with constant stirring and cooling. When the addition of NaOH was completed, the alkaline solution was extracted four times

with diethyl ether. Evaporation of solvent from the ether extract yielded 3.12 grams (0.026 moles) of crude product (78 percent yield; M.P. = 50-53°). The crude product was then vacuum sublimed to obtain pure 3-cyanoaniline, with a melting point of 52-53°C (literature M.P. = 52°C).

4-Methoxypyridine was prepared by catalytic reduction of 4-methoxypyridine-N-oxide by the method of Katritzky and Monro[55]. After purification by vacuum sublimation, 8.87 grams (0.071 moles) of 4-methoxypyridine-N-oxide in 200 ml of dry ethanol was shaken with 0.8 grams of 5% Pd/C under hydrogen (50 p.s.i.) at room temperature for seven hours. After removal of the catalyst by filtration, the picrate derivative was prepared by adding an excess of picric acid in ethanol to the filtered reaction mixture. Upon filtration, 15.7 grams (0.046 moles) of the picrate derivative was obtained (65% yield). The product melted at 168-170° (Literature M.P. = 171-172°). The picrate derivative was dissolved in 0.01 N NaOH and extracted three times with CH_2Cl_2. The combined extracts were allowed to evaporate under a hood until only a small volume remained. This solution was then distilled (B.P. = 35° at 0.5 mm) to obtain colorless 4-methoxypyridine. The n.m.r. spectrum of the product displayed the following absorption peaks: 3.63δ, singlet (3H); 6.75δ, complex doublet (2H); 8.42δ, complex doublet (2H). This spectrum is in accord with the structure of 4-methoxypyridine.

A determination of the enthalpy of ionization or protonation of an organic acid or base generally requires the use of inorganic acids and bases. The perchloric acid and sodium hydroxide solutions used in this research were prepared from 70% w/w perchloric acid and from sodium hydroxide pellets. These solutions were standardized against tris-(hydroxymethyl)-aminomethane (THAM) and potassium hydrogen phthalate (KHP), respectively.

Procedure

Determination of Enthalpies of Ionization

Anilinium Ions and Pyridinium Ions. The enthalpies of ionization of all the anilinium ions and most of the pyridinium ions included in this research were obtained from determinations of the enthalpies of protonation of the respective conjugate bases. Calorimetric determinations were carried out in the previously described reaction vessel, which contained 1-10 mmol of the organic base and 0.241 mmol of sodium hydroxide in 1005 ml of water. The sodium hydroxide was added to insure that less than 0.1% of the sample would be protonated by the solvent. During an experiment a 5-ml sample of 5.63 N perchloric acid was introduced into the system. (A careful analysis of the enthalpies of dilution of aqueous uni-univalent electrolytes[56] reveals that the use of 5.63 N perchloric acid would minimize heat effects due to dilution of the acid.) The total enthalpy determined

for this reaction is the sum of the enthalpy of dilution of perchloric acid from 5.63 N to 0.0279 N, the enthalpy of formation of 0.241 mmol of water, and the enthalpy of protonation of the organic base. From literature data for the enthalpy of dilution of perchloric acid[56] and the enthalpy of ionization of water[57,58], the first two terms are calculated to be 0.19 and 3.17 cal, respectively. These two terms constitute the heat which would be evolved in a blank reaction. The calculated enthalpy of the blank reaction is therefore 3.36 cal.

The enthalpy of the blank reaction was determined in an experiment such as the one described above, but with no organic base in the solution. The average value obtained from several such determinations is 3.41 ± 0.06 cal, which agrees well with the calculated value, and thus establishes both the precision and the accuracy of the calorimetry system. Therefore, in each experiment, the enthalpy of protonation can be directly determined.

$$\Delta\overline{H}(\text{protonation}) = \frac{3.36 - Q(\text{reaction})}{(\text{mmol of organic base})} \qquad (7)$$

Q(reaction = total heat evolved (in calories)

For those organic bases which are too weakly basic to be completely protonated by the above method (pK_a < 3), it

was necessary to determine what fraction of the sample was protonated in each experiment. After each calorimetric determination, an aliquot of the final solution was titrated to a phenolphthalein endpoint with standard sodium hydroxide to accurately determine the concentration of perchloric acid in the solution. If the pK_a of the organic acid and the initial concentration of its conjugate base are also known, the fraction protonated (α) can be calculated.

$$\alpha = \frac{(H+A+K_a) + [(H+A+K_a)^2 - 4HA]^{\frac{1}{2}}}{2A} \qquad (8)$$

where H is the initial concentration of dilute perchloric acid, A is the initial concentration of the organic base, and K_a is the dissociation constant of the organic acid. At this low ionic strength, the ratio of the activity coefficients of H_3O^+ and AH^+ is approximately unity. (A complete derivation of the equation for α is given in the Appendix).

Since these weak organic bases ($pK_a < 3$) are not appreciably protonated by water, it was unnecessary to use sodium hydroxide in these determinations. Therefore, the enthalpy of the blank reaction in these experiments is 0.19 cal, the enthalpy of dilution of perchloric acid[56]. Once α is known, the enthalpy of protonation can be calculated directly.

$$\Delta\bar{H}(\text{protonation}) = \frac{0.19 - Q(\text{reaction})}{\alpha(\text{mmol of organic base})} \quad (9)$$

Since ionization of an organic acid is the reverse reaction of protonation of its conjugate base, the calculated enthalpies of ionization differ only in sign from the experimentally determined enthalpies of protonation. At least five calorimetric determinations were made for each compound studied. The computer program which was used to perform the necessary calculations (HEATPRO) is listed in the Appendix.

Because of the tendency of 4-chloropyridine and 4-bromopyridine to undergo self-quaternization[59], these compounds could be studied only as the commercially available hydrochloride salts. The enthalpies of ionization of 4-chloropyridinium ion and 4-bromopyridinium ion were therefore obtained by determination of the enthalpies of solution of the hydrochloride salts in dilute aqueous perchloric acid ($\Delta\bar{H}_a$) and in dilute aqueous sodium hydroxide ($\Delta\bar{H}_b$). The former reaction was carried out in the previously described reaction vessel, which contained 28.15 mmol of perchloric acid in 1005 ml of water. During an experiment, a 1-5 mmol solid sample of the hydrochloride salt was introduced into the system. The total enthalpy determined for this reaction is simply the enthalpy of solution of the hydrochloride salt ($\Delta\bar{H}_a = \Delta\bar{H}_{sol}$). The enthalpy of solution of the hydrochloride

salt in sodium hydroxide was determined in the above manner with the exception that the sample was introduced into a solution of 24.15 mmol of sodium hydroxide in 1005 ml of water. The total enthalpy determined for this reaction is the sum of the enthalpy of solution of the hydrochloride salt, the enthalpy of ionization of the substituted pyridinium ion, and the enthalpy of formation of water ($\Delta\bar{H}_b = \Delta\bar{H}_{sol} + \Delta\bar{H}_i - \Delta\bar{H}^\circ_w$). By combining $\Delta\bar{H}_a$ and $\Delta\bar{H}_b$ with the enthalpy of ionization of water ($\Delta\bar{H}^\circ_w$ = 13.34 kcal/mol)[57,58], the enthalpy of ionization of the substituted pyridinium ion may be calculated.

Thiophenol. The enthalpy of ionization of thiophenol was obtained from a determination of the enthalpy of neutralization of thiophenol. Calorimetric determinations were carried out in the previously described reaction vessel, which contained 1005 ml of water, 1-3 mmol of freshly distilled thiophenol, and 0.2815 mmol of perchloric acid which was added to prevent ionization of the thiophenol. During an experiment, a 5-ml sample of 4.83 N sodium hydroxide was introduced into the system. (The use of 4.83 N sodium hydroxide minimizes heat effects due to dilution of the base[56]). The total enthalpy determined for this reaction is the sum of the enthalpy of dilution of sodium hydroxide from 4.83 N to 0.0239 N, the enthalpy of formation of 0.2815 mmol of water, and the enthalpy of neutralization of thiophenol.

From literature data for the enthalpy of dilution of sodium hydroxide[56] and the enthalpy of ionization of water[57,58], the first two terms were calculated to be -0.23 and 3.76 cal, respectively. The enthalpy due to neutralization of thiophenol is obtained by subtracting these two terms from the total enthalpy of reaction. When the enthalpy of neutralization is combined with the enthalpy of ionization of water (13.34 kcal/mol), the enthalpy of ionization of thiophenol can be calculated.

All solutions used in these studies were prepared from boiled, nitrogen-saturated water to eliminate oxygen. Unless these precautions were taken, rapid oxidation of the thiophenoxide anion occurred, as evidenced by the formation of a white precipitate of phenyl disulfide. The CALHEAT computer program was used to calculate the enthalpy of neutralization of thiophenol from the experimental data.

Determination of the pK_a of Thiophenol

The pK_a of thiophenol was determined spectrophotometrically at the absorbance maximum of the thiophenoxide anion (37,950 cm^{-1}). The extinction coefficients of thiophenol and thiophenoxide anion were determined in 10^{-4} N hydrochloric acid and in 10^{-3} N sodium hydroxide, respectively. Absorbance measurements in a standard KH_2PO_4-Na_2HPO_4 buffer system (pH=6.86), for which the acidity function $p(a_H\gamma_{Cl})$ has been determined over a wide ionic strength

range, were used to calculate the apparent pK_a values at each ionic strength (pK_{app}) by the method of Bates and Gary[60].

$$pK_{app} = p(a_H\gamma_{Cl}) - \log\frac{(PhS^-)}{(PhSH)} + \log\frac{\gamma_{PhSH}\gamma_{Cl^-}}{\gamma_{PhS^-}} \quad (10)$$

A correction for the effect of the ionization of thiophenol on the acidity function of the buffer was applied to obtain the true pK_a values at each ionic strength[61].

$$pK_a = pK_{app} - \log\left[\frac{(HPO_4^=) + (PhSH)_t}{(HPO_4^=)}\right] \quad (11)$$

$(PhSH)_t$ = total thiophenol concentration

Operation of the Calorimetry System

The procedure for operation of the solution calorimetry system may be divided into several basic steps. Initially, the necessary solutions and samples must be prepared. After being weighed, the organic acid or base is dissolved in 1000 ml of distilled water, the temperature is adjusted to 24.8°, and the solution is quantitatively transferred to the reaction vessel. If needed, other reagents (dilute perchloric acid or sodium hydroxide solutions) may be pipetted directly into the reaction vessel. The sample which is to be introduced into the system during the calorimetric deter-

mination is pipetted into a polyethylene sample bag which has been fitted over the Teflon sample form (see Figure 4). After the sample container is connected to the stirrer shaft (see Figure 3) and the reaction vessel is secured onto the stainless steel joint, the reaction vessel is placed in a stainless steel can whose upper rim forms a water-tight seal with the container lid. The assembled apparatus is placed in a thermally regulated water bath (25.5°) and the calorimetry stirrer is activated.

Once the calorimeter is in the water bath and the external plug is connected to the external receptacle, the electrical system becomes operational. Before a calorimetric determination is begun, the resistance of the heater probe (R_h) is determined. Using the two-volt battery (see Figure 7) as a voltage source, the potential drops across the heater probe (V_h) and across a standard 10-ohm resistor (V_{10}) are determined with a digital voltmeter. Since the 10-ohm resistor is in series with the heater probe, the resistance of the heater probe is given by:

$$R_h = 10V_h/V_{10} \tag{12}$$

Since heat leaks are impossible to eliminate in a calorimetry system, calorimetric determinations are best obtained in a system whose rate of temperature change is

known. The resistance of the thermistor probe is proportional to the temperature, so resistance changes can be used to measure heat effects in the calorimetry system. By maintaining the water bath at a slightly higher temperature than the reaction vessel, the temperature of the reaction vessel will increase slowly with time. The rate of the corresponding resistance change is determined by measuring successively the time interval required for the resistance of the thermistor probe to change by one milliohm. Over a relatively short time period this drift rate is constant, so the contribution of the drift rate to the overall resistance (temperature) change that occurs during a thermal event (electrical or chemical) may be readily calculated.

The thermal events which occur during a calorimetric determination include an initial heat capacity determination, the introduction of the sample, and a final heat capacity determination. Heat capacities (in cal/ohm) are determined by electrically evolving a known amount of heat with the heater probe and measuring the resulting change in the resistance of the thermistor probe. The sample is introduced by supplying power to the sample timing motor, which, in turn, activates the sample introduction motor for a specified length of time. In order to correct the overall resistance change for the contribution of the drift rate during a thermal event, the drift rates before and after the thermal event

must be determined. Therefore, the system must be allowed to return to equilibrium between thermal events.

Switch positions (see Figure 7) for all the previously described measurements are given in Table 2. A sample set of data and a sample calculation are given in the Appendix.

Table 2. Switch Positions for Electrical Measurements and Sample Introduction in the Calorimetry System

Measurement or Operation	Switch Positions				
	A	B	C	D	E
1. Potential Drop Across Heater Probe	Down	Open	Open	Down	Down
2. Potential Drop Across 10-ohm Resistor	Down	Open	Open	Up	Down
3. Drift Rate Determination	Down	Open	Open	Up	Open
4. Heat Capacity Determination	Down	Up	Up	Up	Open
5. Sample Introduction	Down	Down	Down	Up	Open

CHAPTER III

RESULTS

Anilinium Ions and Pyridinium Ions

The enthalpies of ionization of twenty-one substituted anilinium ions and twelve substituted pyridinium ions in aqueous solution were determined calorimetrically at an ionic strength of 0.0287 M. The results of five determinations along with the average value and standard deviation for each anilinium ion are shown in Table 3. Similar results for each pyridinium ion are given in Table 4. The enthalpies of ionization of 4-chloropyridinium ion and 4-bromopyridinium ion were calculated from the enthalpies of solution of the hydrochloride salts in aqueous perchloric acid and in aqueous sodium hydroxide. The pertinent data are given in Table 5. In order to convert the experimental values to the standard state infinite dilution values, it is necessary to know the enthalpies of dilution of the perchlorate salts of the organic bases. Using the enthalpy of dilution of ammonium perchlorate (-37 cal/mol) as an estimate for the enthalpy of dilution of the organic perchlorates, and the enthalpy of dilution of perchloric acid (-54 cal/mol) at an ionic strength of 0.0287, the correction term is approximately -17 cal/mol[56] (see Calculation 3 in the Appendix). Since this

Table 3. Enthalpies of Ionization of Substituted Anilinium Ions

Substituent	$\Delta\bar{H}^{\circ}$ (kcal/mol) Run 1	Run 2	Run 3	Run 4	Run 5	Average	Lit. Values
H	7.43	7.39	7.46	7.44	7.43	7.43 ± 0.02	7.38 (36) 6.52 (39) 7.26 (40) 7.24 (62)
p-OCH_3	8.53	8.50	8.52	8.50	8.51	8.51 ± 0.01	8.34 (38) 7.57 (39) 8.21 (40)
p-OCH_2CH_3	8.56	8.62	8.57	8.48	8.44	8.53 ± 0.07	8.15 (40)
p-CH_3	7.95	7.94	7.75	7.83	7.71	7.86 ± 0.11	8.06 (36) 6.97 (39) 7.59 (40) 7.60 (42)
p-CH_2CH_3	7.75	7.73	7.79	7.70	7.72	7.74 ± 0.03	----
p-F	7.71	7.80	7.79	7.77	7.72	7.76 ± 0.04	7.45 (40)
p-Cl	6.75	6.79	6.66	6.57	6.60	6.67 ± 0.09	6.63 (38) 6.47 (39) 6.42 (40)
p-Br	6.55	6.46	6.55	6.46	6.50	6.50 ± 0.05	6.70 (38) 6.13 (39)
p-I	6.47	6.49	6.52	6.54	6.45	6.50 ± 0.04	6.55 (38) 6.05 (39)
p-CN	4.53	4.66	4.54	4.66	4.50	4.58 ± 0.08	----
p-NO_2	4.12	4.13	4.11	4.13	4.11	4.12 ± 0.01	3.42 (38) 3.11 (39)
m-OCH_3	7.12	7.09	7.10	7.12	7.13	7.11 ± 0.02	7.01 (37) 6.47 (39) 6.89 (40)
m-OCH_2CH_3	7.03	7.09	7.06	7.04	7.02	7.05 ± 0.03	6.66 (40)
m-CH_3	7.57	7.60	7.57	7.56	7.57	7.58 ± 0.02	7.47 (36) 6.51 (39) 7.37 (40) 7.37 (42)
m-CH_2CH_3	7.29	7.26	7.35	7.28	7.36	7.31 ± 0.04	----
m-F	6.57	6.58	6.61	6.56	6.50	6.56 ± 0.04	6.23 (40)
m-Cl	6.43	6.41	6.49	6.45	6.45	6.45 ± 0.03	6.27 (37) 5.63 (39) 6.31 (40)
m-Br	6.58	6.62	6.58	6.60	6.58	6.59 ± 0.02	6.25 (37) 5.55 (39)
m-I	6.76	6.80	6.75	6.74	6.84	6.78 ± 0.04	6.33 (37) 5.88 (39)
m-CN	5.71	5.80	5.75	5.65	5.79	5.74 ± 0.06	----
m-NO_2	5.37	5.40	5.44	5.37	5.30	5.37 ± 0.05	4.98 (37) 4.79 (39)

Table 4. Enthalpies of Ionization of Substituted Pyridinium Ions

Substituent	$\Delta\bar{H}^\circ$ (kcal/mol)						
	Run 1	Run 2	Run 3	Run 4	Run 5	Average	Lit. Values
H	4.76	4.86	4.87	4.76	4.77	4.80 ± 0.06	4.80 (47)
4-NH_2	11.31	11.28	11.24	11.18	11.36	11.27 ± 0.07	11.31 (44) 11.25 (46)
4-OCH_3	6.63	6.79	6.86	6.92	7.05	6.85 ± 0.16	----
4-CH_3	6.10	6.11	6.15	6.13	6.16	6.13 ± 0.03	6.02 (47) 6.10 (44)
4-Cl [a]	(ΔH_a = 3.35 ± 0.05 and ΔH_b = -6.41 ± 0.22)					3.58 ± 0.27	----
4-Br [a]	(ΔH_a = 4.39 ± 0.02 and ΔH_b = -5.44 ± 0.12)					3.51 ± 0.14	----
4-CN	1.25	1.25	1.18	1.30	1.30	1.26 ± 0.05	----
3-NH_2	6.37	6.44	6.39	6.41	6.42	6.41 ± 0.03	6.43 (44)
3-CH_3	5.86	5.86	5.83	5.90	5.90	5.87 ± 0.03	5.64 (47) 5.71 (44)
3-Cl	2.62	2.54	2.56	2.65	2.65	2.60 ± 0.05	2.11 (44)
3-Br	2.81	2.79	2.82	2.74	2.73	2.78 ± 0.04	1.35 (44)
3-CN	0.90	0.86	0.82	0.80	1.02	0.88 ± 0.09	----

[a] $\Delta\bar{H}^\circ$ values determined from the enthalpies of solution of the hydrochloride salts in aqueous perchloric acid (ΔH_a) and in aqueous sodium hydroxide (ΔH_b) in combination with the enthalpy of ionization of water (13.34 kcal/mol).

Table 5. Enthalpies of Solution of 4-Chloropyridine-HCl and 4-Bromopyridine-HCl in Aqueous Perchloric Acid and Sodium Hydroxide Solutions.

Substituent	Reaction[a]	$\Delta\overline{H}$, kcal/mol					
		Run 1	Run 2	Run 3	Run 4	Run 5	Average
4-Cl	$\Delta\overline{H}_a$	3.38	3.36	3.27	3.40	3.35	3.35 ± 0.05
4-Cl	$\Delta\overline{H}_b$	-6.16	-6.26	-6.38	-6.58	-6.69	-6.41 ± 0.22
4-Br	$\Delta\overline{H}_a$	4.41	4.39	4.37	4.39	4.40	4.39 ± 0.02
4-Br	$\Delta\overline{H}_b$	-5.29	-5.53	-5.57	-5.37	-5.46	-5.44 ± 0.12

[a] $\Delta\overline{H}_a$ is the enthalpy of solution in aqueous perchloric acid; $\Delta\overline{H}_b$ is the enthalpy of solution in aqueous sodium hydroxide.

value is within the standard deviation of the best data in Tables 3 and 4, a correction of this magnitude would be superfluous. Therefore, the average values shown in Tables 3 and 4 are the standard enthalpies of ionization of the corresponding anilinium ions and pyridinium ions with an estimated minimum uncertainty of ±50 cal/mol.

The enthalpies of ionization of substituted anilinium ions determined by other workers are included in Table 3. Both Biggs[39], in a preliminary survey, and Bolton[36-38] calculated enthalpies of ionization for several anilinium ions from pK_a-temperature dependence studies. The calorimetric data from this study agrees favorably with the work of Bolton for all compounds studied by both Biggs and Bolton, indicating that the pK_a data of Bolton should be preferred. Differences between the enthalpies of ionization from this study and from Bolton's work tend to become larger than the sum of the experimental uncertainties whenever the pK_a of the anilinium ion is less than 3.6. However, the only serious discrepancy in the data is for the p-nitroanilinium ion, for which the calorimetric value is 700 cal/mol greater than the value reported by Bolton.

Hepler[62] reported a calorimetrically determined value for the enthalpy of ionization of aqueous anilinium ion which is 200 cal/mol lower than the value obtained in this study. Unlike the value obtained in this study, Hepler's

value was derived from the difference between the enthalpy of solution of aniline into aqueous HCl and into pure water. Furthermore, both the ionic strength and sample concentration were much higher in Hepler's study. Therefore, the value obtained in this study is preferred.

In the work of van de Poel[40] on substituted anilinium ions no apparent effort was made to prevent the anilines from being slightly protonated by the solvent before the actual protonation occurred in the calorimeter. If the pK_a of an anilinium ion is greater than 4.5, a significant amount of the aniline will be protonated in aqueous solution at pH 7.0. For example, p-methoxyaniline (pK_a = 5.357) would be about two percent protonated at pH 7.0, thus causing an error of about 170 cal/mol in the enthalpy of ionization. In all likelihood, the pH of the solution was less than 7.0 due to the presence of dissolved carbon dioxide, so the error would be greater than 170 cal/mol. (In the present study, the addition of 0.241 mmol of sodium hydroxide to the solution eliminates this source of error). Since van de Poel's values are consistently 200-400 cal/mol lower than the values obtained in this study, the discrepancy is probably due to a failure to insure that initially the aniline was completely unprotonated.

The enthalpies of ionization of substituted pyridinium ions determined by other workers are included in Table 4.

The results of this research are in excellent agreement with the results recently published by Christensen and coworkers[44] for all the pyridinium ions studied by both researchers with the exception of the 3-chloro- and 3-bromopyridinium ions, for which the results of this research are much higher. However, since the pK_a's of the two acids are almost equal, and since the enthalpies of ionization of 3-chloro- and 3-bromo-substituted acids are almost identical for other acid systems[33,35,37], the results of this research (2.60 and 2.78 kcal/mol, resp.) are preferred over the results of Christensen and coworkers (2.11 and 1.35 kcal/mol, resp.).

Other than the work of Christensen and coworkers, there have been very few determinations of the enthalpies of ionization of substituted pyridinium ions. Bates and Hetzer[46] have reported a value for the enthalpy of ionization of 4-aminopyridinium ion which is in excellent agreement with the results of this research. Sacconi and coworkers[47] have determined the enthalpies of ionization of pyridinium ion and the 2-, 3-, and 4-methylpyridinium ions and have obtained results which are in good agreement with the results of this research.

Combining the pK_a data of Bolton[36-38] and other workers[40,63,64] with the calorimetrically determined enthalpies of ionization ($\Delta\bar{H}°$) from this study, the standard entropies of ionization ($\Delta\bar{S}°$) have been calculated for the

twenty-one anilinium ions included in this study. The $\Delta\bar{S}°$ values for the twelve substituted pyridinium ions were calculated from the pK_a data of Fischer and coworkers[43] and the experimentally determined $\Delta\bar{H}°$ values. The thermodynamic functions for the ionization of substituted anilinium ions and pyridinium ions are summarized in Tables 6 and 7, respectively.

A plot of $\Delta\bar{G}°$ versus $\Delta\bar{S}°$ for both acid systems is given in Figure 8. For substituted anilinium ions, a linear correlation with a slope of -900° and a correlation coefficient of 0.914 is observed. In the case of substituted pyridinium ions, the 4-aminopyridinium ion deviates markedly from the general $\Delta\bar{G}°/\Delta\bar{S}°$ correlation which is exhibited by the other substituents. If this substituent is omitted from least-squares analysis, there is a good correlation between $\Delta\bar{G}°$ and $\Delta\bar{S}°$ with a least-squares slope of -1490° and a correlation coefficient of 0.906. As predicted by electrostatic theory, substituted pyridinium ions, with a shorter proton-dipole distance than substituted anilinium ions, exhibit the more negative substituent-induced $\Delta\bar{G}°/\Delta\bar{S}°$ ratio. However, in contrast to the results reported for the ionization of phenols[33], carboxylic acids[34,35], and thiols[65], the $\Delta\bar{G}°/\Delta\bar{S}°$ ratios for both anilinium ions and pyridinium ions are much more negative than the value of -218° which is predicted by the Bjerrum electrostatic theory[1].

Table 6. Thermodynamics of Ionization of Substituted Anilinium Ions in Aqueous Solution at 25°C

Substituent	$\Delta\bar{G}°$ [a]	$\Delta\bar{H}°$ [a]	$\Delta\bar{S}°$ [a]	Reference [b]
H	6.27	7.43	3.89	36
p-OCH_3	7.31	8.51	4.02	38
p-OCH_2CH_3	7.16	8.53	4.60	40
p-CH_3	6.94	7.86	3.09	36
p-CH_2CH_3	6.82	7.74	3.09	63
p-F	6.34	7.76	4.76	40
p-Cl	5.44	6.67	4.13	38
p-Br	5.30	6.50	4.02	38
p-I	5.21	6.50	4.33	38
p-CN	2.37	4.58	7.41	64
p-NO_2	1.39	4.12	9.16	38
m-OCH_3	5.73	7.11	4.63	37
m-OCH_2CH_3	5.68	7.05	4.60	40
m-CH_3	6.43	7.58	3.86	36
m-CH_2CH_3	6.41	7.31	3.02	63
m-F	4.89	6.56	5.60	40
m-Cl	4.80	6.45	5.53	37
m-Br	4.81	6.59	5.97	37
m-I	4.89	6.78	6.34	37
m-CN	3.75	5.74	6.67	64
m-NO_2	3.35	5.37	6.78	37

[a] $\Delta\bar{G}°$ and $\Delta\bar{H}°$ values in kcal/mol; $\Delta\bar{S}°$ values in cal/deg-mol.

[b] Source of literature $\Delta\bar{G}°$ value.

Table 7. Thermodynamics of Ionization of Substituted Pyridinium Ions in Aqueous Solution at 25°C

Substituent	$\Delta\bar{G}°$ [a]	$\Delta\bar{H}°$ [a]	$\Delta\bar{S}°$ [a]
H	7.11	4.80	-7.75
4-NH_2	12.44	11.27	-3.92
4-OCH_3	8.98	6.85	-7.14
4-CH_3	8.23	6.13	-7.04
4-Cl	5.23	3.58	-5.53
4-Br	5.12	3.51	-5.40
4-CN	2.54	1.26	-4.29
3-NH_2	8.24	6.41	-6.14
3-CH_3	7.74	5.87	-6.27
3-Cl	3.83	2.60	-4.13
3-Br	3.89	2.78	-3.72
3-CN	1.84	0.88	-3.22

[a] $\Delta\bar{G}°$ and $\Delta\bar{H}°$ values in kcal/mol; $\Delta\bar{S}°$ values in cal/deg-mol.

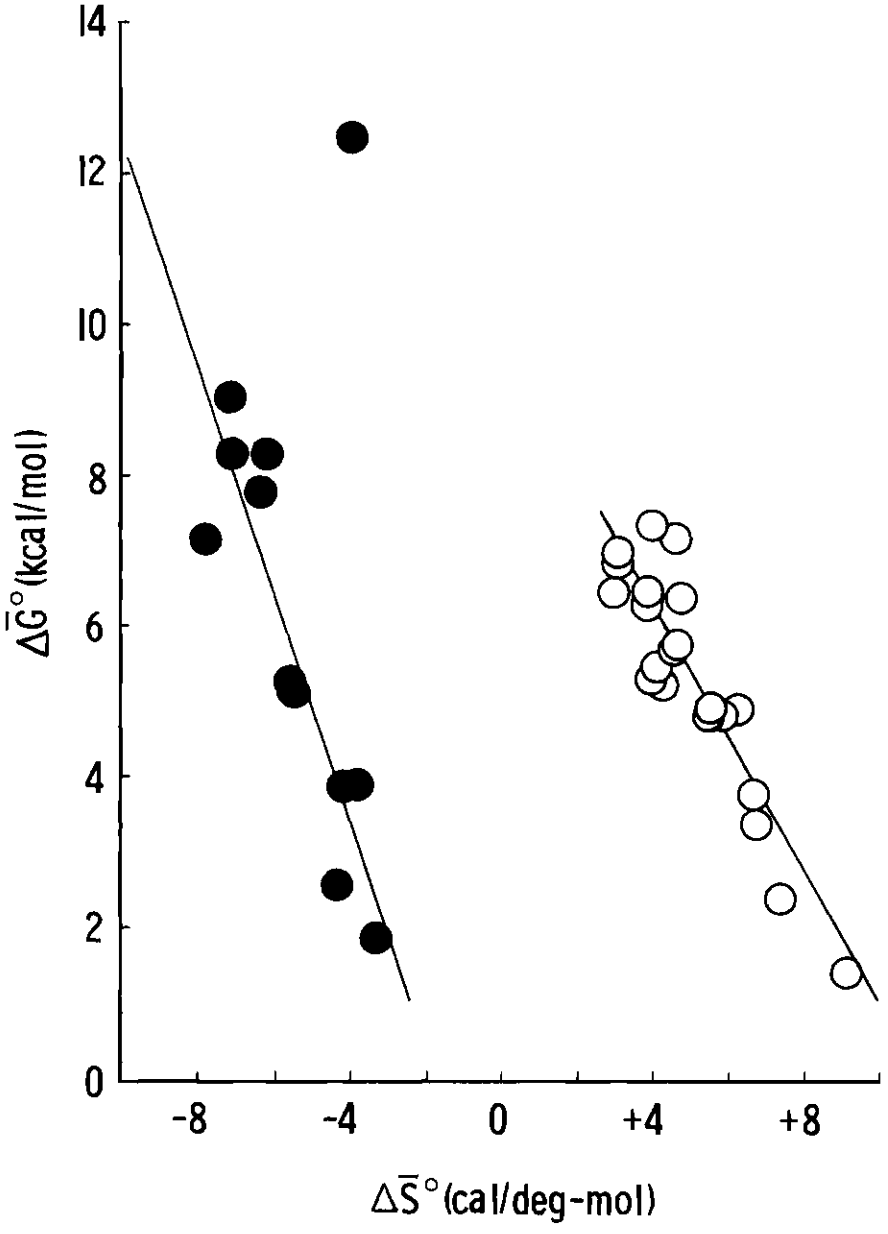

Figure 8. A Plot of $\Delta\bar{G}°$ versus $\Delta\bar{S}°$ for the Ionization of the Substituted Anilinium Ions (◯) and Pyridinium Ions (●) Included in this Study.

A plot of $\Delta\bar{G}°$ versus $\Delta\bar{H}°$ for both acid systems is given in Figure 9. The $\Delta\bar{G}°/\Delta\bar{H}°$ correlation exhibited by substituted anilinium ions is linear with a slope of 1.344 and a correlation coefficient of 0.986. Substituted pyridinium ions also show a linear correlation with a slope of 1.190 and a correlation coefficient of 0.996 (4-aminopyridinium ion has been omitted from least-squares calculations). The magnitudes of the observed $\Delta\bar{G}°/\Delta\bar{H}°$ slopes indicate that the substituent-induced Gibbs free energy changes are predominantly due to enthalpy changes in the ionization of anilinium ions and pyridinium ions (75% and 84%, respectively). On the basis of these results, it appears that both acid systems are unique not only in that substituent-induced Gibbs free energy changes are primarily due to the enthalpy rather than the entropy of ionization, but also in that the system clearly does not seem to fit simple electrostatic theory.

Thiophenol

The extinction coefficients of thiophenol ($\varepsilon_{PhSH} = 575$) and thiophenoxide anion ($\varepsilon_{PhS^-} = 13{,}130$) were determined from absorbance-concentration curves (see Table 14 in the Appendix). Once the extinction coefficients had been determined, it was possible to calculate the concentration of each species in the buffer solutions. The pK_a values at each ionic strength were then calculated using eq 10 and eq 11,

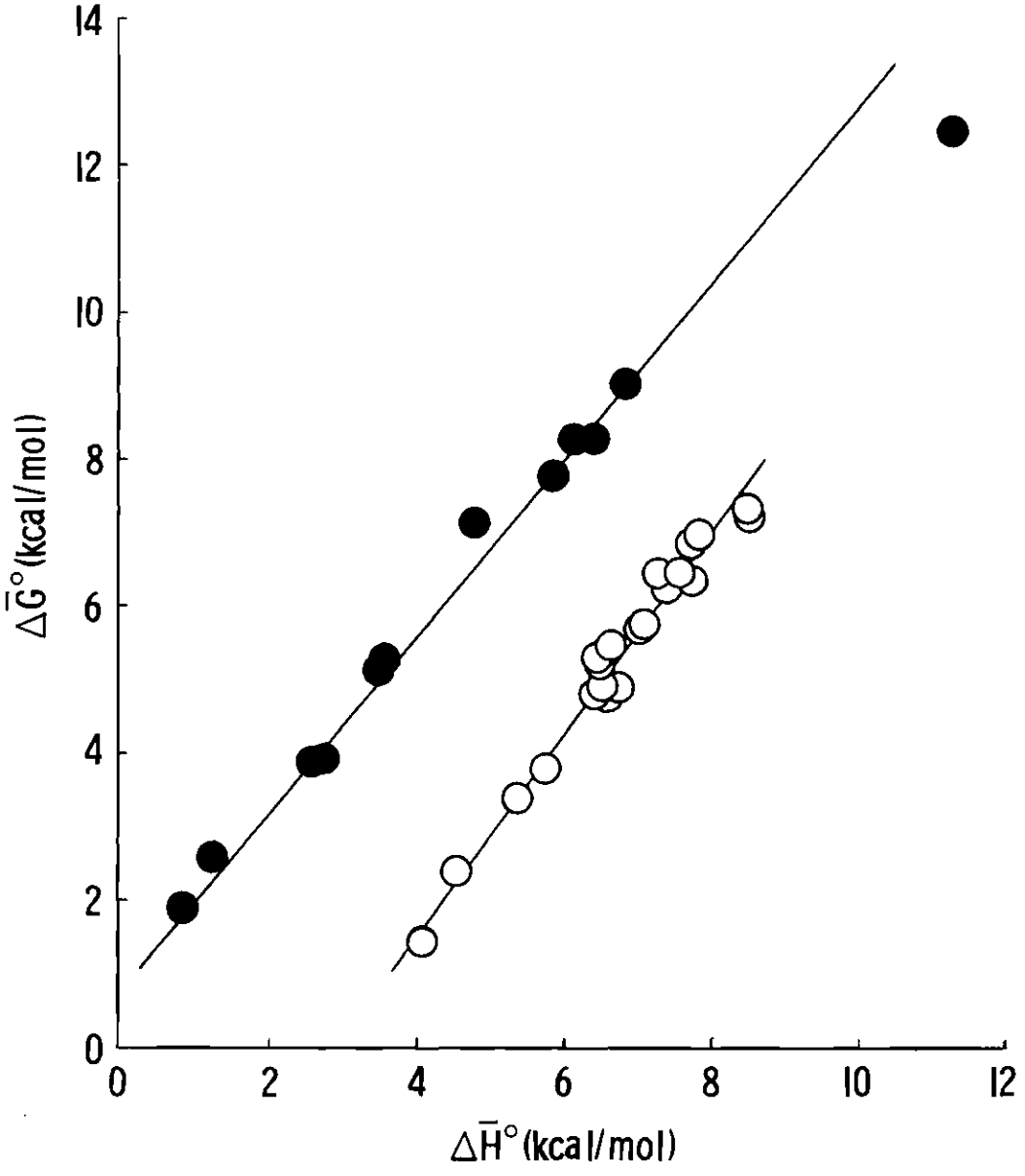

Figure 9. A Plot of $\Delta\bar{G}^\circ$ versus $\Delta\bar{H}^\circ$ for the Ionization of the Substituted Anilinium Ions (○) and Pyridinium Ions (●) Included in this Study.

neglecting the activity coefficient term in eq 10. The absorbance data and pK_a calculations are given in the Appendix.

The pK_a values determined for thiophenol at several ionic strengths are shown in Table 8. Following the procedure of Bates and Gary[60], the data were extrapolated to infinite dilution to obtain the thermodynamic pK_a value (pK_a = 6.488 ± 0.003). This value is in excellent agreement with previously reported values of 6.50[50] and 6.43[51].

The results of five determinations of the enthalpy of neutralization ($\Delta\bar{H}_n$) of thiophenol are given in Table 9. In all of the calorimetric determinations, the ionic strength was less than 0.03. At this ionic strength, the difference between the enthalpies of dilution of sodium hydroxide and sodium thiophenoxide are estimated to be negligible, so that the standard state infinite dilution value for $\Delta\bar{H}_n$ is taken to be the average of the values given in Table 9. When $\Delta\bar{H}_n^\circ$ = -9.32 kcal/mol is combined with the enthalpy of ionization of water[57,58], the standard enthalpy of ionization of thiophenol is calculated to be $\Delta\bar{H}^\circ$ = 4.02 ± 0.08 kcal/mol. Combination of $\Delta\bar{H}^\circ$ with the thermodynamic pK_a yields the standard entropy of ionization of thiophenol ($\Delta\bar{S}^\circ$ = -16.2 cal/deg-mol).

Table 8. The pK_a of Thiophenol in Aqueous Solution at 25°C

PhS^-/PhSH Ratio	Ionic Strength of Buffer	pK_a
3.8515	0.02	6.485
3.7423	0.03	6.479
3.6722	0.04	6.471
3.5706	0.05	6.470
3.4895	0.06	6.467
3.2621	0.10	6.458

pK_a (at I=0) = 6.488 ± 0.003

Table 9. Enthalpy of Neutralization of Thiophenol

mmol of PhSH	Q (corr) cal	$-\Delta\bar{H}_n$ kcal/mol
1.022	9.45	9.25
1.185	11.05	9.32
1.638	15.28	9.33
1.748	16.23	9.33
2.040	19.13	9.38

$\Delta\bar{H}_n$ (avg) = -9.32 ± 0.05

CHAPTER IV

DISCUSSION

Anilinium Ions

Comparison of Anilinium Ions with Primary Ammonium Ions

Protonated primary amines provide a system for which the ionization process is expected to be quite similar to that for anilinium ions. However, in an analysis of the thermodynamics of ionization of a large number of protonated primary amines, Christensen and coworkers have reported that the correlation between $\Delta\bar{G}°$ and $\Delta\bar{S}°$ is rather poor for primary ammonium ions[41], with a least-squares slope of -41.7°. This value is vastly different from both the slope predicted by electrostatic theory and the slope for anilinium ions which was obtained in this study. Included in this analysis are a number of compounds which are known to exist as zwitterions in aqueous solution. If these compounds are deleted from Christensen's data, the resulting plot of $\Delta\bar{G}°$ versus $\Delta\bar{S}°$ for twenty-five primary ammonium ions has a least-squares slope of -439°. Although the correlation coefficient of 0.734 is still rather poor, this slope is much closer to the value predicted from simple electrostatic theory. Furthermore, a plot of $\Delta\bar{G}°$ versus $\Delta\bar{H}°$ for the same primary ammonium ions has a slope of 1.217 and a correlation coefficient of

0.872. This slope is very close to the value of 1.344 found for anilinium ions, which indicates that the two ionization processes are indeed similar. The lack of a good correlation between $\Delta\bar{G}°$ and $\Delta\bar{S}°$ in primary ammonium ions indicates that the phenomena responsible for changes in $\Delta\bar{S}°$ are not simply electrostatic, but are rather a combination of specific solvation and electrostatic effects[41].

Hepler's Theory of Substituent Effects

For symmetrical proton transfer reactions such as eq 1, Hepler[48,49] has proposed that the overall effect of a dipolar substituent may be divided into internal and external contributions. Based on the assumptions that (a) the external contributions to the enthalpy and entropy changes are related by a constant β, and (b) the internal contribution to the entropy is negligible, the following results are obtained:

$$\Delta\bar{G}°_t = \Delta\bar{H}_{int} + (\beta - T)\Delta\bar{S}°_t \qquad (13)$$

$$\Delta\bar{H}°_t = \Delta\bar{H}_{int} + \beta\Delta\bar{S}°_t \qquad (14)$$

where $\Delta\bar{G}°_t$, $\Delta\bar{H}°_t$, and $\Delta\bar{S}°_t$ are the thermodynamic functions of the proton transfer reaction (these values represent the substituent-induced changes in the thermodynamic functions for the acid ionization process).

In order to calculate $\Delta\bar{H}_{int}$ from the measured thermodynamic data, it is necessary to determine a value for β, which Hepler has assigned a value of 280°. Since the assumed value of β is very close to T(298°), it follows that $\Delta\bar{G}^{\circ}_{t} \simeq \Delta\bar{H}_{int}$. Values of $\Delta\bar{H}_{int}$ calculated in this fashion have been found to correlate well with Hammett σ or Taft σ^{*} parameters[38]. Based on the assumption that two different reaction series which show proportional $\Delta\bar{G}^{\circ}_{t}$ values should also show proportional $\Delta\bar{H}_{int}$ values, Bolton and Hall have proposed a general method for the calculation of β values[38]. From eq 14, it can be shown that

$$\Delta\bar{H}^{\circ}_{A} = \theta\Delta\bar{H}^{\circ}_{B} - \theta\beta_{B}\Delta\bar{S}^{\circ}_{B} + \beta_{A}\Delta\bar{S}^{\circ}_{A} \qquad (15)$$

where $\Delta\bar{H}^{\circ}$ and $\Delta\bar{S}^{\circ}$ are the standard substituent-induced enthalpy and entropy changes for reactions series A and B, θ is the ratio of the internal enthalpy changes for series A and B, and β_{A} and β_{B} are the respective Hepler proportionality constants mentioned above. Using the anilinium ion data reported in this study for reaction series A and the thermodynamic data on *m*- and *p*-substituted phenols reported in the recent literature[33] as reaction series B, the parameters θ, β_{A}, and β_{B} were calculated by a multiple parameter least-squares regression method. The calculated values are θ = 2.46 ± 0.15, β_{A} = 640 ± 69° and β_{B} = 190 ± 39°. Bolton and

Hall have reported the following values for these two systems: $\theta = 1.63 \pm 0.17$, $\beta_A = 413 \pm 146°$, and $\beta_B = 240 \pm 17°$. Their calculations, however, were based upon only eleven substituents. The β_B value derived from this study is approximately the same as that of Bolton, whereas the β_A and θ values are substantially different, indicating that this treatment is extremely sensitive to slight changes in the anilinium ion data. Furthermore, because of the small entropy changes associated with the ionization of anilinium ions, the value of β_A used to calculate $\Delta\bar{H}_{int}$ is not very important. Bolton and Hall, using $\beta_A = 413°$ to calculate $\Delta\bar{H}_{int}$, have reported that a plot of $\Delta\bar{H}_{int}$ versus σ for twelve anilinium ions has a slope of -4053 and a correlation coefficient of 0.9969. Using the value of $\beta_A = 640°$ obtained in this study, a plot of the resulting $\Delta\bar{H}_{int}$ values versus σ for twenty anilinium ions has a slope of -5051 and a correlation coefficient of 0.9931.

An interesting result of this treatment is the observed difference between θ and the ratio of the Hammett ρ-values for the reaction series A and B. The former represents the ratio of the substituent-induced internal enthalpy changes (eq 16) while the latter represents the ratio of the respective substituent-induced Gibbs free energy changes in aqueous solution (eq 17).

$$\theta = \frac{(\Delta\overline{H}_{int})_A}{(\Delta\overline{H}_{int})_B} = 2.46 \qquad (16)$$

$$\frac{\rho_A}{\rho_B} = \frac{\Delta\overline{G}^\circ_A\ (aq)}{\Delta\overline{G}^\circ_B\ (aq)} = 1.3 \qquad (17)$$

According to Hepler's theory, θ also represents the ratio of the respective substituent-induced Gibbs free energy changes in the gas phase for reaction series A and B. From this analysis, anilinium ions show a greater susceptibility to substituent effects relative to phenols in the gas phase than in the aqueous phase. While Gibbs free energy changes in aqueous solution result from both enthalpy and entropy changes, Gibbs free energy changes in the gas phase are almost completely due to internal enthalpy changes and are therefore a direct measure of substituent-induced changes in the relative inherent stabilities of the acid and its conjugate base. If both an acid and its conjugate base are stabilized relative to a reference acid by a substituent, the overall effect of that substituent is minimized; however, if an acid is destabilized while its conjugate base is stabilized, or vice versa, the effect of the substituent is maximized. Since anilinium ions exemplify the latter case, gas phase Gibbs free energies of ionization should show larger substituent effects for anilinium ions than for phenols.

Free Energy-Entropy Correlations

If it is assumed that the Gibbs free energy changes for proton transfer reactions such as eq 1 may be divided into a temperature-independent non-electrostatic term and a temperature-dependent electrostatic term, it may be shown that,

$$\Delta\bar{G}^{\circ}_{t}/\Delta\bar{S}^{\circ}_{t} = \left[1 + \frac{\Delta\bar{G}_{non\text{-}el}}{\Delta\bar{G}_{el}}\right] (\partial \ln D/\partial T)^{-1} \qquad (18)$$

where $\mathcal{D}$ is the dielectric constant of the pure solvent if the Bjerrum electrostatic model is employed[1] or the "effective" dielectric constant if the Kirkwood-Westheimer cavity model is used[4-8]. In aqueous solution, the Bjerrum model predicts a value of approximately -218° for $(\partial \ln D/\partial T)^{-1}$ whereas the Kirkwood-Westheimer approach predicts a more negative value since the latter model takes into account the polarizable molecular framework as well as the bulk solvent in calculating the effect of the medium on the work required to remove the proton from the acid.

It is generally assumed that the non-electrostatic contribution to the Gibbs free energy change is negligible in symmetrical proton transfer processes[1], so the ratio of $\Delta\bar{G}^{\circ}_{t}$ to $\Delta\bar{S}^{\circ}_{t}$ should equal $(\partial \ln D/\partial T)^{-1}$. While benzoic acids, $[(\Delta\bar{G}^{\circ}_{t}/\Delta\bar{S}^{\circ}_{t}) = -205°]$[35] and, to a lesser extent, phenols

$[\Delta\bar{G}^{\circ}_t/\Delta\bar{S}^{\circ}_t) = -350°]$[33] appear to be in agreement with the predictions of simple electrostatic theory, anilinium ions $[\Delta\bar{G}^{\circ}_t/\Delta\bar{S}^{\circ}_t) = -900°]$ exhibit a marked deviation from the theoretical predictions.

To determine whether the experimental $\Delta\bar{G}^{\circ}_t/\Delta\bar{S}^{\circ}_t$ ratios of substituted anilinium ions could be explained by the Kirkwood-Westheimer approach, $(\partial \ln D_{eff}/\partial T)^{-1}$ values have been calculated for a variety of *p*-substituted anilinium ions, employing both spherical and oblate ellipsoidal cavities. The cavity volume of a particular *p*-substituted anilinium ion was determined from the partial molal volume of *p*-nitroaniline (95.0 ml/mol)[66] in combination with Traube's rule for the various substituents[67]. The focal radii were calculated from literature bond lengths[68]. The "effective" dielectric constants were calculated by means of the equations developed by Kirkwood and Westheimer[4-7] for the spherical cavity and by Sarmousakis[8] for the oblate ellipsoidal cavity. These equations are of the general form:

$$1/D_{eff} = f_1/D_{H_2O} + f_2/D_{int} \qquad (19)$$

where $\mathcal{D}_{H_2O}$ is the dielectric constant of water (78.36 at 25°)[10], $\mathcal{D}_{int}$ is the temperature-independent dielectric constant of the molecular cavity (usually set equal to 2.0), and f_1 and f_2 are constants which depend on the size and shape

of the molecular cavity. Differentiation and subsequent rearrangement of eq 19 yields

$$(\partial \ln D_{eff}/\partial T)^{-1} = \frac{D_{H_2O}(\partial \ln D_{H_2O}/\partial T)^{-1}}{(f_1)D_{eff}} \quad . \qquad (20)$$

These calculations are more extensively discussed in the Appendix.

From the experimental data for substituted anilinium ions, $\Delta\bar{G}_t^\circ/\Delta\bar{S}_t^\circ$ values were calculated for the proton transfer reaction. A comparison of these values with the calculated $(\partial \ln D_{eff}/\partial T)^{-1}$ values is given in Table 10. Although the $(\partial \ln D_{eff}/\partial T)^{-1}$ values are extremely sensitive to the location of the point dipole, both the spherical and oblate ellipsoidal cavity models yield results which are in reasonably good agreement with the $\Delta\bar{G}_t^\circ/\Delta\bar{S}_t^\circ$ values.

Since phenols, benzoic acids, and anilinium ions may be expected to occupy cavities of similar size and shape in aqueous solution, the results predicted by Kirkwood-Westheimer theory are about the same for all three acid systems. While anilinium ions are in accord with the predictions of Kirkwood-Westheimer theory, phenols and benzoic acids deviate markedly and are actually in better agreement with the predictions of simple electrostatic theory.

From a theoretical point of view, there are several

Table 10. Kirkwood-Westheimer Treatment of Substituted Anilinium Ions

Substituent [a]	$(\Delta\bar{G}^{\circ}_t/\Delta\bar{S}^{\circ}_t)$	$(\partial \ln D_{eff}/\partial T)^{-1}$	
	Experimental	Spherical	Ellipsoidal
p-CH_3 (min)	- 838°	-2317°	-2453°
p-CH_3 (max)	- 838	- 987	-1308
p-Cl	-3458	-2145	-2280
p-Br	-7462	-2165	-2291
p-I	-2409	-2039	-2179
p-CN (min)	-1108	-1301	-1525
p-CN (max)	-1108	- 358	- 808
p-NO_2 (min)	- 926	-1923	-2070
p-NO_2 (max)	- 926	- 822	-1149

[a] In polyatomic substituents (Ø-X-Y) such as p-CH_3, p-CN, and p-NO_2, the point dipole is located either at one-half of the maximum extension of the group as projected on the C-X bond axis (min) or in the middle of the X-Y bond (max).

possible explanations for the anomalous behavior of phenols and benzoic acids. The molecular cavity model of Kirkwood and Westheimer is based on the assumption that no significant interaction occurs between the cavity and adjacent solvent molecules which might distort the solvent continuum in that region. When the proton transfer occurs between uncharged molecular cavities, as in the case of anilinium ions, this assumption is fairly good. However, when the cavities are charged, it is reasonable to assume that solvation of the charged species will result in extensive alteration of the structure of the solvent near the cavity, thus forming a region of solvent whose dielectric constant will be less than that of the bulk solvent. In fact, the dielectric constant of the primary solvation layer around a monovalent ion may be as small as 2.0 in aqueous solution[69]. It is interesting to note that the Tanford modification[9] of Kirkwood-Westheimer theory, in which the radius of the cavity is increased by 1.5Å for dipolar substituents, has proven to be quite useful in the prediction of $\Delta\bar{G}_t^\circ$ values for a variety of neutral organic acids[22-25]; however, this method is even worse than the unmodified theory in the prediction of $\Delta\bar{G}_t^\circ/\Delta\bar{S}_t^\circ$ ratios for phenols and benzoic acids. The radius adjustment has the net effect of increasing the size of the molecular cavity to include a region of solvent whose dielectric constant is approximately the same as that of the molecular cavity.

While this model successfully predicts $\Delta\bar{G}_t^\circ$ values, the differentiation of $\Delta\bar{G}_t^\circ$ with respect to temperature to obtain $\Delta\bar{S}_t^\circ$ does not adequately account for the loss of entropy resulting from ion-induced structure around the molecular cavity, because the primary solvation layer is assumed to be part of the molecular cavity whose dielectric constant is temperature-independent.

While the above explanation appears to be quite reasonable, other alternative explanations of the behavior of these acid systems must be considered. When a proton is removed from an anilinium ion, the cavity containing the conjugate base is uncharged, so the work of proton transfer is totally determined by the magnitude of the difference of the dipole moments of the neutral anilines. Since charge-dipole forces decrease with the inverse square of the charge-dipole separation, most of the work of proton transfer will be expended while the proton is close to the molecular cavity. This system is adequately represented by the Kirkwood-Westheimer model, and thus the predicted $\Delta\bar{G}_t^\circ/\Delta\bar{S}_t^\circ$ ratios agree quite well with the experimental values for substituted anilinium ions.

On the other hand, in the ionization of phenols and benzoic acids, the conjugate base which occupies the cavity bears a unit negative charge which is primarily localized at the reaction center ($-O^-$, $-COO^-$). If the charges are

localized, the work of proton transfer would simply depend on the magnitude of the substituent dipoles. However, if, as suggested by molecular orbital theory, the charge may be delocalized by resonance interactions between the substituent and the reaction center, there could be an incomplete cancellation of charge-charge interactions during the proton transfer reaction. This additional charge-charge interaction, which is inversely related to the proton-charge separation, would result in a larger percentage of the overall electrostatic interaction occurring through the bulk solvent. Therefore, the increased role of the solvent in the ionization of phenols and benzoic acids would cause the $\Delta\bar{G}^{\circ}_{t}/\Delta\bar{S}^{\circ}_{t}$ ratios to approach that of simple electrostatic theory. (Note: This anilinium ion study has recently been published in the Journal of the American Chemical Society[70]).

Pyridinium Ions

Hepler's Theory of Substituent Effects

On the basis of the results obtained in the comparison of the thermodynamics of ionization of anilinium ions and phenols, it appears likely that β values may vary from one reaction to another and might be quite different from the value of 280° suggested by Hepler[48,49]. However, since the calculated β values were based on the assumption that acid systems which show proportional $\Delta\bar{G}^{\circ}_{t}$ values should also exhibit proportional $\Delta\bar{H}_{int}$ values, and since there was con-

siderable uncertainty in the derived β values, it would be quite desirable to directly calculate β values from experimental data without the application of possibly invalid assumptions.

Since ΔH_{int} is actually the gas phase enthalpy of proton transfer, a knowledge of the relative gas phase enthalpies of ionization of acid systems which have also been studied in aqueous solution would provide the necessary experimental data for direct calculation of β values. Recently, Taft and coworkers determined the relative gas phase proton affinities of several 4-substituted pyridines[71]. These researchers reported that a plot of the relative gas phase enthalpies of ionization versus the relative aqueous Gibbs free energies of ionization was linear with a slope of 3.5 ± 0.5, indicating the $\Delta\bar{H}_{int}$ values are much larger than $\Delta\bar{G}^{\circ}_{t}$ values for substituted pyridinium ions. Thus, if the primary assumptions of Hepler's theory are valid, a β value substantially larger than 280° must be employed in this acid system. By rearranging eq 13, the following expression for β is obtained:

$$\beta = T + \frac{\Delta\bar{G}^{\circ}_{t} - \Delta\bar{H}_{int}}{\Delta\bar{S}^{\circ}_{t}} \qquad (21)$$

Combining $\Delta\bar{H}_{int} = 3.5\Delta\bar{G}^{\circ}_{t}$ from the results of Taft and co-

workers with $\Delta\bar{G}^{\circ}_{t}/\Delta\bar{S}^{\circ}_{t}$ = -1490° from this research, a value of β = 4023 ± 745° is obtained. This β value is far greater than the value employed in Hepler's theory and strongly supports the contention that β values vary from one acid system to another.

4-Aminopyridinium Ion

In the previous discussion of Figures 8 and 9, it was noted that the 4-aminopyridinium ion deviates markedly from the general $\Delta\bar{G}^{\circ}/\Delta\bar{S}^{\circ}$ and $\Delta\bar{G}^{\circ}/\Delta\bar{H}^{\circ}$ correlations exhibited by the other substituents. The possibility that this deviation might result from protonation of the amino group is excluded by prior studies which have clearly shown that mono-protonation of 4-aminopyridine (I) occurs on the ring nitrogen rather than on the amino group[72,73]. Furthermore, while the mono-protonated species (II) is only weakly acidic (pK_a = 9.12), the diprotonated species (IV), for which the reported pK_a value is -6.3, can only be obtained in strongly acidic solutions[74]. All of these observations indicate that the monoprotonated species is unusually stable and that this

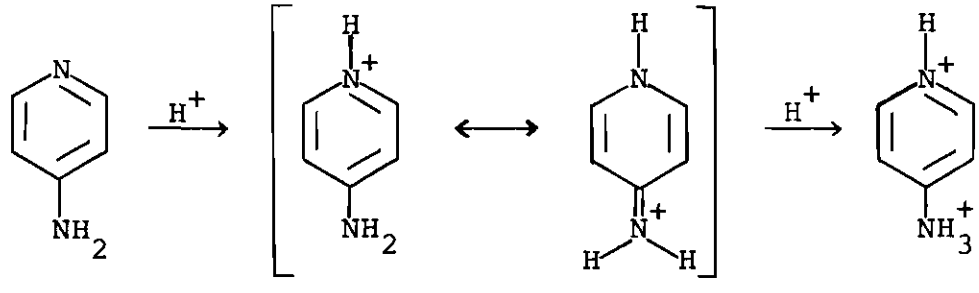

(I) (II) (III) (IV)

stability is destroyed by diprotonation. A substantial resonance contribution by structures such as (III) is in accord with these observations.

The entropy of ionization of the 4-aminopyridinium ion is approximately six cal/deg-mol more positive than predicted by the $\Delta\bar{G}°/\Delta\bar{S}°$ correlation shown in Figure 8. To account for such a deviation, either the absolute entropy of the conjugate base must be unusually large or the entropy of the 4-aminopyridinium ion must be unusually small. While the former possibility cannot be completely discounted, it appears more likely that solute-solvent interactions involving the 4-aminopyridinium ion are the predominant source of the anomalous entropy effects observed for the ionization of this acid. A substantial resonance contribution by structures such as (III) will create a barrier to free rotation around the C-N bond of the amino group which could decrease the entropy of the 4-aminopyridinium ion by as much as three cal/deg-mol[75]. In addition, charge delocalization will result in decreased polarization of the solvent and in increased hydrogen-bonding capacity of the amino group. While the former effect may increase the entropy of the ion-solvent system[33], a decrease in entropy will result from increased hydrogen-bonding interactions. Since the maximum contribution due to hindered rotation is insufficient to account for the overall $\Delta\bar{S}°$ deviation, the net effect of the solute-solvent

interactions apparently results in decreased entropy of the ion-solvent system. Thus the decrease in entropy due to hydrogen-bonding interactions must be greater than the positive entropy effects resulting from decreased polarization of the solvent. Further analysis of the relative importance of these effects awaits the availability of thermodynamic data for the ionization of this acid in the gas phase and in other solvents.

The enthalpy of ionization of the 4-aminopyridinium ion is approximately 1.6 kcal/mol more endothermic than predicted by the $\Delta\overline{G}°/\Delta\overline{H}°$ correlation shown in Figure 9. In view of the previous discussion, it is clear that the unusually positive entropy of ionization of this acid would cause a decrease in $\Delta\overline{G}°$ relative to other substituted pyridinium ions, thus leading to the observed deviation.

Entropy Analysis

In addition to the anomalous behavior of the 4-aminopyridinium ion, pyridinium ion itself deviates from the $\Delta\overline{G}°/\Delta\overline{S}°$ correlation exhibited by the other substituents. In fact, $\Delta\overline{S}°$ is more negative for pyridinium ion than for any of the substituted pyridinium ions, including those with electron-donating substituents. Although experimental proof is lacking, it appears likely that theoretical justification for this anomaly may lie in the relatively large increase in molecular cavity volume which occurs when a substituent is

placed on the pyridine ring. For example, when the partial molal volume of pyridine[76] is combined with Traube's Rule for the substituents[67], the molecular cavity volumes of the substituted pyridines used in this study are predicted to be 13-21 percent larger than the molecular cavity volume of pyridine. Because the charge is somewhat delocalized over the entire molecular cavity in pyridinium ions[77], all solvent molecules around the molecular cavity feel the electrostatic influence of the positive charge. Since a smaller molecular cavity will be in contact with fewer solvent molecules, the entropy of the ion-solvent system will be enhanced for pyridinium ion itself relative to the substituted pyridinium ions. Consequently, $\Delta\bar{S}°$ should be more negative for pyridinium ion than for any of the substituted pyridinium ions.

Another unusual and highly significant result which emerges from the entropy analysis for this acid system concerns the relative magnitudes of the absolute entropies of pyridines and pyridinium ions in aqueous solution. Assuming the entropy of the hydrogen ion to be -5.5 cal/deg-mol in aqueous solution[78], it can be shown that, whenever $\Delta\bar{S}°$ is more negative than -5.5 cal/deg-mol, the entropy of a pyridinium ion must be greater than the entropy of the corresponding pyridine. This effect is observed only for pyridinium ions with electron-donating substituents and for the unsubstituted compound. Such results would seem to indicate that a sub-

stantial amount of hydrophobic water structure may exist around the molecular cavity of the conjugate base, and that the resulting decrease in entropy of the solute-solvent system is of the same order of magnitude as the entropy loss due to solvation of the charged species. A variation of the latter term with the electrical nature of the substituent could thus account for the observed results.

In the previous analysis of anilinium ions, it was found that the experimental $\Delta\bar{G}^\circ_t/\Delta\bar{S}^\circ_t$ ratios of 4-substituted anilinium ions were in good agreement with the values predicted by Kirkwood-Westheimer electrostatic theory. A similar analysis for 4-substituted pyridinium ions predicts that the substituent-induced $\Delta\bar{G}^\circ_t/\Delta\bar{S}^\circ_t$ ratios should be approximately 1.5 times more negative for pyridinium ions than for anilinium ions. This value is in excellent agreement with the value of 1.66 which is derived from the slopes of the respective $\Delta\bar{G}^\circ/\Delta\bar{S}^\circ$ plots shown in Figure 8. This analysis indicates that Kirkwood-Westheimer electrostatic theory correctly predicts the relative magnitude of substituent effects in the ionization of substituted pyridinium ions and anilinium ions.

Thiophenol

Gas Phase versus Aqueous $\Delta\bar{G}^\circ_t$

A comparison of the thermodynamics of ionization of thiophenol and phenol is given in Table 11. Included are

Table 11. Comparison of the Thermodynamics of Ionization of Thiophenol and Phenol in Aqueous Solution and in the Gas Phase at 25°C [a]

	$\Delta\bar{G}°$	$\Delta\bar{H}°$	$\Delta\bar{S}°$	$\Delta\bar{V}°$
PhSH	8.85	4.02	-16.2	-12.76 [c]
PhOH	13.60 [b]	5.48 [b]	-27.2 [b]	-18.01 [c]
eq 6 (aq)	-4.75	-1.46	11.0	5.25
eq 6 (g)	-30.53	-31.14	-2.05	- - -

[a] $\Delta\bar{G}°$ and $\Delta\bar{H}°$ values in kcal/mol; $\Delta\bar{S}°$ values in cal/deg-mol; $\Delta\bar{V}°$ values in ml/mol.

[b] Ref. 33

[c] Ref. 66

the $\Delta\bar{G}°$, $\Delta\bar{H}°$, and $\Delta\bar{S}°$ values for thiophenol (from this study) and for phenol[33], and the partial molal volumes of ionization ($\Delta\bar{V}°$) for thiophenol and phenol[66]. The thermodynamic functions $\Delta\bar{G}°_t$, $\Delta\bar{H}°_t$, $\Delta\bar{S}°_t$, and $\Delta\bar{V}°_t$ for the proton transfer reaction given in eq 6 are also included.

To illustrate the important role of the solvent in acid-base equilibria, a comparison has been made between the thermodynamics of the proton transfer reaction in the gas phase and in aqueous solution. Recently Taft, et al.[71], have shown that the relative gas phase proton affinities of several substituted pyridines are in reasonable agreement with the values calculated by the CNDO/2 method of Pople[79]. Therefore, it has been assumed that a reliable estimate of $\Delta\bar{E}_t$(g, O°K) could be obtained from the semi-empirical calculations. The stabilities of each species in eq 6, calculated by Henneike[80], have been combined to yield an estimate for $\Delta\bar{E}_t$(g, O°K) = -31.1 kcal/mol. This result is only twenty percent larger than the value of -37.7 kcal/mol predicted from the bond dissociation energies of SH and OH[81] and the electron affinities of oxygen and sulfur[82]. When the CNDO/2 results are combined with the molecular parameters and spectroscopic data for each species, the standard Gibbs free energy change at 298°K is determined by standard statistical mechanical methods to be -30.5 kcal/mol (see Calculation 10 in the Appendix). When the reaction is transferred

to the aqueous phase, the magnitude of $\Delta\bar{G}_t^\circ$ is decreased by a factor of 6.7. In the proton transfer reaction for substituted pyridinium ions, an attenuation factor of 3.5 is observed[71]. These results emphasize the important role of the solvent in acid-base equilibria.

Volume Analysis

The volume change for the proton transfer reaction ($\Delta\bar{V}_t^\circ$) can be expressed as a sum of (1) the volume change due to the introduction of a solute molecule into the solvent, assuming the solute and the solvent are hard spheres ($\Delta\bar{V}_{int}$), and (2) the volume change attributed to solute-solvent interactions ($\Delta\bar{V}_{ext}$). The magnitude of $\Delta\bar{V}_{int}$ may be estimated by at least two methods, both of which require the calculation of the van der Waals volume of each of the species in eq 6. The calculated $\Delta\bar{V}_{int}$ values can be combined with the experimental $\Delta\bar{V}_t^\circ$ to provide an estimate of $\Delta\bar{V}_{ext}$ which can then be compared with the predictions of solution theories.

Calculation of $\Delta\bar{V}_{int}$ from van der Waals Volumes. When two atoms, A and B, combine to form AB, the volume of AB is given by

$$\bar{V}_w(AB) = \bar{V}_w(A) + \bar{V}_w(B) - \delta\bar{V}_a - \delta\bar{V}_b \qquad (22)$$

where $\bar{V}_w(A)$ and $\bar{V}_w(B)$ are the van der Waals volumes of A and

β, and $\delta\bar{V}_a$ and $\delta\bar{V}_b$ are the overlapping volume increments, which can be calculated from a knowledge of the van der Waals radii of A and B and the A-B bond length[83]. Using eq 22 and $\bar{V}_w(C_6H_6)$ = 48.36 ml/mol, the van der Waals volume of the phenyl group is found to be $\bar{V}_w(C_6H_5)$ = 47.22 ml/mol. To calculate $\bar{V}_w$(PhOH) and $\bar{V}_w$(PhSH), the van der Waals radii of Bondi[83] and the C-O, O-H, C-S, and S-H bond lengths of methanol and methanethiol were used[68]. In the calculation of $\bar{V}_w(PhO^-)$ and $\bar{V}_w(PhS^-)$, the crystallographic radii of O^- and S^- were employed[84] with the assumption that the $C-O^-$ and $C-S^-$ bond lengths were the same as those in the neutral molecules. The resulting van der Waals volumes are 59.51, 53.52, 67.50, and 55.42 ml/mol for PhSH, PhOH, PhS^-, and PhO^-, respectively. (A detailed calculation of these van der Waals volumes is given in the Appendix). From these volumes, $\Delta\bar{V}_{int}$ is estimated to be +6.09 ml/mol.

Calculation of $\Delta\bar{V}_{int}$ from Cavity Volumes. The $\Delta\bar{V}_{int}$ calculated in the above manner represents the actual change in volume due to the inherent differences in the size of the molecules. Even if there is perfect packing in a solution, there exists a certain quantity of void volume around the solute. Therefore, the $\Delta\bar{V}_{int}$ calculated from the van der Waals volumes assumes that the void volumes cancel for eq 6. An alternate approach is to estimate the cavity volume, $\bar{V}_c$, occupied by each species in eq 6. Reiss, et. al.[85,86], have

derived an expression for the Gibbs free energy of cavity formation accompanying the introduction of a hard sphere into a fluid comprised of hard spheres. This approach has been employed by Pierotti[87,88] to provide reasonable estimates of the thermodynamic parameters for the dissolution of gases into several solvents, including water. Although water is far from being a hard sphere liquid, a favorable comparison between the experimental and calculated values was obtained, probably because the macroscopic parameters of the liquid are an integral part of the calculations. Using Pierotti's method, the molecular cavity volumes, $\bar{V}_c$, are calculated to be 101.27, 92.68, 112.59, and 95.42 ml/mol for thiophenol, phenol, thiophenoxide, and phenoxide, respectively (see Calculation 7 in the Appendix). A value of 8.58 ml/mol is derived for $\Delta\bar{V}_{int}$ by this method. The result is somewhat higher than the value obtained from the van der Waals volumes, indicating that the void volumes may be an important consideration in the calculation of $\Delta\bar{V}_{int}$.

Calculation of $\Delta\bar{V}_{ext}$ from van der Waals Volumes. The estimation of $\Delta\bar{V}_{ext}$ can be divided into two parts: (a) the interaction of the neutral species with the solvent and (b) the electrostriction of the solvent by the anions. At the present time a convenient and reliable method does not exist for calculating the volume change associated with solute-solvent interactions of the neutral species. In

contrast, several methods are available for the estimation of the volume change accompanying the introduction of a charge on the solute.

King[89] has suggested that the partial molal volume of a solute species may be expressed as a combination of at least three contributing factors.

$$\bar{V}° = \bar{V}_w + \bar{V}_v + \bar{V}_{ext} \qquad (23)$$

where $\bar{V}_w$ is the van der Waals volume, $\bar{V}_v$ is the volume of empty space around the solute molecule in solution, and $\bar{V}_{ext}$ is the volume change resulting from solute-solvent interactions. Using the partial molal volumes of thiophenol, phenol, thiophenoxide, and phenoxide (94.09, 86.23, 86.73, and 73.62 ml/mol, respectively)[66], an estimate of the external contribution to the total volume change can be obtained from the difference between $\bar{V}°$ and $\bar{V}_w$ for each of the solute species. The results, however, are ambiguous, since this difference is a measure of the combined $\bar{V}_v$ and $\bar{V}_{ext}$ components, which cannot be separated. In contrast, the cavity model of Pierotti[87,88] avoids this difficulty.

Calculation of $\Delta\bar{V}_{ext}$ from Cavity Volumes. An experimentally based estimate of the relative contribution of the neutral and charged species to $\Delta\bar{V}_{ext}$ can be obtained by calculating the interaction volume ($\bar{V}_i = \bar{V}° - \bar{V}_c - \beta RT$) for

each species, where β is the isothermal compressibility of water. The interaction volume ($\bar{V}_i$) is thus calculated to be -8.29, -7.56, -26.97, and -22.90 ml/mol for thiophenol, phenol, thiophenoxide, and phenoxide, respectively. Combining the contribution of the neutral species (+0.73) with the contribution of the charged species (-4.07), the overall $\Delta\bar{V}_{ext}$ is calculated to be -3.34 ml/mol. The results indicate that the neutral species make only a minor contribution to the overall $\Delta\bar{V}_{ext}$ (approx. 15%).

Calculation of $\Delta\bar{V}_{ext}$ from Electrostriction of Solvent. In an attempt to directly calculate $\Delta\bar{V}_{ext}$ for eq 6, it is assumed that the contribution of the neutral species to $\Delta\bar{V}_{ext}$ is negligible and that $\Delta\bar{V}_{ext}$ is approximately equal to $\Delta\bar{V}_{elect}$, the volume change due to electrostriction of solvent by the anions. The results from the preceding analysis tend to support this approach.

The volume change due to electrostriction by ionic species has usually been calculated by differentiation of the Born equation or a modified version of this relation[90]. Several workers[69] have criticized this approach as unrealistic, since the Born equation is derived via an integration from the periphery of the ion to infinity, assuming a continuum model for the solvent. Bernal and Fowler[91] originally pointed out that the main contribution to the electrostriction volume change ($\Delta\bar{V}_{elect}$) for any ion in aqueous

solution should be the collapse of the water structure in the immediate vicinity of the ion. Recently, Desnoyers, Verrall, and Conway[69] have demonstrated that this collapse of the water structure can be calculated by combining the compressibility relationships for water with the equation of Frank[92] which relates the variation of the volume during the isothermal charging process to the electric field and the pressure[69]. In this approach an effective pressure is calculated which, in the absence of the average electric field in any water layer around the ion, would produce the same volume change in that layer as would the electric field. With this effective pressure the molar volume of the water in the layer can be calculated from the empirical compressibility equation for pure water.

The average electric field, E, in any water layer is $E = -Ze/Dr^2$, where Ze is the charge on the ion, r is the distance from the center of the ion to the center of the water layer, and D is the dielectric constant in this layer. If r can be established, D can be found by simultaneous solution of the field relationship and the empirical equation of Grahame[93] relating D to E.

For monoanions, it is sufficient to consider only those water molecules in the first layer around the ion[69]. However, before $\Delta\bar{V}_{elect}$ for any ion can be calculated by this theory, a molecular model must be constructed which predicts

the average number of water molecules which are in intimate contact with the charge. King[89] has recently utilized this theory to estimate the electrostriction around a formate ion by arbitrarily assuming that two water molecules are associated with each oxygen. Since it is impossible at this time to unambiguously establish the average number of water molecules in the immediate vicinity of the charge of the two anions, $\Delta\bar{V}_{elect}$ is calculated using two solvation models.

The distance from the center of the charge in each anion to the center of the water layer nearest the charge was taken to be the sum of the radius of a water molecule (1.38 Å) and the van der Waals radii of O^- or S^-, respectively. At this distance the average field $\bar{E}$ was calculated as indicated above, and the molar volume of water in this field was obtained from the equation of Desnoyers, et al[69]. If an average coordination number of two is assumed for both the phenoxide and thiophenoxide anions, the value of $\Delta\bar{V}_{elect}$ for the proton transfer reaction is +0.84 ml/mol. Alternatively, the maximum number of water molecules that could be influenced by the electric field can be estimated from the volume accessible to water molecules around atoms containing the charge in the anions. It is estimated from molecular models that the phenyl group effectively prohibits one-half the primary solvation layers of S^- and O^- from containing water molecules. Since the volume of the primary solvation

layers, $\bar{V}_s$, can easily be calculated from the van der Waals radii, the maximum number of water molecules in the primary layer around each of the anions can be estimated as $\bar{V}_s/2\bar{V}$, where $\bar{V}$ is the molar volume of water in the electric field. The value of $\Delta\bar{V}_{elect}$ for eq 6 determined from this model is -0.28 ml/mol. (The electrostriction calculations are given in the Appendix). Although the $\Delta\bar{V}_{elect}$ values calculated from the two solvation models differ in sign, the magnitude of the values obtained is approximately zero.

When $\Delta\bar{V}_{int}$ derived from van der Waals volumes ($\Delta\bar{V}_w$ = 6.09 ml/mol) is combined with the $\Delta\bar{V}_{elect}$ values calculated by the method of Desnoyers, et. al.[69], $\Delta\bar{V}_t^\circ$ is predicted to fall between 5.81 and 6.93 ml/mol. A similar analysis using $\Delta\bar{V}_{int}$ derived from the cavity model ($\Delta\bar{V}_c$ = 8.58 ml/mol) predicts $\Delta\bar{V}_t^\circ$ to be between 8.33 and 9.45 ml/mol. Using either model, the agreement between predicted and observed $\Delta\bar{V}_t^\circ$ is good. In addition, the results indicate that the $\Delta\bar{V}_t^\circ$ is primarily due to $\Delta\bar{V}_{int}$ and only slightly influenced by variations in solute-solvent interactions.

Calculation of $\Delta\bar{V}_t^\circ$ from Packing Densities. The fact that most of $\Delta\bar{V}_t^\circ$ can be accounted for by $\Delta\bar{V}_{int}$ is in agreement with the analysis of King[89] for several carboxylic acids based on packing densities of the acids and conjugate bases. If an "a priori" estimate of the packing densities (d = $\bar{V}_w/\bar{V}^\circ$) of the solute species is available, King's method can

be used to calculate $\Delta\bar{V}^{\circ}_{t}$. For a large number of phenols and phenoxide ions, the packing densities are approximately 0.62 and 0.75, respectively[66]. Using these values for the neutral molecules and ions, the volume change of proton transfer is calculated to be $\Delta\bar{V}^{\circ}_{t}$ = +5.81 ml/mol, which is in good agreement with experimental results.

Entropy Analysis

In order to elucidate the origin of the entropy change for the proton transfer reaction, it is convenient to partition $\Delta\bar{S}^{\circ}_{t}$ into an internal ($\Delta\bar{S}_{int}$) and an external ($\Delta\bar{S}_{ext}$) contribution. The internal contribution, which is the standard gas phase entropy of proton transfer, can be obtained from statistical mechanical calculations of the gas phase entropies of each of the species involved in the reaction. By means of the thermodynamic cycle shown in Figure 10, the external contribution can be attributed to differences in the entropies of hydration ($\Delta\bar{S}^{\circ}_{hyd}$).

Calculation of $\Delta\bar{S}_{int}$. When comparing two structurally similar acids, Pitzer[94] has shown that $\Delta\bar{S}_{int}$ is small. Since thiophenol and phenol are different acid types, this assumption is not valid, so $\Delta\bar{S}_{int}$ must be determined for eq 6. In order to calculate the gas phase entropies of each species involved in the proton transfer reaction, the translational, rotational, and vibrational contributions to the entropies were calculated. The same bond lengths[68] used in the volume

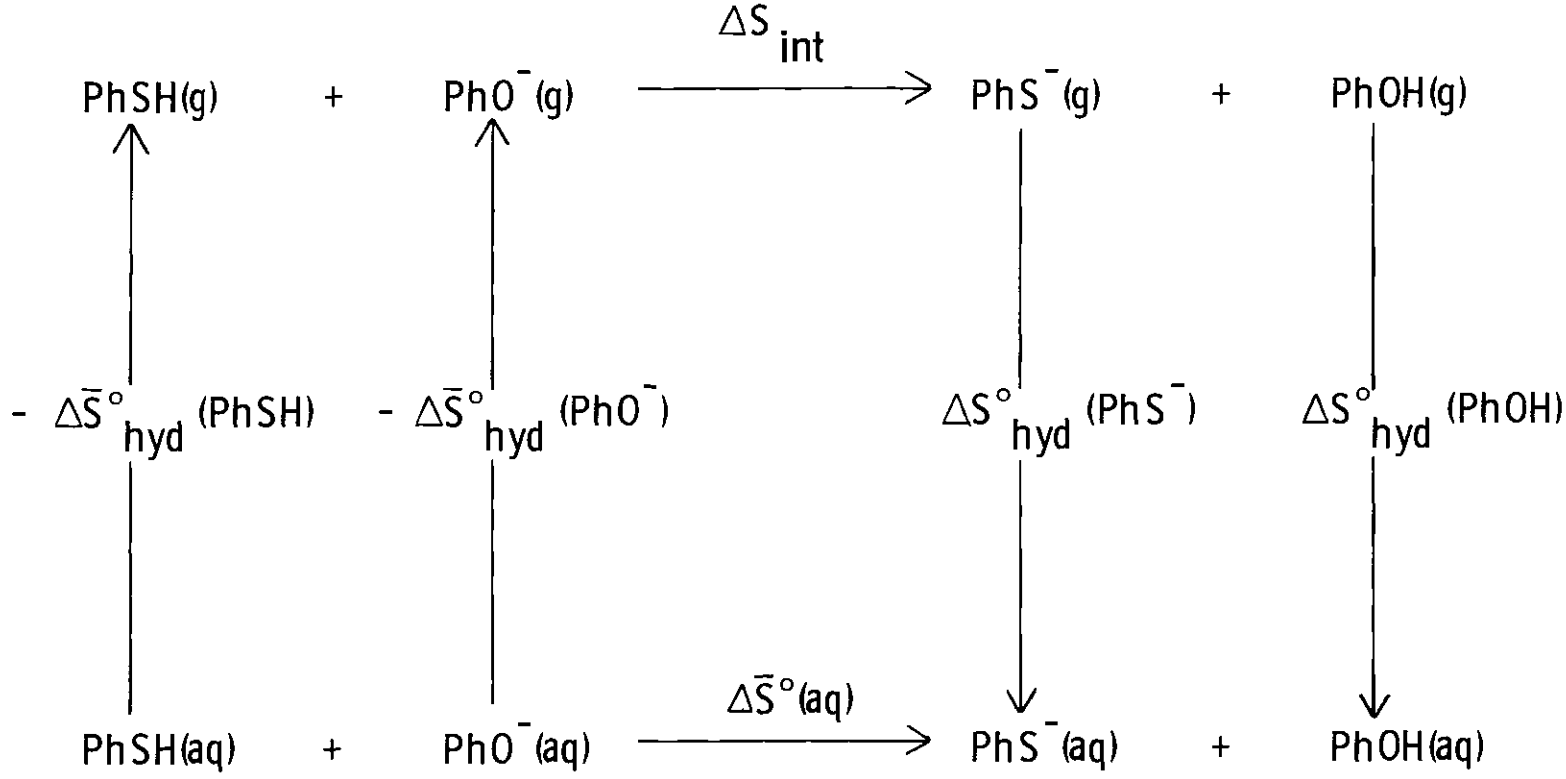

Figure 10. A Thermodynamic Cycle for the Entropy of Proton Transfer in the Thiophenol-Phenol System.

analysis were used to calculate the moments of inertia of the anions. An assignment of the fundamental vibrational frequencies of the anions may be obtained from a comparison of the infrared and laser Raman spectra of the sodium salts[95] with the assignments which have been determined for thiophenol[96] and phenol[97]. All of the low frequency fundamentals were found either in the infrared or Raman spectra of the sodium salts. Consequently, the vibrational contribution to the entropies of the anions is estimated to within ±0.2 cal/deg-mol. Table 12 summarizes the translational, rotational, and vibrational contributions for each ion. The calculated entropies of the anions have been combined with the experimentally derived entropies of thiophenol[96] and phenol[97] (80.51 and 75.44 cal/deg-mol, respectively) to yield $\Delta\bar{S}^{\circ}_{t}(g)$, i.e., $\Delta\bar{S}_{int} = -2.05$ cal/deg-mol.

While $T\Delta\bar{S}^{\circ}_{t}(g)$ accounts for only three percent of the $\Delta\bar{G}^{\circ}_{t}(g)$ at 298°K, $T\Delta\bar{S}^{\circ}_{t}(aq)$ is approximately seventy percent of $\Delta\bar{G}^{\circ}_{t}(aq)$. This drastic variation in the apportionment of $\Delta\bar{G}^{\circ}_{t}$ between $\Delta\bar{H}^{\circ}_{t}$ and $\Delta\bar{S}^{\circ}_{t}$ is a reflection of the influence of the aqueous environment on the thermodynamic properties of the solute species.

Calculation of $\Delta\bar{S}_{ext}$. From the thermodynamic cycle shown in Figure 10, the external contribution to the entropy of proton transfer is given by:

Table 12. Calculated Gas Phase Entropies of Thiophenoxide and Phenoxide Anions

Entropy Contribution [a]	Thiophenoxide Anion	Phenoxide Anion
Translational	39.979	39.505
Rotational	26.389	25.493
Vibrational	8.611	6.965
Total	74.979	71.963

[a] All values in cal/deg-mol.

$$\Delta\bar{S}_{ext} = -\Delta\bar{S}^{\circ}_{hyd}(PhSH) - \Delta\bar{S}^{\circ}_{hyd}(PhO^{-}) \qquad (24)$$

$$+ \Delta\bar{S}^{\circ}_{hyd}(PhS^{-}) + \Delta\bar{S}^{\circ}_{hyd}(PhOH) \quad .$$

The entropies of hydration of the neutral molecules can be calculated from the entropies of solution and vaporization. Rochester[98] has reported that $\Delta\bar{S}^{\circ}_{hyd}(PhOH) = -29.8$ cal/deg-mol based on a calorimetric determination of the enthalpy of solution of phenol, the solubility of phenol at 25°C, and a two-point vapor pressure study. When the more complete vapor pressure data of Biddescombe and Martin[99] is combined with the data of Rochester[98], a value of $\Delta\bar{S}^{\circ}_{hyd}(PhOH) = -29.4$ (±0.2) cal/deg-mol is obtained. The entropy of hydration of thiophenol has been determined from the vapor pressure data of Scott[96] and the temperature dependence of the solubility of thiophenol[100] as $\Delta\bar{S}^{\circ}_{hyd}(PhSH) = -30.8$ (±1.0) cal/deg-mol. From this analysis it is evident that the neutral species contribute only a small fraction of the total $\Delta\bar{S}_{ext}$ for eq 6, since the $\Delta\bar{S}^{\circ}_{hyd}$ for phenol and thiophenol are identical within experimental error. Therefore, neglecting any contribution from the neutral species, $\Delta\bar{S}_{ext}$ is a direct measure of the difference in the entropies of hydration of the anions.

Qualitatively, the positive value found for $\Delta\bar{S}_{ext}$ (13.05 cal/deg-mol) is in agreement with the prediction of

simple electrostatic theory, if the charge of the anions is assumed to be primarily localized on the sulfur and oxygen atoms as indicated by the CNDO/2 results. The positive difference is predicted on the basis of the larger radius of S^- compared to O^-.

However, if simple electrostatic theory is obeyed, then the ratio of $\Delta\bar{S}_{elect}$ to $\Delta\bar{V}_{elect}$ should be constant, where $\Delta\bar{S}_{elect}$ and $\Delta\bar{V}_{elect}$ are the entropy and volume changes for eq 6 resulting from the electrostatic interactions of the anions with the solvent. This ratio is dependent only on the macroscopic properties of the solvent which are well-known for water[10]. A maximum estimate of $\Delta\bar{V}_{elect}$ can be derived by combining $\Delta\bar{V}_{int}$ with $\Delta\bar{V}^{\circ}_{t}$, if $\Delta\bar{V}_{ext}$ is assumed to be totally due to electrostriction effects of the anions. Values of -0.84 and -3.33 ml/mol can be obtained for $\Delta\bar{V}_{elect}$ when the van der Waals and scaled-particle $\Delta\bar{V}_{int}$ values are subtracted from $\Delta\bar{V}^{\circ}_{t}$. Using these values the $\Delta\bar{S}_{elect}$ predicted for eq 6 by simple electrostatic theory is between -2.0 and -8.0 cal/deg-mol. These values have the wrong sign, since the experimentally based $\Delta\bar{S}_{ext}$ for the anions is positive, i.e., +13.05 cal/deg-mol. Therefore, the entropy-volume relationship of electrostatic theory gives completely incorrect results. King[89] has also shown that simple electrostatic theory cannot account for the entropy change observed for similar proton transfer reactions in carboxylic acids.

It now appears that the simple electrostatic entropy-volume relationship is of little value in the correlation of these two thermodynamic parameters.

Since it is reasonable to assume that the negative charge of the anions is localized on the oxygen or sulfur (CNDO/2 results), a modified version of the Born equation, which includes dielectric saturation of the solvent, can be employed to provide a direct estimate[101] for $\Delta\bar{S}_{elect}$.

In order to apply this theory it is necessary to assume that the phenyl group will cause approximately the same change in the electrostatic interactions for both O^- and S^-. With this assumption as a first approximation, $\Delta\bar{S}_{elect}$ for eq 6 is the difference between the entropies of O^- and S^- calculated from the modified Born equation. The predicted $\Delta\bar{S}_{elect}$ found from this approach is 2.05 cal/deg-mol, which has the correct sign but accounts for only one-sixth of the experimental value. A resonance interaction of the phenyl group to delocalize the charge can be shown to be greater for the phenoxide anion by simple orbital size arguments or from the CNDO/2 results. Consequently, any arguments based on resonance delocalization of the charge in the anion would decrease the value of $\Delta\bar{S}_{elect}$ predicted by the Born theory.

CHAPTER V

CONCLUSIONS

From the analysis of the thermodynamics of ionization of substituted anilinium ions and pyridinium ions, it is concluded that substituent effects on the acidities of these acids are primarily manifested in the enthalpy rather than the entropy of ionization. The Gibbs free energy-entropy relationships which are observed for these acids indicate that the acid ionization process for both systems may be adequately described in terms of Kirkwood-Westheimer electrostatic theory. Attempted analyses in terms of Hepler's theory of substituent effects reveal that β values for these acid systems are far greater than the value of 280° which was suggested by Hepler, and that, rather than being constant, β values vary substantially from one acid system to another.

From the comparison of the thermodynamics of ionization of thiophenol and phenol, it is concluded that the greater acidity of thiophenol is due primarily to a more positive entropy of ionization. Combination of the aqueous and gas phase thermodynamic functions of proton transfer (eq 6) in the thiophenol-phenol system reveals that the more positive entropy of ionization of thiophenol is almost entirely due to "looser" solvation of the thiophenoxide anion

in aqueous solution. Although the volume change for the proton transfer reaction can be satisfactorily accounted for in terms of a van der Waals contribution and a small contribution due to electrostriction, none of the theoretical formulations which were employed in this analysis were able to quantitatively account for the large positive entropy change observed for this reaction. The complete failure of electrostatic theory (which predicts a proportionality between entropy and volume changes) to account for the observed entropy change suggests that entropy changes are not related in any simple manner to the corresponding volume changes in aqueous solution. These results substantiate the observation of King[89], who pointed out that the simple molecular model which successfully predicts volume changes is apparently inapplicable when discussing the corresponding entropy changes.

CHAPTER VI

RECOMMENDATIONS

The availability of thermodynamic data for the ionization of organic acids in the gas phase and in nonaqueous solvents is of utmost importance if the role of solvent in the acid ionization process is to be better understood. For example, many questions concerning the anomalous behavior of the 4-aminopyridinium ion will undoubtedly be answered when the gas phase thermodynamic parameters have been determined for this acid. Furthermore, a comparison of the partial molal volumes of ionization of the 4-aminopyridinium ion and the 3-aminopyridinium ion should provide useful information concerning the effect of charge delocalization of the solvation of organic ions in aqueous solution.

Regarding Kirkwood-Westheimer electrostatic theory, thus far only organic acid systems with uncharged or negatively charged molecular cavities have been studied. Since it is generally believed that cation-solvent interactions differ from anion-solvent interactions, the study of an acid system with a positively charged molecular cavity should be undertaken. A series of diprotonated 5-substituted *m*-phenylenediamines would provide such a system.

Finally, the study of thiophenol should be expanded

to include a variety of substituted thiophenols, so that the transmission of substituent effects in this system can be investigated. Again, pertinent gas phase data would be quite useful in the analysis of experimental data.

APPENDIX

Computer Programs

The computer facilities at Georgia State University were routinely used for the analysis of experimental data during the course of this research. The following BASIC programs were used:

1. HEATPRO - This program was used to calculate the enthalpies of protonation of substituted anilines and pyridines.

2. CALHEAT - This program was used to calculate the enthalpies of other miscellaneous reactions.

3. KWELST - This program was used in the analysis of the thermodynamics of ionization of anilinium ions and pyridinium ions in terms of Kirkwood-Westheimer theory.

4. VOLUME - This program was used to calculate the van der Waals volumes and overlapping volume increments for various A-B groups.

5. SPT - This program was used to calculate the cavity volumes of organic solute species in aqueous solution using the scaled-particle theory.

HEATPRØ

```
 25 PRINT "TØDAY'S DATE IS";
 30 INPUT D$
 35 PRINT
 40 PRINT
 45 PRINT
 50 PRINT D$
 55 FØR I=1 TØ 3
 60 READ A(I),B(I),E(I),C(I),D(I)
 65 LET X(I)=A(I)-B(I)-E(I)*(0.0006/C(I)+0.0004/D(I))
 70 NEXT I
 75 FØR I=1 TØ 2
 80 READ I(I),V(I),W(I),T(I)
 85 LET Q(I)=(I(I)↑2*V(I)*T(I)/W(I))*143.403
 90 LET L(I)=Q(I)/X(I)
 95 NEXT I
100 LET L(3)=(L(1)+L(2))/2
105 LET Q(3)=L(3)*X(3)
110 READ M,N,K,HO
115 LET H=(M-Q(3))/N
120 LET A=N/1005
125 LET F=((HO+A+K)-SQR(((HO+A+K)↑2)-4*HO*A))/(2*A)
130 LET H2=H/F
135 READ A$,B$,C$
140 PRINT
145 PRINT
150 PRINT TAB(15);A$;B$;C$
155 PRINT
160 PRINT
165 PRINT TAB(30);"CALIBRATIØN"
170 PRINT
175 PRINT
180 PRINT " I .";TAB(7);"RESISTANCE";TAB(21);"RESISTANCE";
185 PRINT TAB(34);"EQUILIBRATIØN";TAB(51);"DRIFT";TAB(62);"DRIFT"
190 PRINT TAB(9);"BEFØRE";TAB(23);"AFTER";TAB(38);"TIME";
195 PRINT TAB(51);"BEFØRE";TAB(62);"AFTER"
200 PRINT
205 FØR I=1 TØ 2
210 PRINT I;".";TAB(8);A(I);TAB(22);B(I);TAB(37);E(I);
215 PRINT TAB(50);C(I);TAB(61);D(I)
220 NEXT I
225 PRINT
230 PRINT
235 PRINT " I .";TAB(13);"CURRENT";TAB(27);"HEATER";
240 PRINT TAB(41);"STANDARD";TAB(56);"TIME"
245 PRINT TAB(27);"VØLTAGE";TAB(41);"VØLTAGE"
250 PRINT
255 FØR I=1 TØ 2
```

HEATPRØ (Continued)

```
260 PRINT I;".";TAB(13);I(I);TAB(26);V(I);TAB(40);W(I);TAB(55);T(I)
265 NEXT I
270 PRINT
275 PRINT
280 PRINT " I .";TAB(15);"HEAT";TAB(32);"RESISTANCE";TAB(55);"HEAT"
285 PRINT TAB(14);"EVØLVED";TAB(34);"CHANGE";TAB(53);"CAPACITY"
290 PRINT
295 FØR I=1 TØ 2
300 PRINT I;".";TAB(13);Q(I);TAB(31);X(I);TAB(52);L(I)
305 NEXT I
310 PRINT
315 PRINT
320 PRINT TAB(31);"REACTIØN"
325 PRINT
330 PRINT
335 PRINT " I .";TAB(7);"RESISTANCE";TAB(21);"RESISTANCE";
340 PRINT TAB(34);"EQUILIBRATIØN";TAB(51);"DRIFT";TAB(62);"DRIFT"
345 PRINT TAB(9);"BEFØRE";TAB(23);"AFTER";TAB(38);"TIME";
350 PRINT TAB(51);"BEFØRE";TAB(62);"AFTER"
355 PRINT
360 PRINT " 3 .";TAB(8);A(3);TAB(22);B(3);TAB(37);E(3);
365 PRINT TAB(50);C(3);TAB(61);D(3)
370 PRINT
375 PRINT
380 PRINT " I .";TAB(15);"HEAT";TAB(32);"RESISTANCE";TAB(55);"HEAT"
385 PRINT TAB(14);"EVØLVED";TAB(34);"CHANGE";TAB(53);"CAPACITY"
390 PRINT
395 PRINT " 3 .";TAB(13);Q(3);TAB(31);X(3);TAB(52);L(3)
400 PRINT
405 PRINT
410 PRINT TAB(22);"NUMBER ØF MILLIMØLES=";N
415 PRINT
420 IF F>=0.999 THEN 455
425 PRINT TAB(15);"ENTHALPY ØF PARTIAL PRØTØNATIØN =";H
430 PRINT
435 PRINT TAB(22);"FRACTIØN PRØTØNATED =";F
440 PRINT
445 PRINT TAB(18);"ENTHALPY ØF PRØTØNATIØN =";H2
450 GØTØ 500
455 PRINT TAB(18);"ENTHALPY ØF PRØTØNATIØN =";H
460 PRINT
465 DATA 51.93,51.867,300.7,22.99,21.21
470 DATA 51.789,51.724,315.3,20.54,20.2
475 DATA 51.857,51.799,263,21.21,20.54
480 DATA .1314,1.10329,.078305,.9996
485 DATA .13138,1.10329,.078305,1.0011
490 DATA 3.39,3.8559,2.54E-05,.02774
495 DATA ENTHALPY ØF PRØ,TØNATIØN ØF ANI,LINE
500 END
```

Output of HEATPRO Program

TØDAY'S DATE IS?"8/26/71"

8/26/71

ENTHALPY ØF PRØTØNATIØN ØF ANILINE

CALIBRATIØN

I .	RESISTANCE BEFØRE	RESISTANCE AFTER	EQUILIBRATIØN TIME	DRIFT BEFØRE	DRIFT AFTER
1 .	51.93	51.867	300.7	22.99	21.21
2 .	51.789	51.724	315.3	20.54	20.2

I .	CURRENT	HEATER VØLTAGE	STANDARD VØLTAGE	TIME
1 .	.1314	1.10329	.078305	.9996
2 .	.13138	1.10329	.078305	1.0011

I .	HEAT EVØLVED	RESISTANCE CHANGE	HEAT CAPACITY
1 .	34.8718	.494696E-01	704.914
2 .	34.9135	.495486E-01	704.633

REACTIØN

I .	RESISTANCE BEFØRE	RESISTANCE AFTER	EQUILIBRATIØN TIME	DRIFT BEFØRE	DRIFT AFTER
3 .	51.857	51.799	263	21.21	20.54

I .	HEAT EVØLVED	RESISTANCE CHANGE	HEAT CAPACITY
3 .	32.0228	.454371E-01	704.773

NUMBER ØF MILLIMØLES= 3.8559

ENTHALPY ØF PARTIAL PRØTØNATIØN =-7.42571

FRACTIØN PRØTØNATED = .998939

ENTHALPY ØF PRØTØNATIØN =-7.4336

CALHEAT

```
 25 PRINT "TØDAY'S DATE IS";
 30 INPUT D$
 35 PRINT
 40 PRINT
 45 PRINT
 50 PRINT D$
 55 FØR I=1 TØ 3
 60 READ A(I),B(I),E(I),C(I),D(I)
 65 LET X(I)=A(I)-B(I)-E(I)*(0.0006/C(I)+0.0004/D(I))
 70 NEXT I
 75 FØR I=1 TØ 2
 80 READ I(I),V(I),W(I),T(I)
 85 LET Q(I)=(I(I)↑2*V(I)*T(I)/W(I))*143.403
 90 LET L(I)=Q(I)/X(I)
 95 NEXT I
100 LET L(3)=(L(1)+L(2))/2
105 LET Q(3)=L(3)*X(3)
110 READ M,N
115 LET H=(M-Q(3))/N
120 READ A$,B$,C$
125 PRINT
130 PRINT
135 PRINT TAB(15);A$;B$;C$
140 PRINT
145 PRINT
150 PRINT TAB(30);"CALIBRATIØN"
155 PRINT
160 PRINT
165 PRINT " I .";TAB(7);"RESISTANCE";TAB(21);"RESISTANCE";
170 PRINT TAB(34);"EQUILIBRATIØN";TAB(51);"DRIFT";TAB(62);"DRIFT"
175 PRINT TAB(9);"BEFØRE";TAB(23);"AFTER";TAB(38);"TIME";
180 PRINT TAB(51);"BEFØRE";TAB(62);"AFTER"
185 PRINT
190 FØR I=1 TØ 2
195 PRINT I;".";TAB(8);A(I);TAB(22);B(I);TAB(37);E(I);
200 PRINT TAB(50);C(I);TAB(61);D(I)
205 NEXT I
210 PRINT
215 PRINT
220 PRINT " I .";TAB(13);"CURRENT";TAB(27);"HEATER";
225 PRINT TAB(41);"STANDARD";TAB(56);"TIME"
230 PRINT TAB(27);"VØLTAGE";TAB(41);"VØLTAGE"
235 PRINT
240 FØR I=1 TØ 2
245 PRINT I;".";TAB(13);I(I);TAB(26);V(I);TAB(40);W(I);TAB(55);T(I)
250 NEXT I
255 PRINT
```

CALHEAT (Continued)

```
260 PRINT
265 PRINT " I .";TAB(15);"HEAT";TAB(32);"RESISTANCE";TAB(55);"HEAT"
270 PRINT TAB(14);"EVØLVED";TAB(34);"CHANGE";TAB(53);"CAPACITY"
275 PRINT
280 FOR I=1 TØ 2
285 PRINT I;".";TAB(13);Q(I);TAB(31);X(I);TAB(52);L(I)
290 NEXT I
295 PRINT
300 PRINT
305 PRINT TAB(31);"REACTIØN"
310 PRINT
315 PRINT
320 PRINT " I .";TAB(7);"RESISTANCE";TAB(21);"RESISTANCE";
325 PRINT TAB(34);"EQUILIBRATIØN";TAB(51);"DRIFT";TAB(62);"DRIFT"
330 PRINT TAB(9);"BEFØRE";TAB(23);"AFTER";TAB(38);"TIME";
335 PRINT TAB(51);"BEFØRE";TAB(62);"AFTER"
340 PRINT
345 PRINT " 3 .";TAB(8);A(3);TAB(22);B(3);TAB(37);E(3);
350 PRINT TAB(50);C(3);TAB(61);D(3)
355 PRINT
360 PRINT
365 PRINT " I .";TAB(15);"HEAT";TAB(32);"RESISTANCE";TAB(55);"HEAT"
370 PRINT TAB(14);"EVØLVED";TAB(34);"CHANGE";TAB(53);"CAPACITY"
375 PRINT
380 PRINT " 3 .";TAB(13);Q(3);TAB(31);X(3);TAB(52);L(3)
385 PRINT
390 PRINT
395 PRINT TAB(22);"NUMBER ØF MILLIMØLES=";N
400 PRINT
405 PRINT TAB(22);"ENTHALPY ØF REACTIØN =";H
410 DATA 51.92,51.857,305.9,23.41,23.29
415 DATA 51.798,51.735,294.5,22.2,22.26
420 DATA 51.847,51.808,246.7,23.29,22.2
425 DATA .13146,1.09923,.078037,1.0003
430 DATA .13146,1.09923,.078037,.9996
435 DATA 3.53,1.7384
440 DATA ENTHALPY ØF NEU,TRALIZATIØN ØF ,THIØPHENØL
445 END
```

Output of CALHEAT Program

TØDAY'S DATE IS?"1/05/71"

1/05/71

ENTHALPY ØF NEUTRALIZATIØN ØF THIØPHENØL

CALIBRATIØN

I .	RESISTANCE BEFØRE	RESISTANCE AFTER	EQUILIBRATIØN TIME	DRIFT BEFØRE	DRIFT AFTER
1 .	51.92	51.857	305.9	23.41	23.29
2 .	51.798	51.735	294.5	22.2	22.26

I .	CURRENT	HEATER VØLTAGE	STANDARD VØLTAGE	TIME
1 .	.13146	1.09923	.078037	1.0003
2 .	.13146	1.09923	.078037	.9996

I .	HEAT EVØLVED	RESISTANCE CHANGE	HEAT CAPACITY
1 .	34.9191	.499096E-01	699.648
2 .	34.8947	.497521E-01	701.372

REACTIØN

I .	RESISTANCE BEFØRE	RESISTANCE AFTER	EQUILIBRATIØN TIME	DRIFT BEFØRE	DRIFT AFTER
3 .	51.847	51.808	246.7	23.29	22.2

I .	HEAT EVØLVED	RESISTANCE CHANGE	HEAT CAPACITY
3 .	19.755	.282009E-01	700.51

NUMBER ØF MILLIMØLES= 1.7384

ENTHALPY ØF REACTIØN =-9.33329

KWELST

```
  5 PRINT
 10 PRINT
 15 PRINT
 20 PRINT TAB(12);"KIRKWØØD-WESTHEIMER TREATMENT ØF ØRGANIC ACIDS"
 25 PRINT
 30 PRINT
 35 READ N,A$,B$
 40 PRINT TAB(22);A$;B$
 45 PRINT
 50 PRINT
 55 PRINT
 60 PRINT TAB(21);"*** STRUCTURAL PARAMETERS ***"
 65 PRINT
 70 PRINT
 75 PRINT TAB(2);"SUBSTITUENT";TAB(20);"FØCAL";TAB(34);"CAVITY";
 80 PRINT TAB(52);"X";TAB(65);"T/C↑3"
 85 PRINT TAB(19);"RADIUS";TAB(34);"VØLUME"
 90 PRINT
 95 FØR I=1 TØ N
100 READ C$(I),R(I),V(I),G(I),H(I)
105 LET B(I)=(V(I)/4.18879)↑.333333
110 LET T(I)=V(I)/((R(I))↑3)
115 LET X(I)=(R(I)/B(I))↑2
120 PRINT C$(I);TAB(18);R(I);TAB(35);V(I);TAB(49);X(I);TAB(63);T(I)
125 NEXT I
130 PRINT
135 PRINT
140 PRINT
145 PRINT TAB(20);"*** SPHERICAL CAVITY MØDEL ***"
150 PRINT
155 PRINT
160 PRINT TAB(2);"SUBSTITUENT";TAB(20);"F1";TAB(33);"F2";
165 PRINT TAB(45);"EFF-DIELCØNST";TAB(62);"SLØPE"
170 PRINT
175 FØR I=1 TØ N
180 LET A=X(I)↑1.5
185 LET B=SQR(X(I))
190 LET C=1+X(I)
195 LET D=LØG(C)
200 LET E(I)=(8*A/(C↑2))+(4*B/C)-(4*D/B)
205 LET F(I)=1-(4*A/(C↑2))
210 LET D(I)=1/((F(I)/2)+(E(I)/78.36))
215 LET S(I)=(-217.96)*(78.36)/(D(I)*E(I))
220 PRINT C$(I);TAB(18);E(I);TAB(30);F(I);TAB(47);D(I);TAB(60);S(I)
225 NEXT I
230 PRINT
235 PRINT
```

KWELST (Continued)

```
240 PRINT
245 PRINT TAB(16);"*** ØBLATE ELLIPSØIDAL CAVITY MØDEL ***"
250 PRINT
255 PRINT
260 PRINT TAB(2);"SUBSTITUENT";TAB(20);"G1";TAB(33);"G2";
265 PRINT TAB(45);"EFF-DIELCØNST";TAB(62);"SLØPE"
270 PRINT
275 FØR I=1 TØ N
280 LET D(I)=1/((G(I)/2)+(H(I)/78.36))
285 LET S(I)=(-217.96)*(78.36)/(D(I)*H(I))
290 PRINT C$(I);TAB(18);G(I);TAB(30);H(I);TAB(47);D(I);TAB(60);S(I)
295 NEXT I
300 PRINT
305 PRINT
310 PRINT
315 DATA 9,SUBSTITUTED ANI,LINIUM IØNS
320 DATA "4-METHYL(MIN)",2.702,164,.242,.9245
325 DATA "4-METHYL(MAX)",3.077,164,.126,.987
330 DATA "4-CHLØRØ",2.661,155,.237,.928
335 DATA "4-BRØMØ",2.6985,162,.238,.927
340 DATA "4-IØDØ",2.7635,168,.227,.9345
345 DATA "4-CYANØ(MIN)",2.8935,155,.158,.976
350 DATA "4-CYANØ(MAX)",3.2585,155,.072,.9865
355 DATA "4-NITRØ(MIN)",2.7363,158,.216,.9415
360 DATA "4-NITRØ(MAX)",3.0838,158,.114,.9885
365 END
```

Output of KWELST Program

KIRKWØØD-WESTHEIMER TREATMENT ØF ØRGANIC ACIDS

SUBSTITUTED ANILINIUM IØNS

*** STRUCTURAL PARAMETERS ***

SUBSTITUENT	FØCAL RADIUS	CAVITY VØLUME	X	T/C↑3
4-METHYL(MIN)	2.702	164	.633191	8.31358
4-METHYL(MAX)	3.077	164	.821143	5.62939
4-CHLØRØ	2.661	155	.637669	8.22616
4-BRØMØ	2.6985	162	.636739	8.24419
4-IØDØ	2.7635	168	.651788	7.96033
4-CYANØ(MIN)	2.8935	155	.753968	6.39825
4-CYANØ(MAX)	3.2585	155	.956183	4.48
4-NITRØ(MIN)	2.7363	158	.665707	7.71198
4-NITRØ(MAX)	3.0838	158	.845528	5.38764

*** SPHERICAL CAVITY MØDEL ***

SUBSTITUENT	F1	F2	EFF-DIELCØNST	SLØPE
4-METHYL(MIN)	.994265	.244406	7.41336	-2317.15
4-METHYL(MAX)	1.13904	.102571	15.1927	-986.954
4-CHLØRØ	.998472	.240546	7.51794	-2275.29
4-BRØMØ	.997598	.241347	7.49602	-2283.94
4-IØDØ	1.01147	.228544	7.86286	-2147.52
4-CYANØ(MIN)	1.09431	.148771	11.3185	-1378.93
4-CYANØ(MAX)	1.20942	.226443E-01	37.3744	-377.85
4-NITRØ(MIN)	1.0239	.216954	8.22751	-2027.43
4-NITRØ(MAX)	1.15358	.869161E-01	17.1881	-861.381

*** ØBLATE ELLIPSØIDAL CAVITY MØDEL ***

SUBSTITUENT	G1	G2	EFF-DIELCØNST	SLØPE
4-METHYL(MIN)	.242	.9245	7.53023	-2453.33
4-METHYL(MAX)	.126	.987	13.2283	-1308.13
4-CHLØRØ	.237	.928	7.67208	-2398.89
4-BRØMØ	.238	.927	7.64351	-2410.45
4-IØDØ	.227	.9345	7.97285	-2292.34
4-CYANØ(MIN)	.158	.976	10.9343	-1600.41
4-CYANØ(MAX)	.072	.9865	20.5806	-841.231
4-NITRØ(MIN)	.216	.9415	8.33229	-2177.14
4-NITRØ(MAX)	.114	.9885	14.3648	-1202.81

VOLUME

```
 15 DIM A$(30),R(30),L(30),V(30),M(30),X(30),Y(30)
 20 PRINT
 25 PRINT
 30 PRINT
 35 READ A$,R
 40 LET V=4.189*0.6023*(R↑3)
 45 PRINT TAB(18);"VAN DER WAALS VØLUMES ØF ";A$;"-X GRØUPS"
 50 PRINT
 55 PRINT
 60 PRINT TAB(15);"VAN DER WAALS RADIUS ØF ";A$;"-";R;"ANGSTRØMS"
 65 PRINT
 70 PRINT TAB(15);"VAN DER WAALS VØLUME ØF ";A$;"=";V;"ML/MØLE"
 75 PRINT
 80 PRINT
 85 PRINT TAB(2);"GRØUP";TAB(13);"VØLUME ØF";TAB(28);"ØVERLAP VØLUME";
 90 PRINT TAB(48);"ØVERLAP VØLUME"
 95 PRINT TAB(3);A$;"-X";TAB(12);"X (ML/MØLE)";TAB(28);
100 PRINT "ØF ";A$;" (ML/MØLE)";TAB(48);"ØF X (ML/MØLE)"
105 PRINT
110 LET I=1
115 READ A$(I),R(I),L(I)
120 IF R(I)=0 THEN 200
125 LET V(I)=4.189*0.6023*(R(I)↑3)
130 LET M(I)=(R↑2-R(I)↑2+L(I)↑2)/(2*L(I))
135 LET X(I)=1.04725*0.6023*((R-M(I))↑2)*(2*R+M(I))
140 LET Y(I)=1.04725*0.6023*((R(I)-L(I)+M(I))↑2)*(2*R(I)+L(I)-M(I))
145 PRINT TAB(2);A$;"-";A$(I);TAB(13);V(I);TAB(30);X(I);TAB(50);Y(I)
150 PRINT
155 LET I=I+1
160 GØTØ 115
165 DATA "C",1.7
170 DATA "H",1.2,1.084,"C",1.7,1.50,"Ø-",1.76,1.4,"S-",2.19,1.82
175 DATA "Ø",1.52,1.427,"S",1.8,1.818,"F",1.47,1.37,"CL",1.75,1.69
180 DATA "BR",1.85,1.84,"I",1.98,2.1,"N",1.55,1.39,"X",0,0
200 END
```

Output of VOLUME Program

VAN DER WAALS VØLUMES ØF C-X GRØUPS

VAN DER WAALS RADIUS ØF C= 1.7 ANGSTRØMS

VAN DER WAALS VØLUME ØF C= 12.3957 ML/MØLE

GRØUP C-X	VØLUME ØF X (ML/MØLE)	ØVERLAP VØLUME ØF C (ML/MØLE)	ØVERLAP VØLUME ØF X (ML/MØLE)
C-H	4.3598	.695955	2.52418
C-C	12.3957	2.36243	2.36243
C-Ø-	13.755	2.92985	2.63249
C-S-	26.5006	4.1214	2.09774
C-Ø	8.86042	1.67105	2.28258
C-S	14.7143	2.09184	1.83471
C-F	8.01448	1.53927	2.34069
C-CL	13.5219	2.17159	2.0221
C-BR	15.9749	2.25192	1.8534
C-I	19.5848	2.126	1.55389
C-N	9.39546	1.85399	2.42385

SPT

```
 50 PRINT
 55 PRINT
 60 PRINT TAB(15);"CAVITY VØLUMES FRØM SCALED-PARTICLE THEØRY"
 65 PRINT
 70 PRINT
 75 PRINT TAB(3);"SØLUTE";TAB(16);"VAN DER";TAB(27);"MØLAL";
 80 PRINT TAB(35);"HEAT OF CAVITY";TAB(51);"CAVITY";
 85 PRINT TAB(60);"INTERACTIØN"
 90 PRINT TAB(3);"SPECIES";TAB(13);"WAALS VØLUME";TAB(27);"VØLUME";
 95 PRINT TAB(37);"FØRMATIØN";TAB(51);"VØLUME";TAB(63);"VØLUME"
100 PRINT
105 LET D0=2.75E-08
110 LET V0=18.08
115 LET B=4.525E-05
120 LET A=2.55E-04
125 LET N=6.023E23
130 LET R=1.987
135 LET T=298.15
140 LET I=0
145 LET Y=3.14159*(D0↑3)*N/(6*V0)
150 LET I=I+1
155 READ A$(I),W(I),V(I)
160 IF W(I)=0 THEN 255
165 LET D(I)=(6*W(I)/(3.14159*N))↑.333333
170 LET R(I)=(D0+D(I))/2
175 LET F(I)=R(I)/D0
180 LET Y1=6/(1-Y)
185 LET Y2=36*Y/((1-Y)↑2)
190 LET Z(I)=(Y1*(2*(F(I)↑2)-F(I))+Y2*(F(I)↑2-F(I)+.25)+1)
195 LET H(I)=A*R*(T↑2)*(Y/(1-Y))*Z(I)
200 LET C(I)=82.05*(B/A)*(H(I)/(R*T))+W(I)
205 LET I(I)=V(I)-C(I)-82.05*B*T
210 PRINT A$(I);TAB(16);W(I);TAB(26);V(I);TAB(37);H(I);
215 PRINT TAB(50);C(I);TAB(62);I(I)
220 PRINT
225 GØTØ 150
230 DATA PHENØL,53.52,86.23
235 DATA THIØPHENØL,59.51,94.09
240 DATA PHENØXIDE,55.42,73.62
245 DATA THIØPHENØXIDE,67.5,86.73
250 DATA NØNE,0,0
255 END
```

Output of SPT Program

CAVITY VØLUMES FRØM SCALED-PARTICLE THEØRY

SØLUTE SPECIES	VAN DER WAALS VØLUME	MØLAL VØLUME	HEAT ØF CAVITY FØRMATIØN	CAVITY VØLUME	INTERACTIØN VØLUME
PHENØL	53.52	86.23	1593.44	92.6816	-7.5586
THIØPHENØL	59.51	94.09	1699.28	101.273	-8.28973
PHENØXIDE	55.42	73.62	1627.46	95.4176	-22.9045
THIØPHENØXIDE	67.5	86.73	1834.66	112.59	-26.9669

Procedure for Silvering the Reaction Vessel

Heat effects due to thermal radiation can be eliminated in vacuum-jacketed glassware by silvering the inner walls of the vacuum jacket. The calorimetry reaction vessel was thus silvered by the following procedure.

Solutions:

A. Glass washing solution: 3 ml of 48% hydrofluoric acid, 33 ml of concentrated nitric acid, 0.5 g of sodium lauryl sulfate, and 64 ml of distilled water.

B. Silver nitrate solution: Dissolve 25 g of silver nitrate in 1000 ml of distilled water.

C. Potassium hydroxide solution: Dissolve 45 g of potassium hydroxide in 1000 ml of distilled water.

D. Reducing solution: Dissolve 40 g of sucrose in 350 ml of distilled water in a 500 ml volumetric flask. Add 87.5 ml of 95% ethanol, then add 1.5 ml of concentrated nitric acid. Mix well and dilute to 500 ml with distilled water. This solution should be aged for one week before use and will be usable as long as the solution does not turn yellow.

After inlet tubes and outlet tubes are blown onto the lower and upper ends of the vacuum jacket in such a manner that the silvering solution can be admitted between the inner and outer walls of the reaction vessel, the apparatus is washed with a glass cleaning solution (A), and then rinsed repeatedly with distilled water. The volume of the space between the walls of the vacuum jacket is determined by

measuring the volume of distilled water required to fill the space to the desired level. The volume of silvering solution which should be prepared (V) is equal to this volume plus a 25 ml excess.

Using a piece of rubber tubing equipped with a Hoffman clamp, the inlet tube at the bottom of the reaction vessel is attached to a large funnel which is mounted on a ringstand at a height of approximately six inches above the reaction vessel. It is suggested that this assembly be tested by filling the vacuum jacket with distilled water before the silvering process is attempted.

In an adequately large beaker, 0.64V ml of silver nitrate solution (B) is titrated with ammonium hydroxide C.P. until a brown color forms and then almost disappears. Next, 0.32V ml of potassium hydroxide solution (C) is added to the solution and the titration is continued until the brown color almost disappears again. The addition of 0.04V ml of the reducing solution (D) to the titrated solution activates the silvering solution, which is then added smoothly and rapidly through the funnel, using the Hoffman clamp to regulate the flow. After the silvering solution turns a dirty yellow color, the reaction vessel should be drained and rinsed repeatedly with distilled water. This entire process should be repeated three times to insure a thick permanent silver coating. (Note: Best results are obtained when silver is deposited slowly, so cool solutions should be used).

Table 13. Equipment List for Solution Calorimetry System

Bag Sealer (from plastic bag sealer); Sears, Roebuck Co.

Batteries (KS-15544 List 405, two volts); Western Electric.

Calorimetry Stirrer (No. BG8P400C5BK); RMS Motor Corp.

Connecting Rod (8 in. length of 1/32 in. stainless steel rod).

Container Lid (stainless steel); by Ga. Tech machinist.

Cutting Blade (from single-edged stainless steel razor blade).

DC Power Supply [ABC40-0.5(M)]; Kepco, Inc.

Digital Timer (No. PL103, with zero reset); Sodeco, Inc.

Digital Voltmeter (Model 3450-A); Hewlett-Packard Co.

DPDT Pinch-Type Switches (No. 3294); Leeds and Northrup.

Electrical Wiring (RG-58/U, #20 coaxial cable); Belden Co.

External Cable Clamps (AN3057-10); Amphenol.

External Plug (MS3106A-18-1P); Amphenol.

External Receptacle (MS3101A-18-1S); Amphenol.

Galvanometer (No. 2284D, 0.1 μv/mm); Leeds and Northrup.

Galvanometer Reading Device (No. 2100); Leeds and Northrup.

Gears (0.77 in. & 0.43 in.); Boston bevel gears with set screw.

Heater (Manganin #36 wire, 11.92 Ω/ft.); W. B. Driver, Co.

Heater Form (11 cm x 0.6 cm); Polypenco Nylon 101 rod.

Internal Plug (126-195); Amphenol.

Internal Receptacle (126-198); Amphenol.

Mueller Temperature Bridge (No. 8067); Leeds and Northrup.

Outer Calorimeter Can (stainless steel); by machinist.

Table 13. Equipment List for Solution Calorimetry System (Continued)

Precision Clock (Model S-6); The Standard Electric Time Co.

Reaction Vessel (vacuum-jacketed); by Ga. Tech glassblower.

Sample Bags (from 3/4 mil polyethylene film).

Sample Form (from 3 in. length of 7/8 in. Teflon rod).

Sample Introduction Motor (Type 117, 0.5 rpm); Cramer Controls.

Sample Timing Motor (FL108, 0.25 rpm); Haydon Mfg. Co.

Single-Contact Tapping Key (No. 3702); Leeds and Northrup.

Stainless Steel Joint (7651-38, $\overline{\$}$40/50 male); Ace Glass, Inc.

Standard Resistor (Cat. 601244, 10 ohm); J. G. Biddle, Co.

Standard Resistor (Cat. 601245, 100 ohm); J. G. Biddle, Co.

Stirrer Shaft (8 in. length of ¼ in. stainless steel rod).

Temperature Controller (Model 116); Bayley Instrument Co.

Thermistors (No. 44001, 100 ohm); Ysi Components Division.

Tubing Connector (Jaco Berea O, ¼ in. polypropylene).

Water Bath (55 gal.); Drum enclosed in insulated plywood box.

Water Bath Stirrer (Model 18-178); Precision Scientific Co.

Typical Calorimetry Data Sheet

8-26-71 Enthalpy of Protonation of Aniline

Solution Temp: 25.0° $K_a = 2.54 \times 10^{-5}$ $V_h = 1.10329$ v

Water Bath Temp: 25.8° mg = 359.1 $V_{10} = 0.078305$ v

Q(blank) = 3.39 cal mmol = 3.856 $R_h = 140.896$ Ω

$(H^+) = 0.02774$ N

* *

Measurement	Resistance (Ω)	Voltage (v) and Time (min)	Equilibration Time (sec)
Initial Heat	$R_1 = 51.9300$	$V_1 = 1.3140$	300.7
Capacity	$R_2 = 51.8670$	$T_1 = 0.9996$	
Sample	$R_3 = 51.8570$		263.0
Introduction	$R_4 = 51.7990$		
Final Heat	$R_5 = 51.7890$	$V_2 = 1.3138$	315.3
Capacity	$R_6 = 51.7240$	$T_2 = 1.0011$	

Drift Rates (sec/mΩ)

Before R_1	Between R_2 and R_3	Between R_4 and R_5	After R_6
24.1	19.5	20.3	20.2
23.5	21.0	20.8	20.0
22.9	22.4	21.4	19.6
23.0	21.0	20.5	20.2
23.8	21.5	20.4	19.8
22.5	21.8	20.2	20.5
22.2	22.2	20.5	20.7
23.0	20.2	20.5	20.0
22.2	20.0	20.5	20.6
22.7	22.5	20.3	20.4
Avg = 23.0	21.2	20.5	20.2

Calculation 1. Determination of the Enthalpy of a Reaction from the Experimental Calorimetry Data

To determine the actual resistance change resulting from a thermal event in the calorimetry system, the overall resistance change which occurs during the time interval between initiation of the thermal event and re-equilibration of the system must be corrected for the contribution of the drift rate. If it is assumed that, in the absence of a thermal event, the drift rate would remain relatively constant, the contribution of the drift rate to the overall resistance change can be determined by extrapolating the initial drift rate (D_i) through 60% of the equilibration time and the final drift rate (D_f) through the remaining 40% of the equilibration time. (The choice of the point of extrapolation is somewhat arbitrary, but the 60%-40% method gives the best results in this calorimetry system). The actual resistance change due to the thermal event is thus given by:

$$\Delta R = R_i - R_f - E(0.0006/D_i + 0.0004/D_f) \qquad (25)$$

where R_i is the resistance of the thermistor probe at the initiation of the thermal event, R_f is the resistance after the system has re-equilibrated, and E is the equilibration time.

The amount of heat which is electrically evolved

during a determination of the heat capacity of the system is given by:

$$Q = I^2 R_h T \times \frac{60 \text{ sec/min}}{4.1840 \text{ joules/cal}} \qquad (26)$$

where I is the current flowing through the heater circuit, R_h is the resistance of the heater probe, and T is the length of time (in minutes) that power is supplied to the heater circuit. The current (I) is determined by measuring the voltage drop (V) across a standard 10-ohm resistor in series with the heater probe ($I = V/10$).

Once the amount of evolved heat and the corresponding resistance change are known, the heat capacity of the system can be obtained by:

$$C_p = Q/\Delta R \qquad (27)$$

where C_p is an operational heat capacity (in cal/ohm) which is related to the thermodynamically defined heat capacity (in cal/deg) by a constant of proportionality which cancels in the following calculations.

If it is assumed that the heat capacity during sample introduction ($\overline{C}_p$) is the average of the initial and final heat capacities, the amount of heat which is evolved in a chemical reaction is given by:

$$Q_r = \overline{C}_p \Delta R_r \tag{28}$$

where ΔR_r is the corrected resistance change which results from the chemical reaction. The enthalpy of the reaction being investigated is then given by:

$$\Delta\overline{H} = \frac{Q(\text{blank}) - Q_r}{\text{mmol of sample}} \tag{29}$$

where $Q(blank)$ is the amount of heat resulting from dilution of reagents and from the reaction of components of the solution other than the compound being investigated.

Using the typical calorimetry data given on page 115, the following results are calculated for a typical calorimetric determination.

$$\Delta R_1 = 51.9300 - 51.8670 - 300.7(0.0006/23.0 + 0.0004/21.2)$$

$$\Delta R_1 = 0.0495 \text{ ohms}$$

$$\Delta R_r = 51.8570 - 51.7990 - 263.0(0.0006/21.2 + 0.0004/20.5)$$

$$\Delta R_r = 0.0454 \text{ ohms}$$

$$\Delta R_2 = 51.7890 - 51.7240 - 315.3(0.0006/20.5 + 0.0004/20.2)$$

$$\Delta R_2 = 0.0496 \text{ ohms}$$

$$Q_1 = \frac{(0.13140)^2(140.896)(0.9996)(60)}{(4.1840)} = 34.87 \text{ cal}$$

$$Q_2 = \frac{(0.13138)^2(140.896)(1.0011)(60)}{(4.1840)} = 34.91 \text{ cal}$$

$$C_p(i) = (34.87)/(0.0495) = 704.9 \text{ cal/ohm}$$

$$C_p(f) = (34.91)/(0.0496) = 704.7 \text{ cal/ohm}$$

$$\overline{C}_p = \frac{704.9 + 704.7}{2} = 704.8 \text{ cal/ohm}$$

$$Q_r = (704.8)(0.0454) = 32.02 \text{ cal}$$

$$\Delta\overline{H} = \frac{3.39 - 32.02}{3.856} = -7.43 \text{ kcal/mol}$$

These calculations were routinely carried out using the HEATPRO program for enthalpies of protonation and the CALHEAT program for other calorimetric determinations. Both programs are listed in the Appendix.

Calculation 2. Fraction of an Organic Base which is Protonated During a Calorimetric Determination

Since those anilines and pyridines with $pK_a < 3$ cannot be completely protonated by the experimental procedure used in this research, it is necessary to determine the fraction of the sample which is protonated during a calorimetric determination.

Definitions:

K_a = dissociation constant of the organic acid (anilinium ion or pyridinium ion)

H = initial concentration of dilute perchloric acid

A = initial concentration of organic base (aniline or pyridine)

α = fraction of the organic base protonated during a calorimetric determination

For the reaction:

$$A + H^+ \rightleftharpoons AH^+ \qquad (30)$$

the equilibrium constant is given by:

$$K = 1/K_a = \frac{(AH^+)}{(A)(H^+)} \frac{\gamma_{AH^+}}{\gamma_A \gamma_{H^+}} \quad . \qquad (31)$$

Assuming that the activity coefficient of the organic base (γ_A) is unity and that the ratio of the activity coefficients

of AH^+ and H^+ is unity, the following equation is obtained.

$$1/K_a = \frac{\alpha A}{(A-\alpha A)(H-\alpha A)} \tag{32}$$

By rearranging this equation, an expression for α is obtained which can be solved by the quadratic formula.

$$\alpha = \frac{(H+A+K_a) - [(H+A+K_a)^2 - 4HA]^{1/2}}{2A} \tag{33}$$

If the experimentally determined enthalpy for the partial protonation of a weak organic base is $\Delta\bar{H}_{exp}$, the enthalpy of protonation is given by:

$$\Delta\bar{H}_p = \frac{\Delta\bar{H}_{exp}}{\alpha} \tag{34}$$

The HEATPRO computer program, which is used to calculate enthalpies of protonation, calculates α for each calorimetric determination. If $\alpha < 0.999$, the true enthalpy of protonation is calculated by the above method; otherwise, the true value is considered to be equal to the experimental value.

Calculation 3. Conversion of Experimental Enthalpies of Ionization to the Standard State Infinite Dilution Values

The experimentally determined enthalpies of ionization ($\Delta\bar{H}$) were obtained in aqueous solution at an ionic strength of 0.0287. To calculate the standard state infinite dilution value for the enthalpy of ionization ($\Delta\bar{H}°$), the experimental ionization reaction at an ionic strength of "m" is arbitrarily divided into three separate reactions.

The experimental ionization reaction is:

$$AH^+(m) \rightleftharpoons A(m) + H^+(m) \quad . \tag{35}$$

This reaction may also be considered as:

$$AH^+(m) \rightleftharpoons AH^+(\infty) \tag{36}$$

$$AH^+(\infty) \rightleftharpoons A(\infty) + H^+(\infty) \tag{37}$$

$$A(\infty) + H^+(\infty) \rightleftharpoons A(m) + H^+(m) \quad . \tag{38}$$

The overall enthalpy is given by the sum of the enthalpies for each separate reaction.

$$\Delta\bar{H} = \Delta\bar{H}_{dil}(AH^+) + \Delta\bar{H}° - \Delta\bar{H}_{dil}(A) - \Delta\bar{H}_{dil}(H^+) \tag{39}$$

Assuming that the enthalpy of dilution of the neutral organic base is negligible ($\Delta\overline{H}_{dil}(A) \simeq 0$), the following equation is obtained.

$$\Delta\overline{H}^{\circ} = \Delta\overline{H} + \Delta\overline{H}_{dil}(H^{+}) - \Delta\overline{H}_{dil}(AH^{+}) \qquad (40)$$

From literature data for the enthalpies of dilution of aqueous uni-univalent electrolytes[56], the difference between the enthalpies of dilution of H^{+} and AH^{+} is calculated by assuming that the enthalpy of dilution of NH_4^{+} may be substituted for the enthalpy of dilution of AH^{+}. Since the enthalpy of dilution of NH_4ClO_4 was not tabulated, the enthalpies of dilution of HCl (-75.0 cal/mol) and NH_4Cl (-57.5 cal/mol) were used. Therefore, the standard state infinite dilution value for the enthalpy of ionization is given by:

$$\Delta\overline{H}^{\circ} = \Delta\overline{H} + (-75.0) - (-57.5) \quad . \qquad (41)$$

$$\Delta\overline{H}^{\circ} = \Delta\overline{H} - 17.5 \text{ cal/mol} \quad . \qquad (42)$$

This correction term is within the standard deviation of the best data obtained in this research, so the experimental $\Delta\overline{H}$ values are assumed to be the standard state infinite dilution values for the enthalpies of ionization of the organic acids included in this research.

Calculation 4. Calculation of the pK_a of Thiophenol from Absorbance Measurements in a Standard KH_2PO_4-Na_2HPO_4 Buffer System

The pK_a of thiophenol was determined from absorbance measurements in a standard KH_2PO_4-Na_2HPO_4 buffer solution (pH = 6.86) over a range of ionic strengths (0.02 to 0.10). Since appreciable concentrations of thiophenol and thiophenoxide anion are present in these solutions, the concentration of each species must be determined before the pK_a can be calculated.

Definitions:

$(PhSH)_t$ = total concentration of thiophenol

$(PhSH)$ = equilibrium concentration of thiophenol

(PhS^-) = equilibrium concentration of thiophenoxide anion

(ε_{PhSH}) = extinction coefficient of thiophenol

(ε_{PhS^-}) = extinction coefficient of thiophenoxide anion

In a UV cell with a path length of 1.0 cm, the total absorbance of the buffer solution is given by:

$$A = (\varepsilon_{PhSH})(PhSH) + (\varepsilon_{PhS^-})(PhS^-) \quad . \qquad (43)$$

However, since $(PhSH) = [(PhSH)_t - (PhS^-)]$,

$$A = (\varepsilon_{PhSH})(PhSH)_t + [(\varepsilon_{PhS^-}) - (\varepsilon_{PhSH})](PhS^-) \quad . \qquad (44)$$

From the previous equation, it can be shown that

$$\frac{(PhSH)}{(PhS^-)} = \frac{A - (\varepsilon_{PhSH})(PhSH)_t}{(\varepsilon_{PhS^-})(PhSH)_t - A} \qquad (45)$$

Combination of the total thiophenol concentration (1.0048×10^{-4} M) with the extinction coefficients of thiophenol ($\varepsilon_{PhSH} = 575$) and thiophenoxide anion ($\varepsilon_{PhS^-} = 13{,}130$) yields:

$$\frac{(PhSH)}{(PhS^-)} = \frac{A - 0.0578}{1.3193 - A} \quad . \qquad (46)$$

When the $(PhSH)/(PhS^-)$ ratios are combined with the acidity function of the buffer at each ionic strength, the apparent pK_a is given by:

$$pK_{app} = p(a_H\gamma_{Cl}) - \log\frac{(PhS^-)}{(PhSH)} \qquad (47)$$

where $p(a_H\gamma_{Cl})$ is the acidity function of the buffer[60]. (This equation neglects the activity coefficient term shown in eq 10, since this term is approximately unity). A correction for the effect of the ionization of thiophenol on the acidity function of the buffer is applied to obtain the true pK_a value at each ionic strength[61].

$$pK_a = pK_{app} - \log \frac{(HPO_4^{=}) + (PhSH)_t}{(HPO_4^{=})} \qquad (48)$$

The data which are required for the calculation of the true pK_a at each ionic strength are summarized in Table 15. In order to correct for the slight ionic strength dependence of these pK_a values, a plot of pK_a versus ionic strength was extrapolated to zero ionic strength to obtain the standard state infinite dilution value for the pK_a of thiophenol.

Table 14. Absorbance Data for Thiophenol and Thiophenoxide Anion in Aqueous Solution at 37950 cm^{-1}

Solution	Concentration	Absorbance	Ext. Coeff.
Thiophenol in 10^{-4} N HCl	1.850×10^{-4} M	0.106	$\epsilon_{PhSH} = 575$
	4.624×10^{-4} M	0.259	
	9.248×10^{-4} M	0.542	
Sodium Thiophenoxide in 10^{-3} N NaOH	0.925×10^{-5} M	0.119	$\epsilon_{PhS^-} = 13{,}130$
	2.312×10^{-5} M	0.302	
	4.624×10^{-5} M	0.607	

Table 15. Summary of the Experimental Data for the Determination of the pK_a of Thiophenol in a Standard KH_2PO_4-Na_2HPO_4 Buffer Solution

Ionic Strength	$(HPO_4^{=})$	$p(a_{H^+}\gamma_{Cl^-})$	Absorbance	$\frac{(PhS^-)}{(PhSH)}$ [a]	pK_{app}	pK_a
0.02	0.0050	7.080	1.059	3.8515	6.494	6.485
0.03	0.0075	7.058	1.053	3.7423	6.485	6.479
0.04	0.0100	7.040	1.049	3.6722	6.475	6.471
0.05	0.0125	7.026	1.043	3.5706	6.473	6.470
0.06	0.0150	7.013	1.038	3.4895	6.470	6.467
0.10	0.0250	6.974	1.023	3.2621	6.460	6.458

pK_a (at I=0) = 6.488 ± 0.003

[a] A thiophenol concentration of 1.0048×10^{-4} M was used for all measurements.

Calculation 5. The Kirkwood-Westheimer Treatment of the Ionization of Organic Acids

In the molecular cavity model of Kirkwood-Westheimer electrostatic theory, the organic acid molecule is considered to be imbedded in a cavity of low dielectric constant immersed in a solvent continuum whose dielectric constant is that of the solvent. A pictorial representation of this model is given in Figure 11.

For the following reaction:

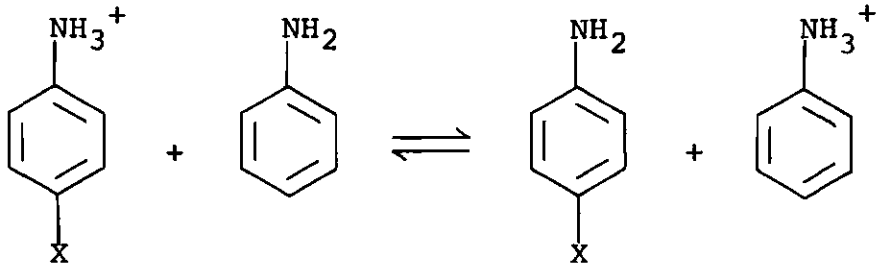

(49)

the Gibbs free energy of proton transfer is given by:

$$\Delta\bar{G}^{\circ}_{t} = \Delta\bar{G}^{\circ}_{X} - \Delta\bar{G}^{\circ}_{H} \qquad (50)$$

where $\Delta\bar{G}^{\circ}_{X}$ and $\Delta\bar{G}^{\circ}_{H}$ are the Gibbs free energies of ionization of the substituted and unsubstituted anilinium ions, respectively. In electrostatic theories of the acid ionization process, it is generally assumed that $\Delta\bar{G}^{\circ}_{t}$ may be divided into a temperature-independent non-electrostatic term and a temperature-dependent electrostatic term. Furthermore, it is

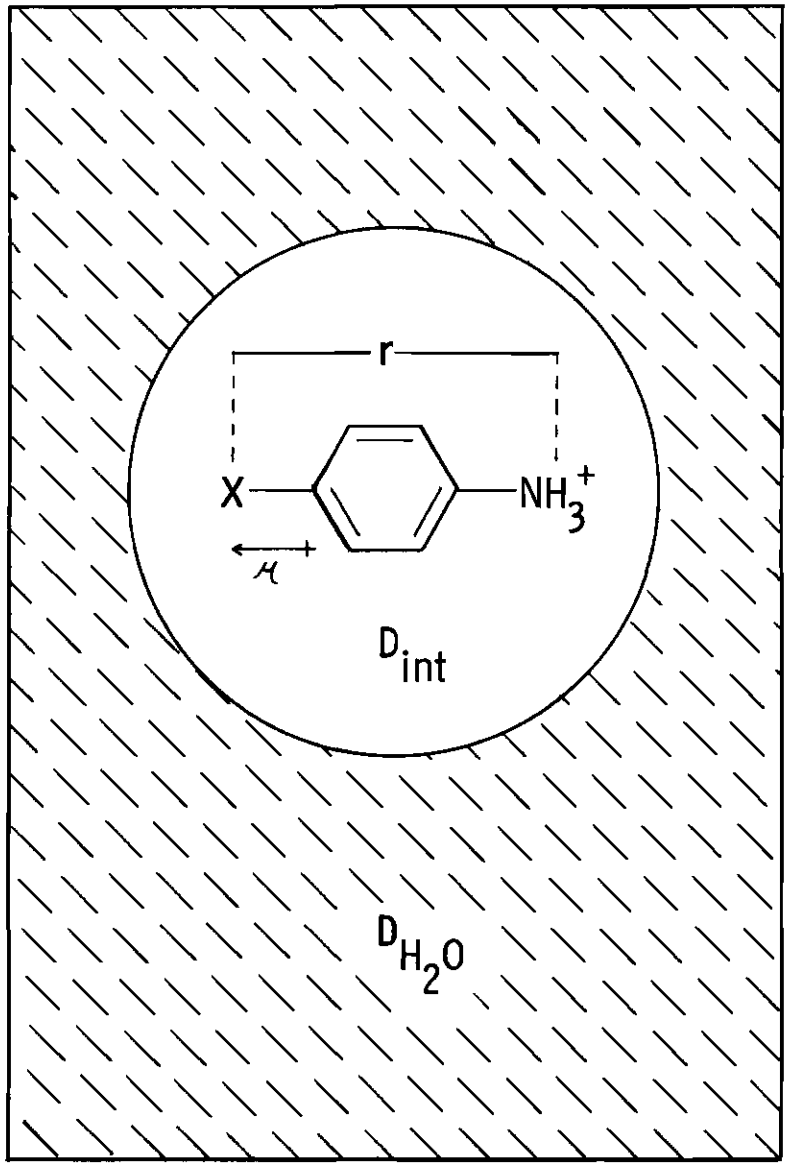

Figure 11. The Spherical Molecular Cavity Model of Kirkwood-Westheimer Electrostatic Theory.

assumed that the non-electrostatic term is negligible in symmetrical proton transfer reactions, so that

$$\Delta\bar{G}^{\circ}_{t} = \Delta\bar{G}_{el} \quad . \tag{51}$$

When the substituted acid contains a dipolar substituent, as is the case for all the anilinium ions and pyridinium ions included in this research, $\Delta\bar{G}_{el}$ is given by:

$$\Delta\bar{G}_{el} = \frac{Ne\mu\cos\phi}{D_{eff}r^2} \tag{52}$$

where N is Avogadro's number, e is the proton charge, μ is the substituent dipole moment, ϕ is the angle between the dipole moment vector and a line connecting the point dipole with the acidic proton, r is the distance between the acidic proton and the point dipole, and D_{eff} is the "effective" dielectric constant as defined by Kirkwood and Westheimer[4-7].

From standard thermodynamic calculations, it can be shown that the electrostatic entropy of proton transfer is:

$$\Delta\bar{S}_{el} = -(\partial\Delta\bar{G}_{el}/\partial T) \quad . \tag{53}$$

Therefore,

$$\Delta\bar{S}_{el} = \frac{Ne\mu\cos\phi}{D_{eff}r^2}(\partial\ln D_{eff}/\partial T) \tag{54}$$

and the ratio of $\Delta\bar{G}_{el}$ to $\Delta\bar{S}_{el}$ is given by:

$$\Delta\bar{G}_{el}/\Delta\bar{S}_{el} = (\partial \ln D_{eff}/\partial T)^{-1} \quad . \tag{55}$$

From Kirkwood-Westheimer theory, D_{eff} is calculated from equations of the following general form:

$$1/D_{eff} = f_1/D_{H_2O} + f_2/D_{int} \tag{56}$$

where D_{H_2O} is the dielectric constant of water, D_{int} is the temperature independent dielectric constant of the molecular cavity (usually set equal to 2.0), and f_1 and f_2 are constants which depend on the size and shape of the molecular cavity. Differentiation of this equation with respect to temperature yields:

$$\frac{1}{D_{eff}}(\partial \ln D_{eff}/\partial T) = \frac{f_1}{D_{H_2O}}(\partial \ln D_{H_2O}/\partial T) + \frac{f_2}{D_{int}}(\partial \ln D_{int}/\partial T). \tag{57}$$

However, since D_{int} is temperature independent, this equation may be simplified and rearranged to yield:

$$(\partial \ln D_{eff}/\partial T)^{-1} = \frac{D_{H_2O}(\partial \ln D_{H_2O}/\partial T)^{-1}}{(f_1)D_{eff}} = \Delta\bar{G}_{el}/\Delta\bar{S}_{el} \quad . \tag{58}$$

These calculations were carried out using the KWELST computer program which is listed in the Appendix.

Table 16. Structural Parameters Used in the Kirkwood-Westheimer Treatment of Substituted Anilinium Ions and Pyridinium Ions

Substituent	Bond Lengths (Å)	Bond Angles	Dipole Moment [a]	Cavity Volume ($Å^3$) [b]	Proton-Dipole Distance (Å) [b,c]
H	C-H = 1.09	None	Zero	138; 128	5.022; 4.290
4-CH_3	C-C = 1.50 C-H = 1.06	CCH = 109.5°	0.37	164; 154	5.404; 4.672 (min) 6.154; 5.422 (max)
4-Cl	C-Cl = 1.69	None	1.72	155; 145	5.322; 4.590
4-Br	C-Br = 1.84	None	1.70	162; 152	5.398; 4.666
4-I	C-I = 2.10	None	1.50	168; ---	5.528; -----
4-CN	C-C = 1.46 C-N = 1.16	CCN = 180°	4.39	155; 145	5.788; 5.056 (min) 6.518; 5.786 (max)
4-NO_2	C-N = 1.39 N-O = 1.20	ONO = 120°	4.21	158; ---	5.472; ----- (min) 6.168; ----- (max)

[a] The dipole moments (in Debyes), which are the difference between the moment of the substituent group and that of hydrogen, are set equal to the moments of the correspondingly substituted benzenes in the vapor state (see Ref. 8).

[b] Data are given for "anilinium ion"; "pyridinium ion".

[c] See footnote on Table 10.

Calculation 6. Calculation of van der Waals Volumes

Whenever two atoms, A and B, combine to form AB, the van der Waals spheres of the two atoms interpenetrate to allow formation of the A-B bond. Thus the van der Waals volume of AB will be somewhat smaller than the sum of the van der Waals volumes of A and B. The difference may be attributed to the overlapping volume increments of A and B. The van der Waals volume of AB is given by:

$$\overline{V}_w(AB) = \overline{V}_w(A) + \overline{V}_w(B) - \delta\overline{V}_a - \delta\overline{V}_b \qquad (59)$$

where $\overline{V}_w(A)$ and $\overline{V}_w(B)$ are the van der Waals volumes of A and B, and $\delta\overline{V}_a$ and $\delta\overline{V}_b$ are the overlapping volume increments, which can be calculated from a knowledge of the van der Waals radii of A and B and the A-B bond length[83].

Using the VOLUME computer program which is given in the Appendix, the van der Waals volumes and overlapping volume increments of a wide variety of A-B groups were calculated. These results are given in Table 17.

Using the van der Waals volume of benzene and the parameters given in Table 17, the van der Waals volumes of thiophenol, phenol, thiophenoxide, and phenoxide are calculated in the following manner.

Since the compounds of interest are of the type C_6H_5-X, it is convenient to calculate the van der Waals volume of the

phenyl group (C_6H_5). Using $\bar{V}_w(C_6H_6)$ = 48.36 ml/mol[83], the value for $\bar{V}_w(C_6H_5)$ can be calculated as follows:

$$\bar{V}_w(C_6H_6) = \bar{V}_w(C_6H_5) + \bar{V}_w(H) - \delta\bar{V}_c(CH) - \delta\bar{V}_h(CH)$$

$$48.36 = \bar{V}_w(C_6H_5) + 4.36 - 0.70 - 2.52$$

$$\bar{V}_w(C_6H_5) = 47.22 \text{ ml/mol}$$

The van der Waals volume of thiophenol is given by:

$$\bar{V}_w(C_6H_5SH) = \bar{V}_w(C_6H_5) + \bar{V}_w(S) + \bar{V}_w(H) - \delta\bar{V}_c(CS)$$

$$- \delta\bar{V}_s(CS) - \delta\bar{V}_s(HS) - \delta\bar{V}_h(HS)$$

$$\bar{V}_w(C_6H_5SH) = 47.22 + 14.71 + 4.36 - 2.09 - 1.83 - 0.65 - 2.21$$

$$\bar{V}_w(C_6H_5SH) = 59.51 \text{ ml/mol}$$

The van der Waals volume of phenol is given by:

$$\bar{V}_w(C_6H_5OH) = \bar{V}_w(C_6H_5) + \bar{V}_w(O) + \bar{V}_w(H) - \delta\bar{V}_c(CO)$$

$$- \delta\bar{V}_o(CO) - \delta\bar{V}_o(HO) - \delta\bar{V}_h(HO)$$

$$\bar{V}_w(C_6H_5OH) = 47.22 + 8.86 + 4.36 - 1.67 - 2.28 - 0.86 - 2.11$$

$$\overline{V}_w(C_6H_5OH) = 53.52 \text{ ml/mol}$$

The van der Waals volume of thiophenoxide anion is given by:

$$\overline{V}_w(C_6H_5S^-) = \overline{V}_w(C_6H_5) + \overline{V}_w(S^-) - \delta\overline{V}_c(C\text{-}S^-) - \delta\overline{V}_s(C\text{-}S^-)$$

$$\overline{V}_w(C_6H_5S^-) = 47.22 + 26.50 - 4.12 - 2.10$$

$$\overline{V}_w(C_6H_5S^-) = 67.50 \text{ ml/mol}$$

The van der Waals volume of phenoxide anion is given by:

$$\overline{V}_w(C_6H_5O^-) = \overline{V}_w(C_6H_5) + \overline{V}_w(O^-) - \delta\overline{V}_c(C\text{-}O^-) - \delta\overline{V}_o(C\text{-}O^-)$$

$$\overline{V}_w(C_6H_5O^-) = 47.22 + 13.76 - 2.93 - 2.63$$

$$\overline{V}_w(C_6H_5O^-) = 55.42 \text{ ml/mol}$$

Table 17. Van der Waals Volumes and Overlapping Volume Increments for A-B Groups [a]

Bond (A-B)	Radius of A	Radius of B	A-B Bond Length	Volume of A	Volume of B	Overlap Volume of A	Overlap Volume of B
C-H	1.70	1.20	1.084	12.40	4.36	0.70	2.52
C-C	1.70	1.70	1.500	12.40	12.40	2.36	2.36
$C-O^-$	1.70	1.76	1.400	12.40	13.76	2.93	2.63
$C-S^-$	1.70	2.19	1.820	12.40	26.50	4.12	2.10
C-O	1.70	1.52	1.427	12.40	8.86	1.67	2.28
C-S	1.70	1.80	1.818	12.40	14.71	2.09	1.83
C-F	1.70	1.47	1.370	12.40	8.01	1.54	2.34
C-Cl	1.70	1.75	1.690	12.40	13.52	2.17	2.02
C-Br	1.70	1.85	1.840	12.40	15.97	2.25	1.85
C-I	1.70	1.98	2.100	12.40	19.58	2.13	1.55
C-N	1.70	1.55	1.390	12.40	9.40	1.85	2.42
C=O	1.70	1.50	1.280	12.40	8.52	1.78	2.63
H-N	1.20	1.55	1.010	4.36	9.40	2.10	0.83
H-S	1.20	1.80	1.330	4.36	14.71	2.21	0.65
H-O	1.20	1.52	0.958	4.36	8.86	2.11	0.86
N-O	1.55	1.52	1.200	9.40	8.86	1.96	2.09

[a] Radii and bond lengths in Angstroms; volumes in ml/mol.

Calculation 7. Calculation of Cavity Volumes from Scaled-Particle Theory

Using the scaled-particle theory[85,86], Pierotti[87,88] has developed a theory of solubility of non-polar solutes in water. In this approach, the solute molecule is treated as a hard sphere of diameter a_2 immersed in a solvent continuum of hard spheres of diameter a_1. According to Pierotti's theory, the cavity volume of a non-polar solute (the volume which the molecule would occupy in aqueous solution in the absence of solute-solvent interactions) is given by:

$$\bar{V}_c = 82.05(\beta/\alpha_p)(\bar{H}_c/RT) + \bar{V}_w \qquad (60)$$

where β and α_p are the isothermal compressibility and the coefficient of thermal expansion of water, respectively, $\bar{H}_c$ is the partial molar enthalpy of cavity formation, R is the gas constant, T is the absolute temperature, and V_w is the van der Waals volume of the solute molecule, which can be calculated from a knowledge of the appropriate van der Waals radii and bond lengths (see Calculation 6). The enthalpy of cavity formation ($\bar{H}_c$) is given by:

$$\bar{H}_c = \alpha_p RT^2[y/(1-y)]\{[6/(1-y)][2(a_{12}/a_1)^2 - (a_{12}/a_1)] +$$

$$[36y/(1-y)^2][(a_{12}/a_1)^2 - (a_{12}/a_1) + \tfrac{1}{4}] + 1\} \qquad (61)$$

where $y = (\pi a_1^3 \rho)/6$, ρ is the number density of water (in molecules/cc), and $a_{12} = (a_1 + a_2)/2$ is the radius of the sphere which excludes the centers of solvent molecules.

If the partial molal volume of the solute in water is also known, the interaction volume ($\bar{V}_i$) can be calculated as follows:

$$\bar{V}_i = \bar{V}^\circ - \bar{V}_c - \beta RT \quad . \tag{62}$$

These calculations were carried out using the SPT computer program which is given in the Appendix.

Calculation 8. Electrostriction Volume Changes in Aqueous Solution.

Using the method developed by Desnoyers and coworkers[69], the following expression may be used to calculate the electrostatic field E at a distance r from the center of an ion in aqueous solution:

$$E^3 + E^2(Ze/n_o^2r^2) + E(D_o/bn_o^2) + Ze/bn_o^2r^2 = 0 \qquad (63)$$

where Ze is the charge on the ion, n_o^2 is the square of the refractive index of water and has the value 1.78 at 25° and 1 atm, D_o is the dielectric constant of water (78.36 at 25°), and b is a constant which has the value 1.08×10^{-8} when E is expressed in electrostatic units.

In using this equation to calculate the electrostatic fields of O^- and S^- at the center of the primary solvation layer around the ions, the r values for O^- and S^- were taken to be the sum of the crystallographic radii of O^- and S^- (1.76 and 2.19Å, respectively)[84] and the radius of a water molecule (1.38Å). Once E has been determined, an effective pressure P, which would produce the same volume change in the absence of an electrostatic field, is determined from the tables compiled by Desnoyers, et. al.[69]. According to the method of Desnoyers and coworkers, the molar volume of water in the electrostatic field of an ion is given by:

$$\log \bar{V} = \log \bar{V}^\circ - 0.1368 \log (1 + P/2.997 \times 10^9) \quad (64)$$

where $\bar{V}^\circ$ is the partial molar volume of pure water in the absence of an electrostatic field (18.07 ml/mol).

Once the molar volume of water in the electrostatic fields of O^- and S^- has been calculated, the electrostriction volume change per mole of water around an ion is obtained by:

$$\Delta\bar{v}_{elect} = \bar{V} - \bar{V}^\circ \quad (65)$$

These calculations yielded the following results:

	O^-	S^-
r(Å)	3.14	3.57
E(esu/cm^2)	2.58×10^5	1.91×10^5
P(dynes/cm^2)	5.20×10^9	3.75×10^9
$\bar{V}$(ml/mol)	15.75	16.17
$\Delta\bar{v}_{elect}$(ml/mol-H_2O)	-2.32	-1.90

The overall electrostriction volume change around an ion is given by:

$$\Delta\bar{V}_{elect} = n\Delta\bar{v}_{elect} \quad (66)$$

where n is the number of solvent molecules in the primary

solvation layer of the ion.

Before $\Delta\bar{V}_{elect}$ can be calculated, the number of water molecules in the primary solvation layer must be known. Since this information is not known for such ions as $C_6H_5O^-$ and $C_6H_5S^-$, two possible model systems were considered. At the very minimum, at least two solvent molecules should be in the primary solvation layer of each ion. Using $n = 2$, electrostriction volume changes of -4.64 and -3.80 ml/mol were calculated for $C_6H_5O^-$ and $C_6H_5S^-$, respectively. In the other model system, it is assumed that the primary solvation layer will contain as many solvent molecules as space will permit. The total amount of available space around the ion is given by

$$\bar{V}_s = \frac{4\pi N}{3}[(r_{ion} + 2.76)^3 - (r_{ion})^3] \qquad (67)$$

where N is Avogadro's number, r_{ion} is the crystallographic radius of the ion and the factor 2.76 is the diameter of a water molecule. This is the volume of the shell which contains the first layer of water molecules around the ion. Using the calculated molar volumes of water in the electrostatic fields of O^- and S^-, and assuming that the phenyl group occupies one-half of the available space around each ion, the maximum number of water molecules which can occupy the primary solvation layer around an ion is calculated by:

$$n = \frac{\overline{V}_s}{2\overline{V}} \quad . \tag{68}$$

Using the calculated n values for $C_6H_5O^-$ and $C_6H_5S^-$ (6.96 and 8.65, respectively), the total electrostriction changes around these ions are -16.15 and -16.43 ml/mol, respectively.

Calculation 9. Statistical Mechanical Calculation of Gas Phase Entropies.

In order to calculate the gas phase entropy of proton transfer in the thiophenol-phenol system, the entropy of each species involved in the reaction must be calculated. From statistical mechanics, the total entropy of a molecule is the sum of translational, rotational, and vibrational contributions.

$$\bar{S}^\circ = \bar{S}^\circ_{trans} + \bar{S}^\circ_{rot} + \bar{S}^\circ_{vib} \quad . \tag{69}$$

The translational entropy is given by:

$$\bar{S}^\circ_{trans} = -R\ln P + \frac{5}{2}R\ln T + \frac{3}{2}R\ln M - 2.3150 \tag{70}$$

where P is the pressure in atm, T is the absolute temperature, and M is the molecular weight.

For thiophenoxide anion,

$$\bar{S}^\circ_{trans} = -R\ln(1) + \frac{5}{2}R\ln(298.15) + \frac{3}{2}R\ln(109.1708) - 2.3150$$

$$S^\circ_{trans} = 39.979 \text{ cal/deg-mol}$$

For phenoxide anion,

$$\bar{S}^{\circ}_{trans} = -R\ln(1) + \frac{5}{2}R\ln(298.15) + \frac{3}{2}R\ln(93.1062) - 2.3150$$

$$S^{\circ}_{trans} = 39.505 \text{ cal/deg-mol}$$

The rotational entropy is given by:

$$\bar{S}^{\circ}_{rot} = \frac{3}{2}R\ln T - R\ln\sigma + \frac{1}{2}R\ln(D \times 10^{117}) - 0.033 \qquad (71)$$

where σ is the symmetry factor (σ = 2), and $\mathcal{D}$ is the product of the principal moments of inertia. (The principal moments of inertia of thiophenoxide anion and phenoxide anion were calculated using a computer program written by C. R. Nave of the Physics Department at Georgia State University).

For thiophenoxide anion, the three principal moments of inertia are 1.47515×10^{-38}, 5.32616×10^{-38}, and 6.80129×10^{-38} g-cm^2, so

$$\bar{S}^{\circ}_{rot} = \frac{3}{2}R\ln(298.15) - R\ln(2) + \frac{1}{2}R\ln(5.34369 \times 10^{4}) - 0.033$$

$$\bar{S}^{\circ}_{rot} = 26.389 \text{ cal/deg-mol}$$

For phenoxide anion, the three principal moments of inertia are 1.47515×10^{-38}, 3.16597×10^{-38}, and

4.64109×10^{-38} g-cm^2, so

$$\bar{S}^\circ_{rot} = \frac{3}{2}R\ln(298.15) - R\ln(2) + \frac{1}{2}R\ln(2.16752 \times 10^4) - 0.033$$

$$\bar{S}^\circ_{rot} = 25.493 \text{ cal/deg-mol}$$

The vibrational entropy is given by:

$$\bar{S}^\circ_{vib} = R\sum_{i=1}^{n}\left[\frac{\mu_i}{(e^{\mu_i} - 1)}\right] - \ln(1 - e^{-\mu_i}) \qquad (72)$$

$$\mu_i = \frac{hc\bar{\nu}_i}{KT}$$

where $\bar{\nu}_i$ is the wavenumber of the i^{th} absorption band, and other symbols have their usual significance. The vibrational bands and the entropy contribution of each band are summarized in Table 18 for the thiophenoxide and phenoxide anions. Summing up all the vibrational entropy contributions, the following results are obtained.

For thiophenoxide anion,

$$\bar{S}^\circ_{vib} = 8.611 \text{ cal/deg-mol}$$

For phenoxide anion,

$$\bar{S}^\circ_{vib} = 6.965 \text{ cal/deg-mol}$$

Thus, the total entropies of these two ions are:

$$\bar{S}^\circ(C_6H_5S^-) = 39.979 + 26.389 + 8.611 = 74.979 \text{ cal/deg-mol}$$

$$\bar{S}^\circ(C_6H_5O^-) = 39.505 + 25.493 + 6.965 = 71.963 \text{ cal/deg-mol}$$

Table 18. Entropy Contributions of the Fundamental Vibrational Frequencies in Thiophenoxide and Phenoxide Anions

Thiophenoxide Anion		Phenoxide Anion	
Wavenumber	Entropy	Wavenumber	Entropy
3100	-----	3100	-----
3071	-----	3071	-----
3055	-----	3055	-----
3045	-----	3045	-----
3042	-----	3042	-----
1580	0.008	1595	0.008
1570	0.009	1585	0.008
1470	0.013	1490	0.012
1460	0.014	1480	0.013
1440	0.015	1450	0.015
1250	0.034	1300	0.027
1180	0.045	1175	0.046
1156	0.050	1168	0.047
1070	0.070	1069	0.071
1020	0.086	1020	0.086
970	0.106	970	0.106
960	0.110	985	0.099
910	0.134	875	0.154
835	0.181	829	0.185
775	0.229	770	0.233
993	0.096	1000	0.094
690	0.320	700	0.306
618	0.420	600	0.450
415	0.909	408	0.934
1080	0.068	1300	0.027
695	0.316	813	0.197
450	0.796	540	0.565
420	0.892	530	0.587
310	1.362	420	0.892
180	2.328	240	1.803
	Total = 8.611		Total = 6.965

Calculation 10. Gas Phase Thermodynamics of Proton Transfer in the Thiophenol-Phenol System.

For the reaction,

$$C_6H_5SH + C_6H_5O^- \rightleftharpoons C_6H_5S^- + C_6H_5OH$$

the thermodynamic parameters $\Delta\bar{G}^\circ_t$, $\Delta\bar{H}^\circ_t$, and $\Delta\bar{S}^\circ_t$ can be calculated by a combination of semi-empirical CNDO/2 calculations and standard statistical thermodynamic procedures.

Using the CNDO/2 method of Pople, Henneike[80] has calculated the total energies of each species in the proton transfer reaction. Values of -1583.5754, -1783.2534, -1561.6549, and -1759.9824 eV/mol were obtained for thiophenol, phenol, thiophenoxide, and phenoxide, respectively. From these values, the gas phase energy of proton transfer at 0°K is calculated to be -1.3505 eV/mol, or $\Delta\bar{E}_t(g,0°K)$ = -31.14 kcal/mol. Since the volume change is zero in a gas phase proton transfer reaction, the enthalpy of proton transfer is given by:

$$\Delta\bar{H}_t(g,0°K) = \Delta\bar{E}_t(g,0°K) = -31.14 \text{ kcal/mol} \qquad (73)$$

By combination of the statistical mechanical calculations of the gas phase entropies of the thiophenoxide and phenoxide anions (see Calculation 9) with the literature

entropies of thiophenol[96] and phenol[97] (80.51 and 75.44 cal/deg-mol, respectively), the entropy of proton transfer is calculated to be:

$$\Delta\bar{S}^{\circ}_{t}(g) = -2.05 \text{ cal/deg-mol}$$

Therefore, assuming that the enthalpy of proton transfer is independent of temperature,

$$\Delta\bar{H}^{\circ}_{t}(g) = -31.14 \text{ kcal/mol} \quad .$$

Furthermore, since at 298°K,

$$\Delta\bar{G}^{\circ}_{t}(g) = \Delta\bar{H}^{\circ}_{t}(g) - T\Delta\bar{S}^{\circ}_{t}(g) \quad . \qquad (74)$$

$$\Delta\bar{G}^{\circ}_{t}(g) = -30.53 \text{ kcal/mol} \quad .$$

BIBLIOGRAPHY*

1. N. Bjerrum, *Z. Phys. Chem.*, *106*, 219 (1923).

2. A. Eucken, *Angew. Chem.*, *45*, 203 (1932).

3. H. M. Smallwood, *J. Amer. Chem. Soc.*, *54*, 3048 (1932).

4. J. G. Kirkwood and F. H. Westheimer, *J. Chem. Phys.*, *6*, 506 (1938).

5. F. H. Westheimer and J. G. Kirkwood, *J. Chem. Phys.*, *6*, 513 (1938).

6. F. H. Westheimer and M. W. Shookhoff, *J. Amer. Chem. Soc.*, *61*, 555 (1939).

7. F. H. Westheimer, W. A. Jones, and R. A. Lad, *J. Chem. Phys.*, *10*, 478 (1942).

8. J. N. Sarmousakis, *J. Chem. Phys.*, *12*, 277 (1944).

9. C. Tanford, *J. Amer. Chem. Soc.*, *79*, 5348 (1957).

10. E. J. King, "Acid-Base Equilibria," MacMillan Co., New York, N. Y., 1965, pp. 161-166.

11. C. G. Derick, *J. Amer. Chem. Soc.*, *33*, 1152 (1911).

12. S. Ehrenson, *Prog. Phys. Org. Chem.*, *2*, 195 (1964).

13. G. E. K. Branch and M. Calvin, "The Theory of Organic Chemistry," Prentice-Hall, Englewood Cliffs, N. J., 1941, pp. 217-232.

14. J. D. Roberts and W. D. Moreland, *J. Amer. Chem. Soc.*, *75*, 2167 (1953).

15. H. D. Holtz and L. M. Stock, *J. Amer. Chem. Soc.*, *86*, 5188 (1964).

16. C. F. Wilcox and J. S. McIntyre, *J. Org. Chem.*, *30*, 777 (1965).

---

* For complete titles of journals cited, see *Access*, 1969.

17. C. D. Ritchie and E. W. Lewis, *J. Amer. Chem. Soc.*, *84*, 591 (1962).

18. F. W. Baker, R. C. Parish, and L. M. Stock, *J. Amer. Chem. Soc.*, *89*, 5677 (1967).

19. C. F. Wilcox and C. Leung, *J. Amer. Chem. Soc.*, *90*, 336 (1968).

20. S. Siegel and J. M. Kormarmy, *J. Amer. Chem. Soc.*, *82*, 2547 (1960).

21. H. Stetter and J. Mayer, *Chem. Ber.*, *95*, 667 (1962).

22. C. L. Liotta, W. F. Fisher, G. H. Greene, Jr., and B. L. Joyner, *J. Amer. Chem. Soc.*, *94*, 4891 (1972).

23. C. L. Liotta, W. F. Fisher, E. L. Slightom, and C. L. Harris, *J. Amer. Chem. Soc.*, *94*, 2129 (1972).

24. C. L. Liotta, W. F. Fisher, and C. L. Harris, *J. Chem. Soc.*, *D*, (1971), 1312.

25. C. L. Liotta, W. F. Fisher, and G. H. Greene, Jr., *J. Chem. Soc.*, *D*, (1969), 1251.

26. C. A. Grob, A. Kaiser, and E. Renk, *Chem. Ind. [London]*, (1957), 598.

27. C. A. Grob, E. Renk, and A. Kaiser, *Chem. Ind. [London]*, (1955), 1222.

28. R. Golden and L. M. Stock, *J. Amer. Chem. Soc.*, *88*, 5928 (1966).

29. L. M. Stock, *J. Chem. Educ.*, *49*, 400 (1972).

30. L. P. Hammett, *J. Amer. Chem. Soc.*, *59*, 96 (1937).

31. J. Hine, "Physical Organic Chemistry," McGraw-Hill, New York, N.Y., 1962, pp. 81-103.

32. H. H. Jaffe, *Chem. Rev.*, *53*, 191 (1953).

33. J. W. Larson and L. G. Hepler, "Solute-Solvent Interactions," J. F. Coetzee and C. D. Ritchie, Ed., Marcel Dekker, New York, N.Y., 1969, Ch. 1.

34. J. J. Christensen, R. M. Izatt, and L. D. Hansen, *J. Amer. Chem. Soc.*, *89*, 213 (1967).

35. P. D. Bolton, K. A. Fleming, and F. M. Hall, *J. Amer. Chem. Soc.*, *94*, 1033 (1972).

36. P. D. Bolton and F. M. Hall, *Aust. J. Chem.*, *20*, 1797 (1967).

37. P. D. Bolton and F. M. Hall, *Aust. J. Chem.*, *21*, 939 (1968).

38. P. D. Bolton and F. M. Hall, *J. Chem. Soc.*, *B*, (1969), 259.

39. A. I. Biggs, *J. Chem. Soc.*, (1961), 2572.

40. W. Van de Poel and P. J. Slootmaekers, *Bull. Soc. Chim. Belges*, *79*, 223 (1970).

41. J. J. Christensen, R. M. Izatt, D. P. Wrathall, and L. D. Hansen, *J. Chem. Soc.*, *A*, (1969), 1212.

42. W. F. O'Hara, *Can. J. Chem.*, *46*, 1965 (1968).

43. A. Fischer, W. J. Galloway, and J. Vaughan, *J. Chem. Soc.*, (1964), 3591.

44. J. J. Christensen, D. E. Smith, M. D. Slade, and R. M. Izatt, *Thermochim. Acta*, *5*, 35 (1972).

45. A. R. Katritzky and J. M. Lagowski, *Adv. Heterocyclic Chem.*, *1*, 339 (1963).

46. R. G. Bates and H. B. Hetzer, *J. Res. Nat. Bur. Stand.*, *64A*, 427 (1960).

47. L. Sacconi, P. Paoletti, and M. Ciampolini, *J. Amer. Chem. Soc.*, *82*, 3831 (1960).

48. P. D. Bolton and L. G. Hepler, *Quart. Rev. Chem. Soc.*, *25*, 521 (1971).

49. L. G. Hepler, *Can. J. Chem.*, *49*, 2803 (1971).

50. M. M. Kreevoy, B. E. Eichinger, F. E. Stary, E. A. Katz, and J. H. Sellstedt, *J. Org. Chem.*, *29*, 1641 (1964).

51. W. P. Jencks and K. Salvesen, *J. Amer. Chem. Soc.*, *93*, 4433 (1971).

52. W. F. O'Hara, C. H. Wu, and L. G. Hepler, *J. Chem. Educ.*, *38*, 512 (1961).

53. C. Plato and A. R. Glasgow, Jr., *Anal. Chem.*, *41*, 330 (1969).

54. G. M. Dyson, H. J. George, and R. F. Hunter, *J. Chem. Soc.*, (1927), 436.

55. A. R. Katritzky and A. M. Monro, *J. Chem. Soc.*, (1958), 1263.

56. V. B. Parker, *Nat. Stand. Ref. Data Ser., Nat. Bur. Stand.*, NSRDS-NBS2, 50, (1965).

57. J. D. Hale, R. M. Izatt, and J. J. Christensen, *J. Phys. Chem.*, *67*, 2605 (1963).

58. C. E. Vanderzee and J. A. Swanson, *J. Phys. Chem.*, *67*, 2608 (1963).

59. J. P. Wibaut and W. J. Holmes-Kamminga, *Bull. Soc. Chim. Fr.*, (1958), 424.

60. R. G. Bates and R. Gary, *J. Res. Natl. Bur. Stand.*, *65A*, 495 (1961).

61. R. A. Robinson and A. I. Biggs, *Trans. Faraday Soc.*, *51*, 901 (1955).

62. W. F. O'Hara, H. C. Ko, M. N. Ackermann, and L. G. Hepler, *J. Phys. Chem.*, *71*, 3107 (1967).

63. A. de Courville and D. Peltier, *Bull. Soc. Chim. Fr.*, (1967), 2164.

64. M. M. Fickling, A. Fischer, B. R. Mann, J. Packer, and J. Vaughan, *J. Amer. Chem. Soc.*, *81*, 4226 (1959).

65. R. J. Irving, L. Nelander, and I. Wadsö, *Acta Chem. Scand.*, *18*, 769 (1964).

66. C. L. Liotta, H. P. Hopkins, Jr., and A. Abidaud, unpublished data.

67. K. B. Wiberg, "Physical Organic Chemistry," John Wiley and Sons, Inc., New York, N. Y., 1964, p. 284.

68. G. W. Wheland, "Resonance in Organic Chemistry," John Wiley and Sons, New York, N. Y., 1955, pp. 696-784.

69. J. E. Desnoyers, R. E. Verrall, and B. E. Conway, *J. Chem. Phys.*, *43*, 243 (1965).

70. C. L. Liotta, E. M. Perdue, and H. P. Hopkins, Jr., *J. Amer. Chem. Soc.*, *95*, 2439 (1973).

71. M. Taagepera, W. G. Henderson, R. T. C. Brownlee, J. L. Beauchamp, D. Holtz, and R. W. Taft, *J. Amer. Chem. Soc.*, *94*, 1369 (1972).

72. A. Albert, R. Goldacre, and J. Phillips, *J. Chem. Soc.*, (1948), 2240.

73. S. J. Angyal and C. L. Angyal, *J. Chem. Soc.*, (1952), 1461.

74. M. L. Bender and Y. L. Chow, *J. Amer. Chem. Soc.*, *81*, 3929 (1959).

75. K. S. Pitzer, "Quantum Chemistry," Prentice-Hall, New York, N. Y., 1953, p. 498.

76. S. D. Hamann and S. C. Lim, *Aust. J. Chem.*, *7*, 329 (1954).

77. R. D. Brown and M. L. Heffernan, *Aust. J. Chem.*, *12*, 554 (1959).

78. R. W. Gurney, "Ionic Processes in Solution," McGraw-Hill, New York, N. Y., 1953, Ch. 10.

79. J. A. Pople and M. Gordon, *J. Amer. Chem. Soc.*, *89*, 4253 (1967).

80. H. F. Henneike, Department of Chemistry, Georgia State University, private communication.

81. F. A. Cotten and G. Wilkinson, "Advanced Inorganic Chemistry," Interscience, New York, N. Y., 1966, p. 100.

82. M. C. Day, Jr., and J. Selbin, "Theoretical Inorganic Chemistry," Reinhold Book Corp., New York, N. Y., 1962, p. 110.

83. A. Bondi, *J. Phys. Chem.*, *68*, 441 (1964).

84. "Handbook of Chemistry and Physics, 46th Ed.," Chemical Rubber Co., Cleveland, Ohio, 1965, p. F-117.

85. H. Reiss, H. L. Frisch, and J. L. Lebowitz, *J. Chem. Phys.*, *31*, 369 (1959).

86. H. Reiss, H. L. Frisch, E. Helfand, and J. L. Lebowitz, *J. Chem. Phys.*, *32*, 119 (1960).

87. R. A. Pierotti, *J. Phys. Chem.*, *67*, 1840 (1963).

88. R. A. Pierotti, *J. Phys. Chem.*, *69*, 281 (1965).

89. E. J. King, *J. Phys. Chem.*, *73*, 1220 (1969).

90. M. Born, *Z. Phys.*, *1*, 45 (1920).

91. J. D. Bernal and R. H. Fowler, *J. Chem. Phys.*, *1*, 515 (1933).

92. H. S. Frank, *J. Chem. Phys.*, *23*, 2023 (1955).

93. D. C. Grahame, *J. Chem. Phys.*, *21*, 1054 (1953).

94. K. Pitzer, *J. Amer. Chem. Soc.*, *59*, 2365 (1937).

95. H. P. Hopkins, Jr., unpublished data.

96. D. W. Scott, J. P. McCullough, W. N. Hubbard, J. F. Messerly, I. A. Hossenlopp, F. R. Frow, and G. Waddington, *J. Amer. Chem. Soc.*, *78*, 5463 (1956).

97. J. H. S. Green, *J. Chem. Soc.*, (1961), 2236.

98. G. H. Parsons, C. H. Rochester, and C. E. C. Wood, *J. Chem. Soc.*, *B*, (1971), 533.

99. D. P. Biddescombe and J. F. Martin, *Trans. Faraday Soc.*, *54*, 1316 (1958).

100. C. L. Liotta, E. M. Perdue, and H. P. Hopkins, Jr., unpublished data.

101. K. J. Laidler and C. Pegis, *Proc. Roy. Soc. (London)*, *A241*, 80 (1957).

VITA

Edward Michael Perdue, the son of Mr. and Mrs. Edward P. Perdue, is a native of Waycross, Georgia. He received his Bachelor of Science degree in Chemistry from Georgia Tech in June, 1969. In the fall of that year, he entered the Ph.D. program in the School of Chemistry at Georgia Tech and began his studies in physical organic chemistry under the direction of C. L. Liotta.

From September, 1969 to September, 1970, he worked as a research assistant with J. H. Reuter in the School of Geophysical Sciences at Georgia Tech. From September, 1970 to July, 1973, he was engaged in his thesis research under the direction of C. L. Liotta and H. P. Hopkins, Jr. of Georgia State University. This research was funded by the Office of Water Resources Research.

In the fall of 1973, Mike will join the faculty at Portland State University in Portland, Oregon, where he has accepted an assistant professorship in the Department of Chemistry.

Mike is married to the former Kathryn Elizabeth Wilder, who is also a native of Waycross, Georgia.